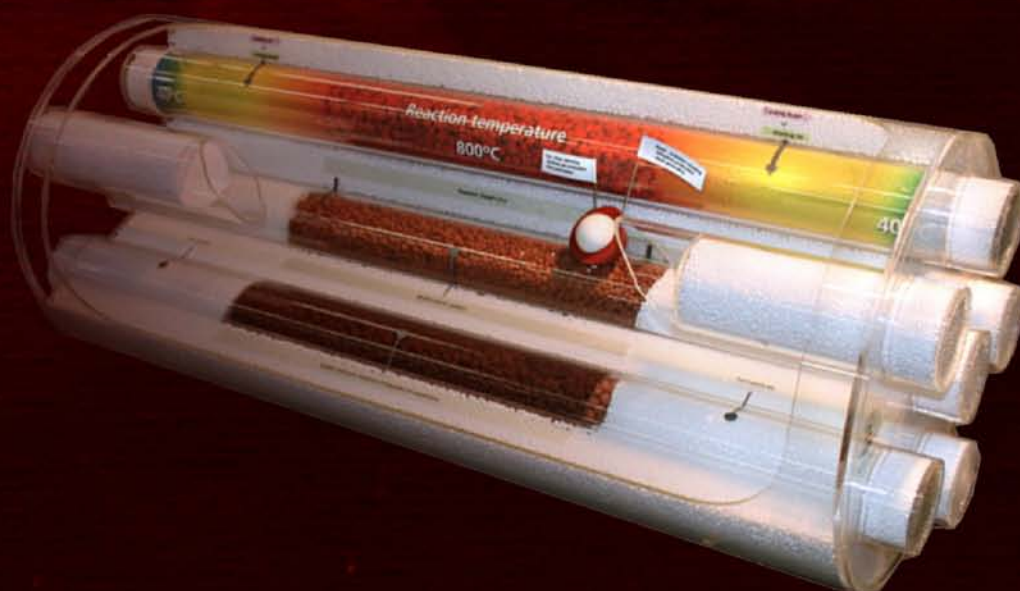


Combining oxidative coupling and reforming of methane

Vision or Utopia?



Patrick Graf



University of Twente
Enschede - The Netherlands

Combining oxidative coupling and reforming of methane

Vision or Utopia?

Patrick Graf

Promotie Commissie

Voorzitter:	Prof.dr. G. van der Steenhoven	Universiteit Twente
Promotor:	Prof. dr. ir L. Lefferts	Universiteit Twente
Assistant promotor:	Dr. B. L. Mojet	Universiteit Twente
	Dr. J. G. van Ommen	Universiteit Twente
Lid:	Prof.dr.ir. J.A.M. Kuipers	Universiteit Twente
	Prof.dr.ir. A. Nijmeijer	Universiteit Twente
	Prof. J.R.H. Ross	University of Limerick
	Dr. D. van Oeffelen	Dow Benelux B.V.
	Prof.dr. F. Kapteijn	Technische Universiteit Delft
	Prof.dr.ir. H. van den Berg	Universiteit Twente

The research described in this thesis was performed under the auspices of the Dutch Institute for Research in Catalysis (NIOK). Financial support ACTS-NWO Project No. 053.62.008 (ASPECT) is gratefully acknowledged.

Cover design: Ing. Bert Geerdink, Catalytic Processes and Materials (CPM),
University of Twente, Enschede, The Netherlands.

ISBN 978-90-365-2778-1

Copyright © 2008 by Patrick Graf, Enschede, The Netherlands

Printed by Gildeprint, Enschede

No part of this book may be reproduced in any form of print, photo print, microfilm or any other means without permission from the author / publisher

COMBINING OXIDATIVE COUPLING AND REFORMING OF METHANE

VISION OR UTOPIA?

PROEFSCHRIFT

ter verkrijging van
de graad van doctor aan de Universiteit Twente,
op gezag van de rector magnificus,
prof. dr. H. Brinksma
volgens besluit van het College voor Promoties
in het openbaar te verdedigen
op vrijdag 23 januari 2009 om 16.45 uur

door

Patrick Oliver Graf

geboren op 19 augustus 1979

te Aachen

Dit proefschrift is goedgekeurd door de promotor

Prof. dr. ir. L. Lefferts

En de assitant promotoren

Dr. B. L. Mojet

Dr. J.G. van Ommen

Contents

Inhoudsopgave

Summary		1
Samenvatting		5
Chapter 1	Introduction	11
Chapter 2	Comparative study of steam reforming of methane, ethane and ethylene on Pt, Rh and Pd supported on yttrium-stabilized zirconia	35
Chapter 3	Influence of potassium on the competition between methane and ethane in steam reforming over PtYSZ	57
Chapter 4	The effect of potassium addition to Pt supported on YSZ on steam reforming of mixtures of methane and ethane	77
Chapter 5	Reactive separation of ethylene from the effluent gas of methane oxidative coupling via alkylation of benzene to ethylbenzene on ZSM-5	101
Chapter 6	New insights in the water gas shift mechanism on Pt/ZrO₂: the role of hydroxyl groups elucidated	121
Chapter 7	Conclusions	141
Dankwoord		153
Publications		157
Curriculum Vitae		159

Summary

Methane, which is the principal component of natural gas reserves, is currently being used for home and industrial heating and for the generation of electrical power. In many aspects methane is an ideal fuel because of its availability in most populated centres, its ease of purification and the fact that it has the largest heat of combustion compared to the amount of CO₂ formed, among all hydrocarbons. On the other hand, methane is an under-utilised resource for chemicals and liquid fuels. Known resources of natural gas are enormous and rival those of liquid petroleum. Moreover, the known reserves of methane are increasing more rapidly than those of liquid petroleum.

Large amounts of methane are found in regions that are located far away from industrial complexes and often methane is found off shore. This means its transportation is uneconomical or even impossible. Transportation problems and the increasing oil price have led to world-wide efforts for directly converting methane into easy transportable value added products, such as ethylene (feedstock for petrochemicals), aromatics and liquid hydrocarbon fuels. The main goal of the work described in this thesis was the development of an auto thermal process, combining the exothermic oxidative coupling of methane (1) and highly exothermic combustion (side)reactions (2) with the endothermic processes of methane steam reforming (3) and methane dry reforming (4). The desired products are ethylene and synthesis gas.

Summary



The research discussed in this thesis and the parallel work by Tymen Tiemersma evaluated the possibilities of combining the oxidative coupling and reforming of methane in one multifunctional reactor. Several aspects related to catalyst and reactor development were investigated and are described in the two PhD theses.

Chapter 2 discusses a comparative study of methane, ethane and ethylene steam reforming on Pt, Rh and Pd on YSZ (yttrium-stabilized zirconia). The intention was to develop a methane selective steam reforming catalyst, showing low reactivity towards ethane and ethylene. Both reactivity and composition of products varied depending on the reforming catalyst. The order of activity of separate hydrocarbons on Rh was $\text{C}_2\text{H}_6 > \text{C}_2\text{H}_4 > \text{CH}_4$. On Pt, methane reacted faster than the C2 hydrocarbons: $\text{CH}_4 > \text{C}_2\text{H}_6 \approx \text{C}_2\text{H}_4$. Concerning the target process of methane coupling combined with reforming, Pt is considered the most promising metal because C2 hydrocarbons are converted less than methane. Additionally, Pt/YSZ was the most stable catalyst. On Pt/YSZ, the steam reforming reactions resulted in synthesis gas exclusively. It was shown that on Rh/YSZ, additionally to synthesis gas, methane was formed during steam reforming of ethane on Rh/YSZ. Hydrogenolysis of ethane occurred on this catalyst as a consecutive reaction, converting hydrogen produced in ethane steam reforming and unconverted ethane *via* hydrogenolysis to methane. This showed that effective steam reforming of higher hydrocarbons can only be achieved when the activity for hydrogenolysis is limited, avoiding production of methane.

Chapter 3 and 4 discuss the potassium modification of Pt supported on Yttrium stabilized zirconia. Reforming experiments with mixtures of methane/ethylene showed that preferential conversion of ethylene occurred on PtYSZ. It was also found that in methane/ethane mixtures, methane and ethane competed for active sites on Pt. It was found that ethane provides a high surface coverage of C_xH_y fragments and that

in mixtures of methane and ethane on PtYSZ, water activation is the rate limiting step. The addition of potassium to PtYSZ resulted in a weaker adsorption of methane and ethane on the Pt surface, indicated by weakened adsorption of CO in FT-IR TPD on Pt4K700. With potassium addition the hydrocarbon activation on Pt became rate determining for mixtures of methane and ethane, induced by low surface coverage of methane and ethane in this case. As a result, competition effects of methane and ethane were diminished on potassium modified PtYSZ, enabling simultaneous conversion of methane and ethane. Unfortunately, ethane conversion is not suppressed by the addition of potassium. A catalyst that clearly suppresses ethane conversion would be needed to make the overall concept of oxidative coupling combined with steam reforming applicable in one reactor compartment. In conclusion, it can be said that it is unlikely that a methane selective catalyst for the steam reforming process can be developed.

Chapter 5 discusses the separation of ethylene from the effluent gas of oxidative coupling, which has been a challenging issue for several years. Separation of ethylene is necessary between oxidative coupling and reforming processes to avoid ethylene conversion to synthesis gas in the steam reforming process. Reactive separation of ethylene, via alkylation of benzene to ethylbenzene (EB) is a promising option in comparison to earlier proposed concepts like cryogenic distillation. Ethylene was successfully converted to the useful chemical intermediate ethylbenzene using ZSM-5. Yields of EB up to 90% were found at above 95% conversion and more than 90% selectivity at 360°C. None of the additional components present in the effluent gas of oxidative coupling (CO, CO₂, CH₄, C₂H₆ and H₂O) influences activity or selectivity of the alkylation catalyst. Stability of ZSM-5 is also not influenced by the added components, with the exception of water, which even increases stability.

The activation of water on zirconia was investigated in Chapter 6, using water gas shift as a model reaction. The water gas shift reaction converts water and CO to CO₂ and hydrogen. It was shown that water induces the presence of two types of hydroxyl groups on monoclinic zirconia: mono- and multi-coordinated hydroxyls. Both types are active in the water gas shift mechanism, but they have different functionalities, as demonstrated on a PtZrO₂ catalyst. Mono coordinated hydroxyls are involved in reaction with CO to the intermediate formate, while multi coordinated hydroxyls play

Summary

a role in formate decomposition. Platinum was not necessary for formate formation and is suggested only to play a role in formate decomposition/product formation. The reaction products, CO₂ and H₂ were formed on Pt/ZrO₂ when subjected to CO, even in the absence of water. However, without water product formation was temporary. Subsequent treatment with water regenerated the hydroxyls on the ZrO₂ support. Continuous production of CO₂ and H₂ was observed in presence of water. These observations led to the conclusion that the role of water in the process is to regenerate the catalyst and avoid depletion of hydroxyl groups. The mechanistic insights gained in this study provide new possibilities to improve water gas shift catalysts by optimizing the availability of mono- and multi-coordinated groups on the support.

In chapter 7, results from previous chapters are summarized and translated into ideas for possible reactor concepts for the combined process of oxidative coupling and reforming of methane. Because of the high reforming activity of ethane and ethylene, contact between C₂ hydrocarbons and the reforming catalyst should be avoided. This led to two proposed concepts for future research: The first concept combines oxidative coupling and reforming in structured spherical catalyst particles, consisting of an outer layer of oxidative coupling catalyst and a core of a reforming catalyst. Essential challenges in this concept are optimising the diffusion of methane and steam to the center of the particle and limiting the combustion of ethylene on the oxidative coupling catalyst in the last part of the reactor. The second concept combines oxidative coupling and reforming in different reactor compartments, still facilitating heat exchange between both processes. After oxidative coupling, reactive separation of ethylene by alkylation with benzene is performed. The remaining mixture is fed to the reforming compartment of the reactor, yielding synthesis gas. The total process will convert methane, oxygen and benzene to synthesis gas and ethylbenzene. Efficient heat exchange between reactant and product streams is needed to make this concept feasible. Experimental demonstration of both concepts offers a challenging task for future research.

Samenvatting

Methaan, de hoofdcomponent in aardgas, wordt momenteel vooral gebruikt voor verwarming in particuliere en industriële toepassingen en voor het opwekken van elektriciteit. Methaan is een ideale brandstof door beschikbaarheid in dicht bevolkte gebieden, door de eenvoudige zuivering en de hoge verbrandingswaarde vergeleken bij de CO₂ uitstoot. Methaan zou in de toekomst een belangrijke grondstof voor chemicaliën en vloeibare brandstoffen kunnen vormen. De beschikbare aardgasreserves zijn enorm en vergelijkbaar met de ruwe olie reserves. Sterker nog, steeds meer nieuwe aardgas voorraden worden ontdekt, terwijl voor ruwe olie de prijs stijgt en de beschikbaarheid niet toeneemt.

Grote hoeveelheden additioneel methaan zijn te vinden in ver afgelegen gebieden, op grote afstand van industriële complexen en vaak zelfs in zeegebieden. Dit betekent dat transport van aardgas vaak niet economisch rendabel of zelfs onmogelijk is. Deze transportproblemen hebben geleid tot wereldwijde onderzoeksinitiatieven om aardgas om te zetten naar hoogwaardige en efficiënt te vervoeren producten, bijvoorbeeld ethaan, aromatische verbindingen en vloeibare brandstoffen. De doelstelling van het werk in dit proefschrift was de ontwikkeling van een autotherm en dus energie efficiënt proces, waarbij de exotherme oxidatieve koppeling van methaan (1) en de zeer exotherme verbrandingsreacties (2) gecombineerd worden met de endotherme steam (3) en dry (4) reforming van methaan. De gewenste producten hierbij zijn ethaan en synthesegas (H₂ + CO).

Samenvatting



In samenwerking met Tymen Tiemersma zijn in dit project de mogelijkheden tot combinatie van oxidatieve koppeling en reforming van methaan in een multifunctionele reactor geëvalueerd. Hierbij stond de ontwikkeling van efficiënte katalysatoren voor beide processen en het ontwerpen van een geschikt reactorconcept centraal.

In hoofdstuk 2 wordt de reforming activiteit van methaan, ethaan en etheen op Pt, Rh en Pd katalysatoren vergeleken. Alle metalen werden op een drager van yttrium-gestabiliseerd zirconia (YSZ) getest. De vraagstelling hierbij was of een katalysator gevonden kan worden die selectief methaan omzet en tegelijkertijd een lage reactiviteit t.o.v. ethaan en etheen vertoont. Afhankelijk van de gebruikte katalysator zijn grote verschillen tussen de metalen gevonden, zowel op het gebied van reactiviteit als wat betreft productsamenstelling. The activiteit van de separaat gevoede koolwaterstoffen in steam reforming op RhYSZ was $\text{C}_2\text{H}_6 > \text{C}_2\text{H}_4 > \text{CH}_4$. Op PtYSZ reageerde methaan sneller dan de C2-koolwaterstoffen: $\text{CH}_4 > \text{C}_2\text{H}_6 \approx \text{C}_2\text{H}_4$. Daarnaast was PtYSZ de meest stabiele katalysator in de testen. Om deze redenen werd Pt geselecteerd als meest geschikte metaal voor verder onderzoek. Opvallend was de vorming van methaan naast synthese gas op RhYSZ bij steam reforming van ethaan, terwijl op PtYSZ uitsluitend synthese gas geproduceerd werd. De methaanvorming op RhYSZ werd toegeschreven aan hydrogenolyse van ethaan, waarbij ethaan met in steam reforming geproduceerde waterstof wordt omgezet naar methaan. Dit laat zien dat de hydrogenolyse activiteit van een steam reforming katalysator beperkt moet worden om te voorkomen dat ethaan naar methaan kan terugreageren.

In hoofdstuk 3 en 4 wordt kalium modificatie van PtYSZ besproken. Op ongemodificeerd PtYSZ bleek in mengsels van etheen/methaan voornamelijk etheen

omgezet te worden. In mengsels van ethaan/methaan werd competitieve conversie tussen ethaan en methaan gevonden. De toevoeging van kalium aan PtYSZ had een significant effect op de steam reforming van ethaan/methaan mengsels. De adsorptiesterkte van de koolwaterstoffen werd verzwakt. Door de resulterende lage bedekkingsgraden van methaan en ethaan werd het competitie-effect in steam reforming opgeheven. Hierdoor werd gelijktijdige omzetting van beide koolwaterstoffen mogelijk. De conversie van ethaan werd echter niet onderdrukt door de toevoeging van kalium aan de katalysator. Een katalysator met duidelijke onderdrukking van de ethaanconversie zou voor de toepassing van het totaalconcept van oxidatieve koppeling en steam reforming in een reactorbuis nodig zijn. Uit de uitgevoerde experimenten werd de conclusie getrokken dat het onwaarschijnlijk is dat een compleet methaan selectieve reforming katalysator ontwikkeld kan worden.

In hoofdstuk 5 wordt de scheiding van etheen uit het productmengsel van de oxidatieve koppeling onderzocht, welke al verschillende jaren een grote uitdaging vormt. Afscheiding van etheen is noodzakelijk tussen oxidatieve koppeling en reforming, om etheennomzetting naar synthesegas in het reforming proces te voorkomen. Voor deze scheiding is alkylering van benzeen met etheen naar ethylbenzeen een veelbelovende optie, vergeleken met bijvoorbeeld de eerder onderzochte cryogene destillatie. Experimenteel werd etheen over een ZSM-5 zeoliet omgezet naar ethylbenzeen met een opbrengst tot 90%, waarbij de selectiviteit en conversie respectievelijk boven de 95% en 90% lagen. Methaan en ethaan in de voeding werden hierbij niet omgezet en kunnen voor steam reforming gebruikt worden in het totaalproces. Alle componenten in de productstroom van oxidatieve koppeling (CO_2 , CO en water, ethaan en methaan) hadden geen invloed op de selectiviteit en activiteit van ZSM-5. De componenten hadden ook geen invloed op de stabiliteit, met uitzondering van water dat zelfs voor een verhoogde stabiliteit van de katalysator zorgde.

De activering van water op zirconia wordt in hoofdstuk 6 besproken aan de hand van de water gas shift reactie, die CO en water omzet naar waterstof en CO_2 . Water kan op zirconia twee types hydroxyl groepen vormen: mono en multi gecoördineerde hydroxylgroepen. Beide zijn actief in het water gas shift proces maar hebben verschillende functies in het mechanisme, zoals werd aangetoond op een PtZrO_2

Samenvatting

katalysator. De mono groepen op zirconia reageren met CO naar een formaatcomplex, dat als intermediair van de reactie beschouwd kan worden. Multi gecoördineerde hydroxylgroepen zijn betrokken bij de ontleding van het formaat complex. Er werd aangetoond dat Pt niet nodig is bij het vormen van het formaat maar wel een belangrijke rol speelt bij de formaatontleding naar de gasfase producten H₂ en CO₂. Op PtZrO₂ kon door pulsen van CO de reactie tijdelijk plaatsvinden, zelfs in afwezigheid van water. De tijdelijke productie van waterstof en CO₂ stopte met de uitputting van de hydroxyl groepen op het zirconia oppervlak. Omdat na waterbehandeling weer tijdelijke reactie mogelijk was en de reactie in aanwezigheid van water continu verliep, werd geconcludeerd dat de rol van het water in het mechanisme bestaat uit het regenereren van hydroxyl groepen. De nieuwe mechanistische inzichten leiden tot de conclusie dat het optimaliseren van de aanwezigheid van mono en multi gecoördineerde hydroxylgroepen essentieel is voor een goede water gas shift katalysator.

In hoofdstuk 7 worden de belangrijkste resultaten uit de vorige hoofdstukken samengevat en naar ideeën voor mogelijke reactorconcepten voor een gecombineerd proces van oxidatieve koppeling en reforming van methaan vertaald. Contact tussen ethaan en etheen met de reforming katalysator moet hierbij vermeden worden, gezien de hoge reforming activiteit van beide koolwaterstoffen. Uiteindelijk worden twee reactorconcepten gepresenteerd waarvan de haalbaarheid in verder onderzoek in detail bekeken kan worden. Het eerste concept combineert oxidatieve koppeling en reforming in een multifunctioneel katalysatordeeltje. Het deeltje is opgebouwd uit een katalysatorlaag voor oxidatieve koppeling aan de buitenkant en een reforming katalysator in de kern van het bolvormige katalysatordeeltje. Een optimale diffusie van methaan en stoom naar de reforming kern van het deeltje en de beperking van de etheen en ethaan verbranding aan de buitenkant op de oxidatieve koppelingskatalysator in de het laatste deel van het katalysatorbed zijn de belangrijkste uitdagingen in dit concept. Het tweede concept combineert oxidatieve koppeling en reforming in verschillende reactor compartimenten, waarbij warmte-uitwisseling tussen beide processen nog steeds voor een autotherm proces zorgt. Na de oxidatieve koppeling wordt etheen reactief uit de productstroom afgescheiden door alkylering van benzeen naar ethylbenzeen. Het resterende mengsel wordt vervolgens

naar het reforming proces geleid en omgezet naar synthesegas. Uiteindelijk worden in dit proces methaan, benzeen en zuurstof naar synthesegas en ethylbenzeen omgezet. Efficiënte warmteoverdracht tussen reactant- en productstromen vormt de grootste uitdaging in het tweede concept. De experimentele demonstratie van beide concepten biedt interessante mogelijkheden voor toekomstig onderzoek.

Chapter 1

Introduction

1.1 Introduction

Methane, which is the principal component of natural gas reserves, is currently being used for home and industrial heating and for the generation of electrical power. In many aspects methane is an ideal fuel because of the existence of distribution systems in most populated centres, its ease of purification and the fact that it has the largest heat of combustion compared to the amount of CO₂ formed, among all hydrocarbons. On the other hand, methane is an under-utilised resource for chemicals and liquid fuels. Known resources of natural gas are enormous and rival those of liquid petroleum. Moreover, the known reserves of methane are increasing more rapidly than those of liquid petroleum and it is expected that this trend will extend into the 21st century [1].

Large amounts of methane are found in regions that are located far away from industrial complexes and often methane is found off shore. This means its transportation is uneconomical or even impossible. Parts of the methane obtained, is re-injected, flared or vented at the moment, which is waste of hydrocarbon resource. Both methane and CO₂ are greenhouse gases responsible for global warming and more strict regulations about letting out or flaring are expected in the future.

These transportation and environmental problems and the increasing oil price have led to world-wide efforts for directly converting methane into easy transportable value

added products, such as ethylene (feedstock for petrochemicals), aromatics and liquid hydrocarbon fuels.

Direct and indirect methods are known for methane valorisation. The indirect routes are based on partial oxidation. The most used reaction is the highly energy consuming steam reforming to produce synthesis gas (CO and H₂). The synthesis gas is converted either to liquid fuels through Fischer Tropsch or to methanol and subsequently to olefins or gasoline. These two or three steps processes require high investments in production plants. Considerable efforts have been made for many years to develop direct conversion reactions producing partially oxidised compounds (mainly methanol) and products derived from oxidative coupling of methane (ethane and ethylene).

The main goal of the work described in this thesis is the development of an auto thermal process, combining the exothermic oxidative coupling of methane and highly exothermic combustion (side)reactions with the endothermic processes of methane steam reforming and methane dry reforming in a new multifunctional reactor. The intention is to convert the combustion products of the OCM reaction, e.g. CO₂ and H₂O, to CO and hydrogen via reforming reactions with remaining methane. By integrated catalyst and reactor development the activity for the oxidative coupling and reforming will be optimised. In this first chapter a literature overview of oxidative coupling and reforming of methane and higher hydrocarbons will be given. Topics like catalysts formulations and process conditions will be discussed.

1.2 Oxidative coupling of methane

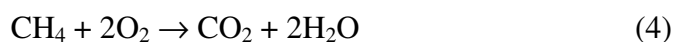
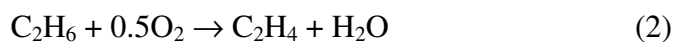
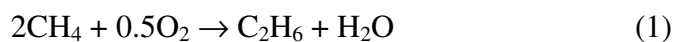
1.2.1 Introduction and challenges

The major difficulty of oxidative coupling of methane (OCM) is to overcome the energy barrier of the strong first C-H bond in methane (435 kJ mol^{-1}). This implies that coupling reactions have to be carried out at high temperatures (more than 700°C), leading to the following challenges [2, 3]:

- Occurrence of homogeneous gas phase reactions, giving a complex pattern of parallel reactions
- Kinetic stabilization of the products could be a problem, because of consecutive reactions. As ethylene is more reactive than methane high selectivity can only be obtained at low conversions
- Presence of mass transfer limitations can influence the catalytic reactions
- The process requires a catalyst with high thermal and hydrothermal stability. The evaporation of volatile/low melting catalytically active components or chemical interactions with the support may lead to catalyst deactivation.
- When a high CH_4/O_2 ratio is used in the process, the selectivity for C_2 -hydrocarbons is high but the methane conversion is low. At lower CH_4/O_2 ratios, a lower selectivity is obtained. This also leads to a more exothermic and hazardous process, due to occurrence of combustion reactions at a larger extent. Also the process is less efficient, due to low selectivity
- The low ethylene concentrations in the product stream lead to high separation cost. Cryogenic distillation has been considered for separation, operating around -160°C [4, 5]. This implies a large temperature difference between oxidative coupling and separation.
- Due to low yield a large methane recycle will be required in the oxidative coupling process

1.2.2 Reaction mechanism

In the OCM process the following reactions occur simultaneously [3]:



The reactions indicate that in a first step the coupling to ethane takes place (1). Ethylene can be produced by dehydrogenation of ethane (3). Oxidative dehydrogenation to ethylene is also possible (reaction 2), but occurs at a much slower rate [4]. Reactions (4) and (5) show the side combustion reactions of methane, while equation (6) indicates combustion reactions of the products. It should be noted that the oxidative coupling reactions (1) & (2) are slightly exothermic and the combustion reactions (3), (4) & (5) are highly exothermic, leading to excessive heat formation in the oxidative coupling process.

Even if the gas-phase reactions play an important role in the overall process, the presence of a catalyst is essential. According to different sources [2, 3, 6, 7] methane dehydrogenates on the catalyst surface and produces methyl radicals, which can react on the surface or in the gas phase. The abstraction of a hydrogen atom is caused by an oxygen ion present on the surface of the catalyst. Next to the efficient formation of methyl radicals, coupling of the radicals is also essential. It is generally accepted that coupling of $\text{CH}_3\bullet$ -radicals takes place in gas phase [3]. Several catalyst systems and reactor configurations have been used and a short overview will be given in the next paragraphs.

1.2.3 Performance of various catalysts

A large number of catalysts with or without support have been evaluated for their performance in the OCM process with the objective of developing a highly selective, active and stable catalyst [1-3, 6, 8-26]. Comparison of catalysts is not straight

forward as different conditions and reactor configurations were used in the different studies presented. Among experimental conditions temperature, feed compositions and space velocity (contact time) were the main variables. Furthermore fixed bed reactors of different sizes (ranging from micro reactors to scale up tubes) and various other reactor types (different membrane reactors, solid electrolyte or gas recycle) were used. In Table 1.1 gives an overview of the best catalysts, concerning C2(+)-yield, selectivity, stability and experimental conditions:

The Mn/Na₂WO₄/SiO₂ system was an excellent catalyst in terms of both stability and activity. It was also called the most effective catalyst in a review by Lunsford [27]. Other systems that have approximately the same activity show stability problems or stability has not been investigated.

Table 1.1: Comparison of the best OCM catalysts: conditions, performance and stability

catalyst	Temp (°C)	Ratio CH₄:O₂:He	C2+-yield (%)	Selectivity (%)	Stability (h)
Eu ₂ O ₃ [12]	725	6.7:1:0	17.7	72.4	?
Ce/La ₂ O ₃ [12]	775	4-5:1:0	22.3	66.0	?
Li/MgO [3]	750	4:1:0	+/- 19	65	up to 100
La-Ce/MgO [12]	850	4-5:1:0	16.1	72.4	high*
Mn/Na ₂ WO ₄ /SiO ₂ [6, 16, 21-23]	800/850	various	20 – 26	80	>100
Mn/K ₂ WO ₄ /SiO ₂ [16]	800	3.2:1:0	18.5	62.4	>5
Mn/Na ₂ WO ₄ /MgO [6, 22]	800	7.4:1:0	20	75	40
Na/S/P/Zr/Mn [14, 15]	790	3:1:0	27.8	73.5	>10

*stability was only reported for La/MgO and >100 hours

The multi component system by Huang [13, 14] shows questionable stability as experiments were only carried out for about 10 hours. The maximum yield of 27.8% in single pass packed bed operation approaches the theoretical limit of 28% as calculated by San Su et al. [7]. They optimized the yield to ethylene in the oxidative coupling reaction by setting optimal parameters for an elementary step surface mechanism combined with gas phase rate constants and thermodynamic property data compiled by Mims [28]. However, the maximum yield of 28% has already been exceeded in a membrane reactor by Akin et al. [8, 9].

A temperature of about 800°C is needed to reach the best results for most of the catalysts. Generally diluting the reaction mixture with an inert gas (He) leads to better results as homogeneous gas phase reactions are reduced.

1.2.4 Process improvements in oxidative coupling

The results mentioned in the last paragraph were obtained with single-pass flow reactors. Next to the development of various catalyst systems the following process modifications have been made in order to overcome the limitations of OCM.

Distribution of O₂ feed

Per-pass methane conversion and C₂ yield are limited because of the limit for the O₂ concentration in the feed, due to explosion limits of CH₄/O₂ mixture. A second point is that in general high oxygen partial pressure promotes over-oxidation. With increasing O₂ concentration methane conversion increases but the selectivity to C₂-hydrocarbons decreases, making the process more exothermic and hence more hazardous. Using a membrane to distribute the oxygen feed could provide low oxygen concentration over the entire reactor length and limit combustion reactions, leading to lower exothermicity and higher C₂-yield of the oxidative coupling process.

Akin et al. [8, 9] used a catalytically active fluorite structured Bi_{1.5}Y_{0.3}Sm_{0.2}O_{3-δ} (BYS) membrane tube. In their reactor the oxygen is fed on one side of the membrane and methane on the other. Only oxygen can permeate through the membrane via ionic conductivity and reaction thus takes place on the surface exposed to methane. The main advantage of this membrane reactor is avoiding direct contact between the reactants, leading to minimization of gas-phase complete oxidation reactions. Also with an ion conducting membrane the expensive generation of pure oxygen could be avoided: only oxygen can be transported through the membrane and air can be used as oxygen source. With this concept, up to 30% C₂-yield was accomplished at 900°C, more than ever reported in any other single pass reactor. The selectivity and methane conversion were 60% and 50%, respectively. This was almost twice as high as obtained in co-feed experiments in the same reactor. High yields were found especially at low methane partial pressures. The system showed stable activity for 5 days at 900°C.

Kao et al. [16] used porous ceramic membranes (alumina or zirconia) in their reactor. In this case a separate catalyst is used for the OCM reaction and the membrane only acts as oxygen supply. Kao et al. chose the Li/MgO system as OCM catalyst. At 750°C a maximum yield of 30% was reached at 53% C₂ selectivity, compared to 20.7% yield and 52.5% selectivity in a fixed bed reactor under the same conditions. Both, use of atmospheric air and lowering the membrane permeability improved the performance, showing that a lower oxygen flux leads to higher yield and selectivity. Haag et al. [29] used ionic oxygen conducting membranes, demonstrating that oxygen supply rates of the membrane and consumption in oxidative coupling have to be balanced. It was also stated that more active catalysts for oxidative coupling have to be developed to reach the optimal potential of the ionic conducting membrane reactor.

Alternative reactor concepts

Makri et al. [19] investigated the OCM process, using a gas recycle reactor with Mn/Na₂WO₄/SiO₂ as catalyst. To separate ethylene, Linde 5A molecular sieve pellets were placed after the reactor. This material was found to be effective in trapping of ethylene and only partially trapped ethane. Methane and CO were not trapped at all. The combustion products CO₂ and H₂O were also stored in the trap. Trapping takes place at room temperature and reactions at 770°C-850°C, requiring a lot of cooling and heating. The products can be collected from the trap by heating to 250°C. Continuous operation is possible by switching between two parallel traps. C₂ yield values up to 53% were reached. Tonkovich et al. [30, 31] used a separative chemical reactor that simulated a countercurrent moving bed. High C₂ selectivity (80%) and methane conversion (65%) could be obtained with a Sm₂O₃ catalyst at 725°C, leading to around 50% C₂ yield.

Coupling of exothermic and endothermic reactions

A promising coupling concept of exothermic and endothermic reactions was presented by Czechowicz et al. [10]. In a serial process, oxidative coupling was carried out in the first part of the reactor over a Li/MgO-catalyst. After the catalyst bed naphtha was introduced. In the second part of the reactor (containing no catalyst) the endothermic pyrolysis of naphtha took place. It was demonstrated that such a

process could be realized, always giving an increase in the C₂H₄ yield as compared to both single processes.

Direct conversion of ethylene into less volatile products

Choudhary et al. [3] reported two possible processes to overcome separation problems with ethylene by converting it to value-added products. Both options show only a low methane conversion and still recycling of methane is required.

- Two step process for methane to gasoline conversion. In a first step the catalytic OCM is performed. The second step consists of conversion of ethylene into LPG (C₃-C₄ hydrocarbons) and gasoline (C₅-C₁₀ hydrocarbons) with the use of a bifunctional pentasil zeolite catalyst. Up to 90% ethylene conversion and 80% aromatic selectivity were obtained with the diluted ethylene stream. The mixture produced in oxidative coupling can directly be used in the second step, avoiding separation steps between the two processes [3, 32].
- Multi-step process for methane to ethylene oxide conversion. First methane coupling to ethylene is carried out. Afterwards selective oxidation of carbon monoxide to carbon dioxide and separation of the traces of CO from the resulting gas stream is performed. In the last step, vapor phase oxidation of the ethylene present in the product stream of step 2 is carried out, producing ethylene oxide over a supported silver catalyst. This process was found to be technically feasible.

1.2.5 Conclusions oxidative coupling

Efficient production of ethylene through oxidative coupling requires a selective catalyst and optimal process operation and conditions. It was found that the Mn/Na₂WO₄/SiO₂ catalyst gives the highest yield for the coupling process. Application of a ceramic membrane reactor in combination with this catalyst seems a promising option, but a thorough comparison between membrane and co-feed with the Mn/Na₂WO₄/SiO₂ catalyst is needed. Tymen Tiemersma, a second PhD student involved in the current project, will investigate the oxidative coupling reaction in both co-feed and membrane operation. His results are described in his PhD thesis (Tymen Tiemersma, Fundamentals of Chemical Reaction Engineering, University of Twente). The most important results about the oxidative coupling process were also used in this

thesis and the most relevant findings are included in the conclusions of this thesis in chapter 7.

1.3 Steam and dry reforming of methane

1.3.1 Introduction

As mentioned in the previous paragraph, OCM is always accompanied by highly exothermic side combustion reactions producing CO₂ and H₂O. The thermal energy and side products can be used for the endothermic steam and dry reforming reactions of methane [33, 34]:



The steam reforming reaction (7) creates synthesis gas with a H₂:CO ratio of 3:1 and in the dry reforming reaction (8) a H₂:CO ratio of 1 is produced. Both reactions take place simultaneously and thus a H₂:CO ratio between 1 and 3 will be achieved. Applications of synthesis gas include Fischer Tropsch, CH₃OH, CH₃COOH or NH₃ synthesis or iron ore reduction. Both steam reforming reactions are highly endothermic and are carried out typically above 700°C, where the products are thermodynamically favored. Under reforming conditions the water gas shift reaction also occurs.



The products of steam reforming are dictated by thermodynamics of reaction (7), (8) and (9) [35]. In presence of oxygen the catalytic partial oxidation of methane is also possible (10):



In the next paragraphs, the reaction mechanism of the methane reforming process and the activity of several catalysts on various supports will be discussed. Furthermore catalyst deactivation and reforming activity for higher alkanes will be discussed.

1.3.2 Reaction mechanism

Wei et al. [36] presented a comprehensive reaction scheme for the reforming process with both CO₂ and H₂O, that also includes water gas shift reaction. The mechanism is shown in Figure 1.1. It was stated that this mechanism is applicable to all metal

catalysts. As also reported by Dicks [37], it is stated that the rate limiting step in the process is the formation of radicals from methane. This means that CH_4 decomposes to chemisorbed carbon (C^*) via sequential elementary H-abstraction steps. As abstraction of the first hydrogen atom seems to have the highest activation energy, the surface will be mainly occupied by C^* and have low CH_x coverages. The chemisorbed carbon is then removed by reactions with CO_2 and H_2O .

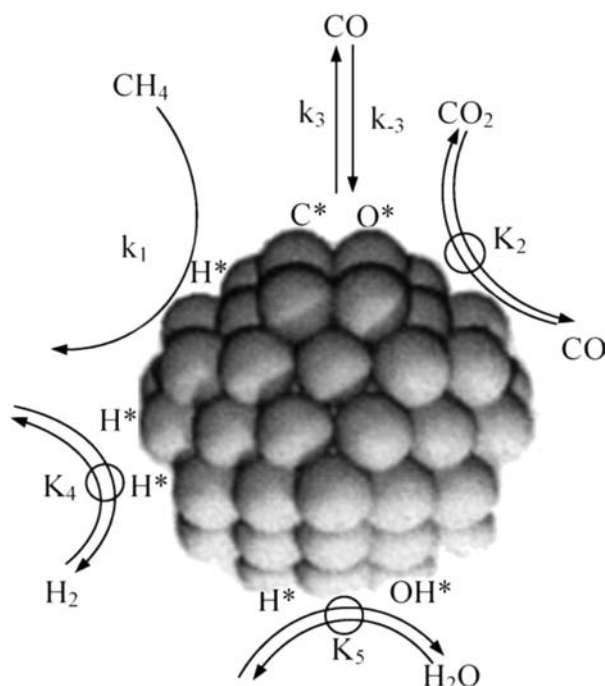


Figure 1.1: Reaction mechanism for Methane steam reforming, dry reforming and water gas shift reaction. Hydrogen, water and carbon dioxide steps are on equilibrium. Carbon monoxide dissociation is reversible and methane activation rate determining. [36]-Reproduced by permission of The Royal Society of Chemistry

In isotopic experiments with D_2 instead of H_2 and $^{13}\text{CH}_4$ instead of $^{12}\text{CH}_4$ it was shown that steps involving H_2O and CO_2 were much faster than kinetically relevant C-H bond activation steps. For example dissociation of CO_2 to CO and oxygen occurred in both directions many times during each CH_4 chemical conversion turnover. The same was found for the H_2O activation steps, meaning that the water gas shift reaction would always be equilibrated during reforming [35]. In the overall process reactions with water, carbon dioxide and hydrogen are at equilibrium. The

dissociation of CO is determined by kinetics instead of thermodynamics and the hydrogen abstraction from methane determines the reaction progress.

1.3.3 Catalysts used for reforming reactions

Industrial practice in reforming reactions relies on Ni-catalysts [38], because of cost and availability concerns about noble metals. Ni-catalysts however show a tendency to deactivate. Two potential causes of deactivation exist [39]: coke deposition and sintering of the metal particles.

The relative activities of different metals for steam and dry reforming have been compared by several authors [33, 40-43]. Hegarty et al. [33] compared 1wt% of Co, Cu, Fe, Ni, Pd and Pt supported on zirconia for steam reforming between 400°C and 800°C. Ni showed much less activity compared to Pt or Pd. Low activity and significant deactivation due to carbon deposition was found on Fe, Cu and Co. Pt/ZrO₂ was not only the most active but also the most stable catalyst. Rostrup Nielsen [42] and Quin [40] found Rh and Ru as the most active metals in steam reforming. Some main group metals were also investigated as alternatives for Ni or noble metal catalysts [44-46], but all materials showed relatively low activity.

1.3.4 Catalyst deactivation

The most common deactivation of steam reforming catalysts occurs by carbon deposition. Coke originates mainly from two reactions: methane decomposition to C and H₂ and carbon monoxide disproportionation via the Boudouard reaction (11). The former is endothermic and favored at high temperatures and low pressures, while the latter is exothermic and favored at low temperatures and high pressures. Noble metals however were found resistant to coking and appeared stable for long periods.



The role of the support was tested by Nagaoka et al. [39], O'Connor et al. [47] and Bitter et al. [48, 49]. Nagaoka compared Pt on Al₂O₃ and Pt on ZrO₂ in methane dry reforming. Pt/ZrO₂ was found to be stable for more than 500 hours at 900 K, while Pt on alumina deactivated rapidly under the same conditions. It was stated that the stability of Pt catalysts strongly depends on the nature of the support and its ability to form carbonates, leading to carbon deposition. The deactivation of Pt on alumina was

mainly ascribed to coke formation. High temperature regeneration with CO₂ was possible, ruling out sintering of Pt as the cause of deactivation. Coke can be removed by the reverse Boudouard reaction (11), as high temperature thermodynamically favors the CO-side.

It was stated that coke formation on Pt/alumina occurred on Pt and on Lewis acid sites of the support through decomposition of CH₄, as also stated by Wei [36]. This coke can be removed with CO₂ at high temperatures. Coke on Pt supported on ZrO₂ was considered more reactive than on alumina. Additionally, CH₄ decomposition during dry reforming was slower on the zirconia support than on alumina [39]. In case of zirconia, this leads to a balanced combination of carbon formation on Pt and its oxidation by activated CO₂. Coke hardly accumulates on Pt/ZrO₂ and thus the material is a stable catalyst in CO₂ reforming. O' Connor et al. [47] and Sauvet et al. [46] confirmed that noble metals deposited on ZrO₂ had a much higher stability for both reforming reactions compared to silica or alumina supported noble metals.

In the combined process of OCM and steam and dry reforming, alkali poisoning might be relevant as OCM catalysts usually contain alkali components, for example Na in the Mn/Na₂WO₄/SiO₂-system. Often potassium is added as a promoter to steam reforming catalysts, which can also lead to poisoning effects in case of too high concentrations of potassium. Effects of potassium on Ni catalysts are well described, but the effects to noble metals, e.g. Pt, in steam reforming of methane and ethane have not been reported so far.

Two effects of alkali addition are described in literature. Addition of potassium and other alkali can limit carbon formation but can also reduce catalytic activity. It is claimed that K prevents carbon formation on Ni catalysts by blocking step sites which are believed to be the nucleation sites for graphite formation [50]. In addition, potassium on Ni catalysts enhances coke gasification [51]. It was reported by Dicks et al. [37] that small amounts of potassium reduce the risk of carbon deposition by decreasing the acidity of the catalyst support.

A decreasing activity of Ni/Al₂O₃ [52] was reported in methane dry reforming with increasing potassium concentration in the catalyst. A reduction in catalytic activity by

potassium was also confirmed by Trimm [53] and Rostrup-Nielsen [41]. The activity of Ni/MgO-Al₂O₃ for methane steam reforming was reported to decrease by 85% when 1.1wt% of K was added [54]. Decreasing reforming activity by addition of potassium was also found on Rh/La-Al₂O₃ [55]. Alkali poisoning to reforming catalysts often occurs in molten carbonate fuel cells, as alkali may be transported to the reforming catalyst either by the vapor phase or by creep along the walls of the fuel cell. According to Rostrup-Nielsen [56] the poisoning effect of K₂CO₃ is much stronger than the effect of Na₂CO₃ and Li₂CO₃.

1.3.5 Reforming of higher alkanes

It is well known that higher hydrocarbons are also reactive in reforming. Trimm reports in a review that all kinds of hydrocarbons can be reformed, e.g. alkanes, olefins, aromatics and oxygenates [57]. Ethane and ethylene are produced in the OCM process and it is desired that these products are not converted to CO and H₂. Only a few studies have compared reactivity of various hydrocarbons.

Sutton et al. [58] investigated dry reforming of a gas stream containing mol percentages of H₂ (42), CO (15.5), CH₄ (5.1), CO₂ (19) and C₃H₈ (18.3) over Ni/Al (co-precipitated), Ru/Al₂O₃ and Pt/ZrO₂. A higher reactivity of propane was found compared to methane. Wang et al. [59] investigated steam reforming of methane, ethane, n-butane and some higher hydrocarbons on Pd/ceria for temperatures ranging from 620 to 770 K. The production of CO_x increased with carbon number, indicating higher reactivity for higher hydrocarbons.

Via thermochemical calculations, Sinev [35] determined that activation of light alkanes through formation of free radicals is energetically favored compared to other activation mechanisms like proton abstraction or molecular ionization. Among alkanes, methane had the highest activation energy, indicating lower reactivity compared to other alkanes.

1.3.6 Conclusions reforming processes

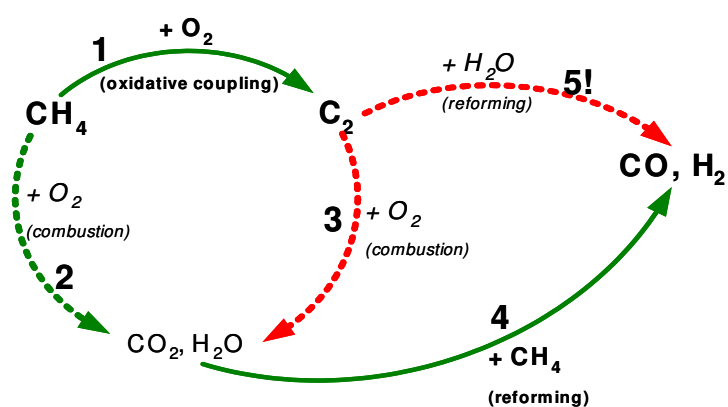
A few conclusions about the steam reforming reaction can be drawn, summarizing the data available in literature. Ni is often used but deactivation by carbon deposition is a problem. The deactivation through coke formation will be more pronounced when reforming of ethane and ethylene is included [53, 57]. Pt or Pd supported on zirconia

are promising catalysts as they showed high activity and stability. In general, catalyst activity and stability are largely dependent on the support. In the combined process of methane coupling and reforming, alkali deactivation of the reforming catalyst, released from the oxidative coupling catalyst could be a problem. Alkali deactivation is not well investigated for Pt-systems and will be discussed in this thesis.

The major challenge in the steam reforming process is the reactivity of higher hydrocarbons; reforming of higher hydrocarbons produced in the oxidative coupling reaction should be avoided. At the same time high reactivity towards methane is desired in steam reforming. Higher alkanes were found to be more reactive than methane in reforming processes for the catalysts tested until now. A more detailed approach of comparing several catalysts in their reforming activity towards methane and C₂-hydrocarbons will be part of this thesis.

1.4 Problem definition & aspects of integration

The main goal of the overall process of oxidative coupling and reforming of methane is to produce ethylene and synthesis gas (CO and H₂) in one multifunctional reactor. The possible reactions are shown in Scheme 1. Methane coupling takes place oxidatively, resulting in C₂ hydrocarbons (ethane and ethylene) and water (1). The side combustion reactions of methane (2) and C₂-hydrocarbons (3) produce water and CO₂, which can react with the remaining methane through steam or dry reforming to CO and H₂ (4). The main challenge in the reaction concept is to suppress steam/dry reforming of ethane and ethylene (5!) in order to avoid complete reaction to synthesis gas.



Scheme 1: Reactions occurring in combined process of methane coupling and steam reforming

The processes of oxidative coupling and reforming of methane can be integrated on several levels. Figure 1.2 shows several possibilities for the combination of both processes, ranging from integration on catalyst particle scale (Figure 1.2-I) to reactor scale (Figure 1.2-V). It should be noted that matching of reaction rates of oxidative coupling and reforming is required for autothermal operation.

The type of concept that can be used strongly depends on the following issues.

1. Oxidation reactions of hydrocarbons on steam reforming catalyst should be prevented, e.g. by
 - using a reforming catalyst that is not active in oxidation reactions
 - preventing exposure of the reforming catalyst to oxygen
2. Reforming activity of ethane and ethylene can convert the complete mixture to synthesis gas and should be prevented as well, e.g. by
 - limiting reforming activity of reforming catalyst towards ethane and ethylene
 - avoiding contact of ethane and ethylene with the reforming catalyst
3. The overall process combines the highly exothermic coupling and combustion reactions with the endothermic reforming, requiring optimized heat transfer between both processes. This can be achieved by
 - combining both processes in one catalyst particle or using one multifunctional catalyst and keep production and consumption of energy close to each other
 - optimizing heat transfer in separate reaction zones or reactor compartments
4. High oxygen concentration leads to unselective oxidation reactions in the OCM section, producing CO_2 and H_2O . To increase C_2 yield and minimize combustion reactions a low oxygen partial pressure is needed in the OCM section. This can be achieved by distributed feeding of oxygen.

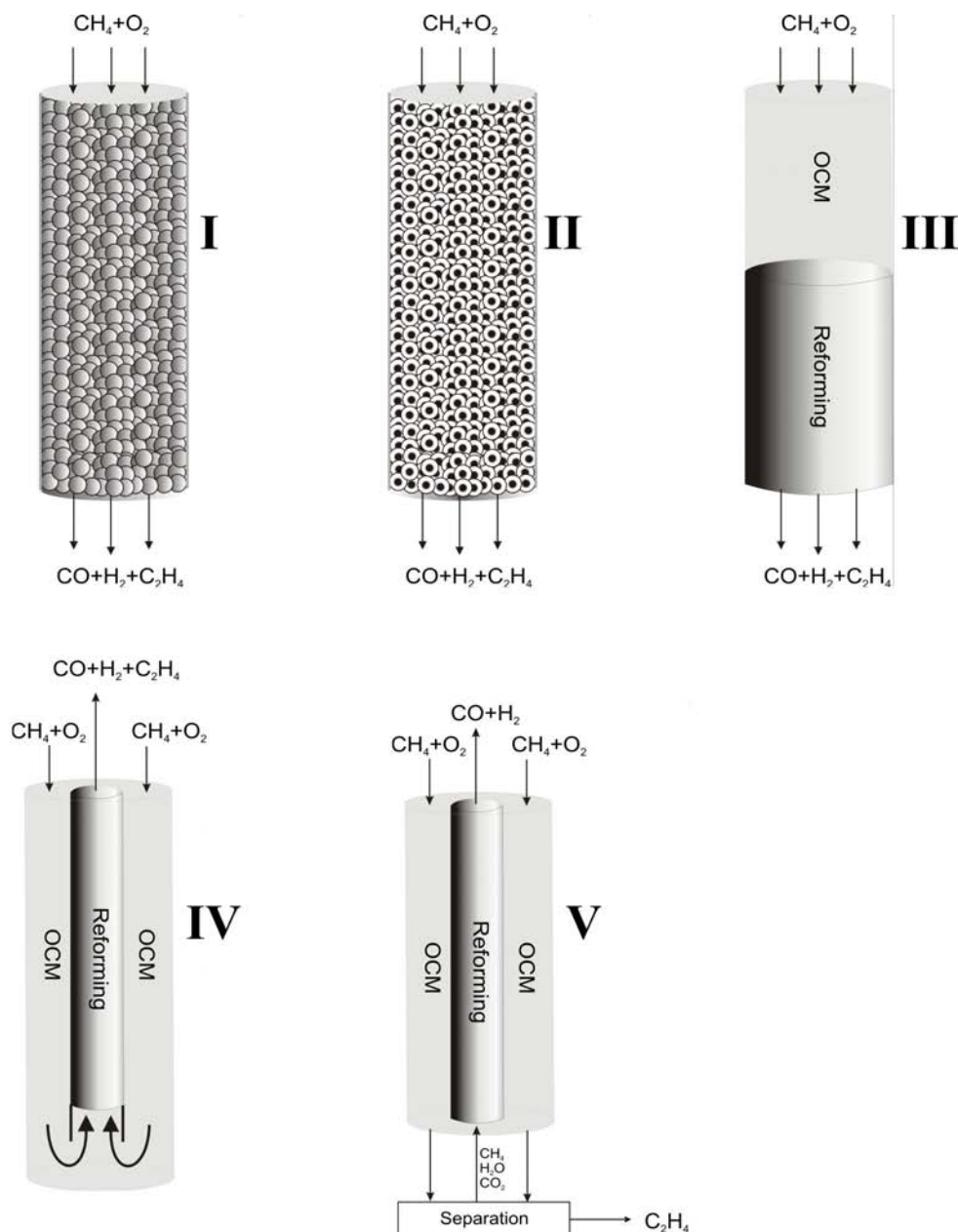


Figure 1.2: Different levels of integration of oxidative coupling and reforming of methane, ranging from particle scale (I) to reactor scale (V)

The reactor concepts shown in Figure 1.2 are shortly discussed below:

- I. Combining the processes on particle scale, means in an ideal case combining both functions in one uniform multifunctional catalyst particle (Figure 1.2-I). In this concept, combustion activity for all hydrocarbons and reforming activity of the reforming catalyst towards ethane and ethylene need to be avoided. Heat exchange is very efficient in this concept. It should be noted that reducing the

combustion activity of reforming catalysts is expected to be very difficult as reforming is performed on Ni or noble metal catalysts, that are very active in catalyzing combustion. Research in this thesis will not focus on this aspect. Therefore, reactor concepts that avoid contact between oxygen and the reforming catalyst are required.

- II. An eggshell catalyst can be applied (Figure 1.2-II) to avoid contact between oxygen and the hydrocarbons on the reforming catalyst, eliminating combustions reactions on the reforming catalyst. The oxidative coupling catalyst is placed in the shell and the reforming function in the core of the catalyst. Oxygen present in the gas phase should be consumed in the outer layer of the particle to avoid diffusion to the core. In the core, a methane selective reforming catalyst is required to avoid reforming of ethane and ethylene. This shell and core system enable excellent heat exchange between the processes, requiring support materials with good conductivity.
- III. Figure 1.2-III displays the combination of oxidative coupling and reforming in separate catalyst zones, within one reactor: a reforming zone in the center of the reactor can be combined with a catalyst zone for oxidative coupling on the outside of the reactor. Oxygen is consumed completely in the OCM section, avoiding combustion on the reforming catalyst. Reforming of ethane and ethylene still has to be avoided and efficient heat exchange between both processes is extremely difficult because of large exothermic and endothermic zones in the reactor, located far away from each other.
- IV. Figure 1.2-IV also displays the combination of oxidative coupling and reforming placed in separate sections but now in a parallel configuration, improving heat transfer between the processes. Oxygen has to be exhausted after the OCM section, avoiding combustion on the reforming catalyst. A reforming catalyst that selectively reforms methane and does not convert ethane and ethylene is required for this concept. For efficient heat exchange between both processes it is important to limit the distance between exothermic and endothermic zones, e.g. using small reactor tubes or even micro reactor systems.
- V. Figure 1.2-V displays a concept of completely separate reactor compartments for oxidative coupling and reforming. In this case, reforming of ethane and

ethylene and combustion of hydrocarbons on the reforming catalyst can be completely avoided by including separation steps between oxidative coupling and reforming. Efficient heat exchange between both processes can be achieved by limiting the distance between exothermic and endothermic zones, e.g. using small reactor tubes or micro reactor systems.

It should be noted that distributed feeding of oxygen (4) can be integrated in all presented concepts, to optimize operation of OCM reaction, increasing C₂ yield by applying low oxygen concentration over the entire reactor length. As an example, concept 1-2-V is shown with distributed oxygen feeding in Figure 1.3.

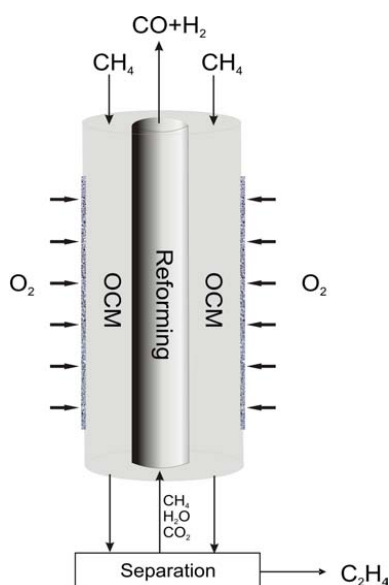


Figure 1.3: Reactor concept for combining oxidative coupling with distributed oxygen feeding with reforming; including separation of ethylene.

Research in this thesis and the parallel work by Tymen Tiemersma will focus on selection of a suitable reactor concept and catalysts for a combined process of oxidative coupling and reforming. This thesis will consist of a total of seven chapters, covering the following topics:

- Reforming competition between methane, ethane and ethylene will be the central topic of chapters 2, 3 and 4 of this thesis. The reforming of methane, ethane and ethylene on Rh, Pt and Pd will be discussed in *chapter 2*. The influence of potassium modification of Pt supported on yttrium-stabilized

zirconia (PtYSZ) on the steam reforming competition of methane and ethane will be described in *chapter 3*. The underlying mechanism of the effect of potassium to PtYSZ will be described in *chapter 4* on the basis of XRD, FT-IR CO spectroscopy and including CO TPD measurements.

- *Chapter 5* discusses a reactive separation of ethylene to ethylbenzene in the mixture obtained in oxidative coupling.
- The activation of water on oxidic supports is a highly relevant process in steam reforming reactions and not well understood until now. In *chapter 6* the activation of water on ZrO_2 will be investigated, using water gas shift as a model reaction, With FT-IR characterization of hydroxyl groups, the activation of water and the role of these hydroxyl groups in water gas shift reaction on Pt/ ZrO_2 will be investigated.
- Finally, *chapter 7* will discuss and combine results of the earlier chapters, leading to possible reactor concepts and future possibilities for the combined process of oxidative coupling and reforming of methane.

1.5 References

- [1] J.H. Lunsford, *Catalysis Today* 63 (2000) 165.
- [2] R. Spinicci, P. Marini, S. De Rossi, M. Faticanti, P. Porta, *Journal of Molecular Catalysis A-Chemical* 176 (2001) 253.
- [3] T.V. Choudhary, D.W. Goodman, *Catalysis Today* 77 (2002) 65-78.
- [4] L. Mleczko, M. Baerns, *Fuel Processing Technology* 42 (1995) 217-248.
- [5] S.N. Vereshchagin, V.K. Gupalov, L.N. Ansimov, N.A. Terekhin, L.A. Kovrigin, N.P. Kirik, E.V. Kondratenko, A.G. Anshits, *Catalysis Today* 42 (1998) 361-365.
- [6] S. Pak, P. Qiu, J.H. Lunsford, *Journal of Catalysis* 179 (1998) 222.
- [7] Z.-Y. Ma, C. Yang, W. Wei, W.-H. Li, Y.-H. Sun, *Journal of Molecular Catalysis A: Chemical* 231 (2005) 75-81.
- [8] F.T. Akin, Y.S. Lin, *Catalysis Letters* 78 (2002) 239.
- [9] F.T. Akin, Y.S. Lin, *Aiche Journal* 48 (2002) 2298.
- [10] D. Czechowicz, K. Skutil, A. Torz, M. Taniewski, *Journal of Chemical Technology and Biotechnology* 79 (2004) 182.
- [11] A.G. Dedov, A.S. Loktev, I.I. Moiseev, A. Aboukais, J.F. Lamonier, I.N. Filimonov, *Applied Catalysis A-General* 245 (2003) 209.
- [12] C. Hoogendam, 1996.
- [13] K. Huang, F.Q. Chen, D.W. Lu, *Applied Catalysis A-General* 219 (2001) 61.
- [14] K. Huang, X.L. Zhan, F.Q. Chen, D.W. Lu, *Chemical Engineering Science* 58 (2003) 81.
- [15] S.F. Ji, T.C. Xiao, S.B. Li, L.J. Chou, B. Zhang, C.Z. Xu, R.L. Hou, A.P.E. York, M.L.H. Green, *Journal of Catalysis* 220 (2003) 47.
- [16] Y.K. Kao, L. Lei, Y.S. Lin, *Catalysis Today* 82 (2003) 255.
- [17] S. Kus, M. Otremba, M. Taniewski, *Fuel* 82 (2003) 1331.
- [18] S. Kus, M. Otremba, A. Torz, M. Taniewski, *Applied Catalysis A: General* 230 (2002) 263.
- [19] M. Makri, C.G. Vayenas, *Applied Catalysis A-General* 244 (2003) 301.
- [20] A. Malekzadeh, M. Abedini, A.A. Khodadadi, M. Amini, H.K. Mishra, A.K. Dalai, *Catalysis Letters* 84 (2002) 45.
- [21] S. Pak, J.H. Lunsford, *Applied Catalysis A: General* 168 (1998) 131.
- [22] A. Palermo, J.P.H. Vazquez, A.F. Lee, M.S. Tikhov, R.M. Lambert, *Journal of Catalysis* 177 (1998) 259.
- [23] S. Ramasamy, A.R. Mohamed, S. Bhatia, *Reaction Kinetics and Catalysis Letters* 75 (2002) 353.
- [24] S. Takenaka, T. Kaburagi, I. Yamanaka, K. Otsuka, *Catalysis Today* 71 (2001) 31.
- [25] J.E. Tenelshof, H.J.M. Bouwmeester, H. Verweij, *Applied Catalysis A-General* 130 (1995) 195.
- [26] V.R. Choudhary, S.A.R. Mulla, B.S. Uphade, *Fuel* 78 (1999) 427.
- [27] J.H. Lunsford, F.J.J.G. Janssen, R.A. Van Santen, in: G.J. Hutchings (Ed.), *Environmental Catalysis*, 2000, p. 87.

- [28] C.A. Mims, R. Mauti, A.M. Dean, K.D. Rose, *J. Phys. Chem.* 98 (1994) 13357-13372.
- [29] S. Haag, A.C. van Veen, C. Mirodatos, *Catalysis Today* 127 (2007) 157-164.
- [30] A. Ray, A.L. Tonkovich, R. Aris, R.W. Carr, *Chemical Engineering Science* 45 (1990) 2431-2437.
- [31] A.L. Tonkovich, R.W. Carr, R. Aris, *Science* 262 (1993) 221-223.
- [32] V.R. Choudhary, S.A.R. Mulla, *Industrial & Engineering Chemistry Research* 36 (1997) 3520-3527.
- [33] M.E.S. Hegarty, A.M. O'Connor, J.R.H. Ross, *Catalysis Today* 42 (1998) 225.
- [34] J.R.H. Ross, A.N.J. van Keulen, M.E.S. Hegarty, K. Seshan, *Catalysis Today* 30 (1996) 193.
- [35] M.Y. Sinev, *Journal of Catalysis* 216 (2003) 468.
- [36] J.M. Wei, E. Iglesia, *Physical Chemistry Chemical Physics* 6 (2004) 3754.
- [37] A.L. Dicks, *Journal of Power Sources* 71 (1998) 111.
- [38] K.H. Hou, R. Hughes, *Chemical Engineering Journal* 82 (2001) 311.
- [39] K. Nagaoka, K. Seshan, K. Aika, J.A. Lercher, *Journal of Catalysis* 197 (2001) 34.
- [40] D. Qin, J. Lapszewicz, *Catalysis Today* 21 (1994) 551-560.
- [41] J.R. Rostrup-Nielsen, *Journal of Catalysis* 31 (1973) 173.
- [42] J.R. Rostrup-Nielsen, J.H.B. Hansen, *Journal of Catalysis* 144 (1993) 38-49.
- [43] K. Tomishige, M. Nurunnabi, K. Maruyama, K. Kunimori, *Fuel Processing Technology* 85 (2004) 1103.
- [44] A.J. Brungs, A.P.E. York, J.B. Claridge, C. Marquez-Alvarez, M.L.H. Green, *Catalysis Letters* 70 (2000) 117.
- [45] E. Ramirez-Cabrera, A. Atkinson, D. Chadwick, *Applied Catalysis B-Environmental* 47 (2004) 127.
- [46] A.L. Sauvet, J.T.S. Irvine, *Solid State Ionics* 167 (2004) 1.
- [47] A.M. O'Connor, J.R.H. Ross, *Catalysis Today* 46 (1998) 203.
- [48] J.H. Bitter, W. Hally, K. Seshan, J.G. van Ommen, J.A. Lercher, *Catalysis Today* 29 (1996) 349-353.
- [49] J.H. Bitter, K. Seshan, J.A. Lercher, *Journal of Catalysis* 171 (1997) 279.
- [50] J. Sehested, *Catalysis Today* 111 (2006) 103-110.
- [51] J.W. Snoeck, G.F. Froment, M. Fowles, *Industrial and Engineering Chemistry Research* 41 (2002) 3548-3556.
- [52] J. Juan-Juan, M.C. Roman-Martinez, M.J. Illan-Gomez, *Applied Catalysis A: General* 301 (2006) 9-15.
- [53] D.L. Trimm, *Catalysis Today* 49 (1999) 3.
- [54] M. Matsumura, C. Hirai, *Journal of Chemical Engineering of Japan* 31 (1998) 734.
- [55] S.Y. Choung, M. Ferrandon, T. Krause, *Catalysis Today* 99 (2005) 257-262.
- [56] J.R. Rostrup-Nielsen, L.J. Christiansen, *Applied Catalysis A-General* 126 (1995) 381.
- [57] D.L. Trimm, *Catalysis Today* 37 (1997) 233.
- [58] D. Sutton, S.M. Parle, J.R.H. Ross, *Fuel Processing Technology* 75 (2002) 45.

[59] X. Wang, R.J. Gorte, *Applied Catalysis A: General* 247 (2003) 157-162.

Chapter 2

Comparative study of steam reforming of methane, ethane and ethylene on Pt, Rh and Pd supported on yttrium-stabilized zirconia

Abstract

Steam reforming of methane, ethane and ethylene was compared on Pt, Rh and Pd supported on Yttrium stabilized zirconia (YSZ). Both, reactivity and product distribution changed with the use of different catalysts. The order of activity for the hydrocarbons on Rh was $C_2H_6 > C_2H_4 > CH_4$. On Pt, methane reacted faster than the C2 hydrocarbons: $CH_4 > C_2H_6, C_2H_4$. The lowest coking tendency was observed on Pt/YSZ. Pd/YSZ showed a high tendency to coke formation and blocked the reactor. Pt/YSZ produced synthesis gas (CO and H₂) only, for all hydrocarbons. However, more importantly, in this study all significant reactions during ethane steam reforming on Rh/YSZ have been clarified. Methane formation additionally to synthesis gas production on this catalyst was assigned to hydrogenolysis of ethane by consecutive conversion of hydrogen produced in ethane steam reforming.

2.1 Introduction

With the depletion of mineral oil and simultaneous increase in known natural gas reserves, it is expected that methane will eventually become a major resource for chemicals and liquid fuels. Much of the methane is found in regions that are far removed from industrial complexes and often offshore, implying that transport is uneconomical or even impossible. This has led to worldwide efforts for directly converting methane into easy transportable value-added products.

Direct and indirect methods are known for methane valorisation. The indirect routes are mainly based on the steam reforming to produce synthesis gas (CO and H₂), which can then be converted to the desired liquid fuels. Since reforming is a highly energy consuming process, considerable efforts have been made for many years to develop direct conversion routes. One of the possibilities in this respect is the slightly exothermic oxidative coupling of methane that leads to ethylene (1).



In the coupling process also ethane is formed. Next to reaction (1) the highly exothermic complete oxidation of methane is unavoidable (2).



As a high selectivity to reaction (1) is always compromised with a low conversion, methane conversion will never be complete. Limitations of the reaction in a co-feed reactor of methane and oxygen have led to recent development of several alternatives. Makri et al used a gas recycle reactor [1], Choudhary proposed the use of a countercurrent moving bed [2]. Also research on plasma [3] and solid-state electrolyte reactors [4] has been carried out. Additionally combinations with other reactions have been proposed: catalytic oxidative coupling and gas phase partial oxidation [5], co-generation of ethylene and electricity through oxidative coupling [6], oxidative coupling of methane and oxidative dehydrogenation [7] and oxidative coupling of methane and pyrolysis of naphtha [8]. All of the processes face difficulties with economic and/or technical feasibility.

Comparative study of reforming of methane, ethane and ethylene

A closer look at equations 1 and 2 shows that the side products of the coupling process can also react with methane through the endothermic steam and dry reforming reactions (3) & (4).



The idea of the current research is creating an auto thermal process, combining the exothermic oxidative coupling of methane and highly exothermic combustion (side) reactions with the endothermic reactions of methane steam and dry reforming. The intention is to convert methane to ethylene and synthesis gas (CO and H₂) in one multifunctional reactor. Allowing the side combustion reactions next to oxidative coupling to increase the methane conversion, and auto thermal operation including energy consumption *via* steam and dry reforming of remaining methane are important issues in this concept.

Two side reactions are involved that can disturb the process. In the oxidative coupling reaction combustion of C₂-hydrocarbons can also occur. This, however, can be minimized by avoiding the contact of oxygen and the coupling products.

The second challenge is the activity of ethane and ethylene in the reforming reactions [9]. As a result of the methane coupling reaction, a mixture of methane, ethane and ethylene is present (next to CO₂, H₂O and CO). To avoid complete reaction to synthesis gas, steam/dry reforming of ethane and ethylene has to be limited. High temperature is required in the overall process. Under these conditions water gas shift reaction will convert most of the CO₂ to H₂O (5). Therefore main focus in this study is on steam reforming.



Only few publications are available in the field of steam reforming of higher hydrocarbons than methane. Wang et al [10] measured steam reforming rates for methane, ethane, n-butane and some higher hydrocarbons on Pd/ceria for temperatures ranging from 620 to 770 K. The production of CO_x increased with carbon number, pointing out higher reactivity for higher hydrocarbons. The same tests

were also carried out on Pt/ceria which had similar catalytic properties, leading to identical rates and selectivity for both catalysts.

Takeguchi et al [11] compared steam reforming of methane, ethane and ethylene on Ni-YSZ cermets. C₂-hydrocarbons were completely converted to CO/CO₂ at 800°C while methane conversion was about 85% under these conditions. Complete conversion of methane was found at temperatures higher than 850°C.

While most researchers focused on separate reforming of hydrocarbons, Sutton et al [12] studied dry reforming of a gas mixture containing both CH₄ and C₃H₈ over Ni/Al (co-precipitated), Ru/Al₂O₃ and Pt/ZrO₂. At 800°C propane was completely consumed and CH₄ partially remained unconverted, showing higher reactivity of the larger hydrocarbon.

Sperle et al [13] determined the coking tendency for steam reforming of methane in presence of minor amounts of C₂ and C₃ hydrocarbons. A Ni/MgAl₂O₄ catalyst was used between 480 and 550°C. It was found that coking increased with carbon number and a dramatic increase was noted for olefins. Sidjabat and Trimm [14] also found higher deactivation rates for ethane and propane compared to methane in steam reforming on Ni/MgO at 500°C.

An ideal reforming catalyst in the combined process of oxidative coupling and reforming of methane would selectively react with methane in presence of ethane/ethylene at temperatures comparable to oxidative coupling conditions. Comparative studies between different metal catalysts have been limited to methane until now [15, 16]. Attention is focused on low temperature measurements and highly dispersed catalysts. So far the relative reactivity in mixtures of methane, ethane and ethylene has not been published. Also a comparison of methane, ethane and ethylene separately on different metal catalysts is not available. The latter issue will be studied first, while behaviour in mixtures will be studied in future work.

Usually Ni or noble metals like Ru, Rh, Pd, Ir and Pt are used as active metal in steam reforming catalysts. Compared to Rh and Ir, Pt and Pd are well known for low reactivity in splitting the C-C bond [17, 18] and were therefore considered promising in this study. Metals with even lower reactivity towards C-C bonds, for example Cu

Comparative study of reforming of methane, ethane and ethylene

and Au, show hardly any activity in C-H splitting [19], which would be necessary to activate any alkane. Rh was also included in this study as it shows high steam reforming activity. In case of C2 reforming and especially ethylene, coking is an issue. This eliminated the use of Ni. In this study Yttrium stabilized zirconia (YSZ) was selected as catalyst support, as zirconia supported catalysts are well-known for high resistance to coking [20]. In this publication, results of a comparative study of steam reforming of methane, ethane and ethylene on Rh, Pd and Pt supported on YSZ are discussed.

2.2 Experimental

Catalysts were prepared by wet impregnation of Yttrium stabilized zirconia (YSZ) obtained from TOSOH (TZ-8Y). The precursors were RhCl_3 , PdCl_2 and H_2PtCl_6 obtained from Alfa Aesar. Around 10 g of support was impregnated with a solution containing 0.01 g Rh, Pt or Pd per ml aqueous solution. Catalysts were calcined at 900°C in case of Rh and at 750°C for Pt and Pd. Synthetic air (ml/min) was used during the 15 h calcination period (ramp 5°C min^{-1}).

Activity tests were carried out in a micro reactor flow setup. The reactor consisted of a quartz tube with inner and outer diameter of respectively 4 and 6 mm. 200mg of catalyst was loaded between quartz wool. Catalyst particles with a diameter between 0.3 and 0.6 mm were loaded in the reactor, resulting in a pressure drop around 0.1 bar.

Methane (Hoekloos 4.5), ethane (Indugas 4.0) and ethylene (Indugas 3.5) were fed separately on all three catalysts. To ensure constant water/carbon ratio, methane concentration was chosen twice as high as ethane and ethylene. The reaction mixtures had the following composition: 10vol.% of methane or 5vol.% of ethane or ethylene in Ar (Hoekloos 5.0). A total flow rate of $200\text{ml}\cdot\text{min}^{-1}$ was applied. Water was added through a double saturation step of the gas mixture. In a first saturator the gas stream was contacted with water at 65°C , followed by condensation at 55°C in a second saturator. This led to a stable water concentration of 12vol.%, resulting in a constant water/carbon ratio of 1.2 for all experiments. Before activity test the samples were heated to 500°C in argon and reduced in 2.5vol.% H_2 (Indugas 5.0) / Ar for 1 h (flow rate: $200\text{ml}/\text{min}$).

Conversion of hydrocarbons was measured between 500 and 800°C for Rh/YSZ with intervals of 50°C . To avoid extensive sintering of the Pt and Pd samples, the maximum temperature applied was 700°C . The product and reactant gas composition was analysed by a Varian 3800 Gas Chromatograph equipped with two columns (Molsieve 5A and PoraPlotQ) and two TCD detectors. For all experiments the water gas shift constant was calculated by equation 5a:

$$K = \frac{[\text{H}_2][\text{CO}_2]}{[\text{H}_2\text{O}][\text{CO}]} \quad (5a)$$

Comparative study of reforming of methane, ethane and ethylene

Values calculated based on the observations are compared to theoretical equilibrium values calculated using HSC chemistry 4.0 software. HSC Chemistry was also used to calculate equilibrium compositions of the reaction mixtures.

For all experiments 200 mg of catalyst was used and total flow rate was 200ml/min. During water gas water gas shift measurements, 1 vol.% of CO in Argon with 12vol.% of water was fed. A mixture of CO₂ (10vol.%), H₂O (12vol.%) and H₂ (20vol.%) in Ar was used for methanation on Rh/YSZ; hydrogenolysis was studied using a H₂ (20vol.%) / ethane (5vol.%) mixture in Ar.

Metal dispersion was determined with H₂-chemisorption on a Micromeritics ChemiSorb 2750 pulse chemisorption apparatus. Elemental composition of the samples was determined with XRF on a Philips PW 1480 x-ray spectrometer. A H/Me ratio of 1 was assumed.

2.3 Results

2.3.1 Catalyst characterization

Table 2.1 displays the elemental analysis and results of the dispersion measurements for Pt/YSZ, Rh/YSZ and Pd/YSZ. The XRF results show that around 1wt% of metal is present in all catalysts. As expected, metal dispersion values (Table 2.1) of Pt/YSZ and Rh/YSZ were low because of high calcination temperatures and low surface area of the support material (16 m²/g).

Table 2.1: Metal dispersion and elemental composition for Pt/YSZ, Rh/YSZ and Pd/YSZ

Catalyst	Metal dispersion ¹	Metal content ²
1wt% Pt/YSZ	1.5%	1.04 wt% Pt
1wt% Rh/YSZ	6.3%	0.99 wt% Rh
1wt% Pd/YSZ	n.d.	0.99wt% Pd

¹ Determined by H₂ chemisorption, H/Me ratio of 1

² Determined by XRF

2.3.2 Rh/YSZ

Steam reforming of methane, ethane and ethylene was tested on Rh/YSZ in separate experiments. The initial conversions of methane, ethane and ethylene as a function of temperature are shown in Figure 2.1. It can be seen that the reactivity of ethylene and ethane is much higher than of methane, complete conversion of C₂-hydrocarbons already occurs at temperatures around 600°C. In case of ethylene reforming, Rh/YSZ deactivated at 500°C and 550°C (not shown). The conversion of ethylene decreased by 10% within the first hour of reaction at 500°C, whereas the decrease was limited to 2% in the first hour at 550°C. Thermodynamic calculations confirmed that carbon formation can be a factor under these conditions, as the equilibrium leads to carbon next to synthesis gas. Oxidation at 850°C reactivated the catalyst. Experiments at temperatures above 600°C with ethylene as well as all experiments with ethane and methane showed stable conversion with time on-stream. The carbon mass balances was closed within 5% for all experiments.

Comparative study of reforming of methane, ethane and ethylene

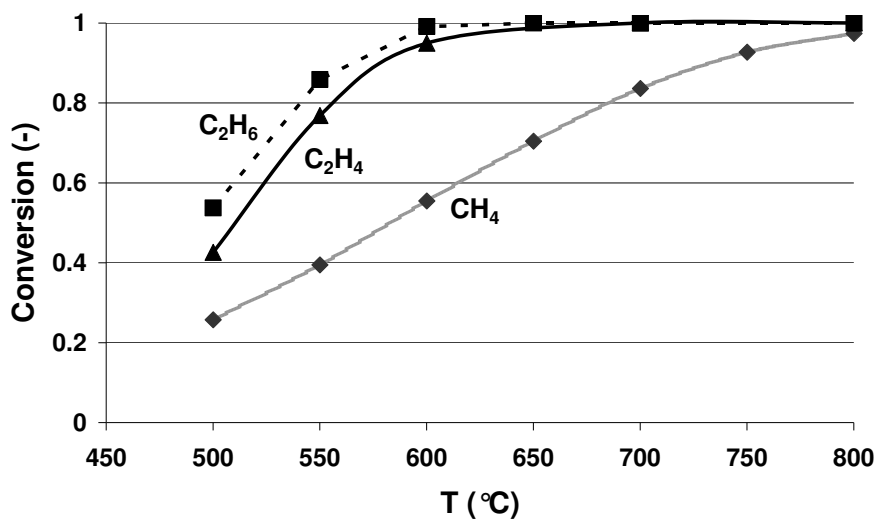


Figure 2.1: Conversion of methane (10vol.%), ethane (5vol.%) and ethylene (5vol.%) when fed separately in steam reforming on Rh/YSZ between 500°C and 800°C

Methane reforming produces mainly H₂ and CO₂ at temperatures up to 500°C. CO formation becomes notable at 550°C. Relatively more CO is formed at higher temperatures. In Figure 2.2 the WGS constant, calculated from the experimental product concentrations, is compared to the theoretical equilibrium value as a function of temperature for all three experiments. For methane, equilibrium is achieved during

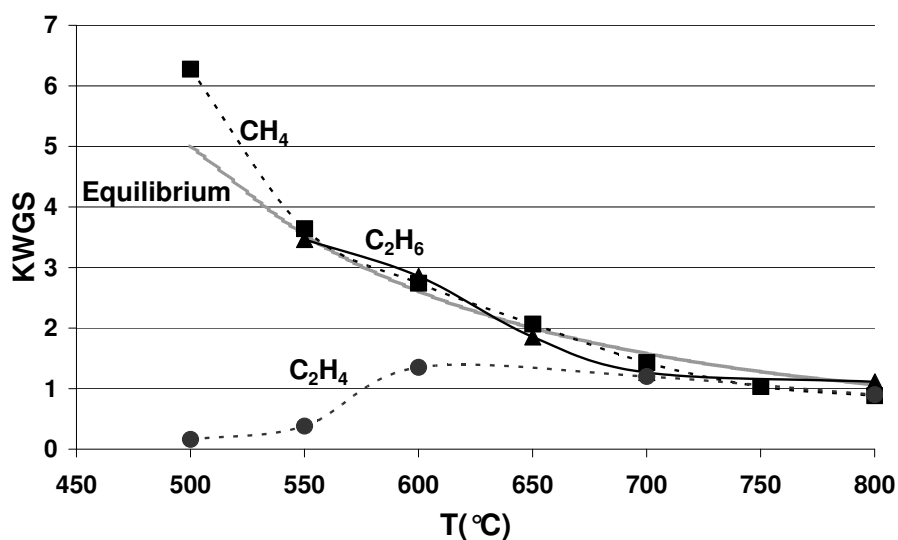


Figure 2.2: WGS equilibrium values between 500°C and 800°C compared to calculated WGS constants for steam reforming of methane, ethane and ethylene on Rh/YSZ

steam reforming at all temperatures (Figure 2.2). For reforming of ethane, the water gas shift reaction is also equilibrated. Clearly, WGS equilibrium is not reached in ethylene reforming. CO was the main product besides hydrogen under all conditions, while only minor amounts of CO₂ were formed.

The conversion of ethane is slightly higher than that of ethylene (Figure 2.1), while ethylene is generally considered more reactive. Therefore, a closer look is taken at the difference in product composition in both experiments. In case of ethane reforming (Figure 2.3a), interestingly, methane is one of the products next to the expected CO, CO₂ and H₂ mixture. The highest methane yield, almost 30%, is observed at 600°C. Higher temperatures increase selectivity to synthesis gas. The product composition in case of ethylene reforming is shown in Figure 2.3b. Under all conditions measured, the main product is a mixture of CO, CO₂ and H₂. Only minor amounts of methane and ethane were formed

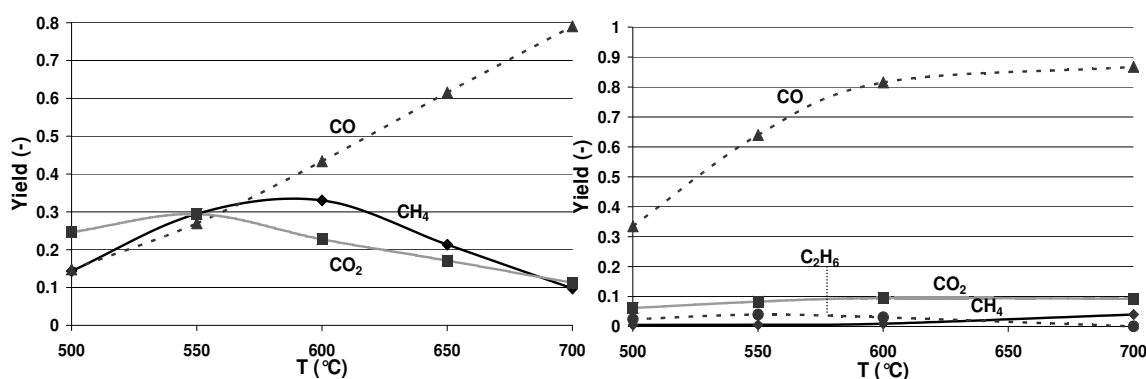
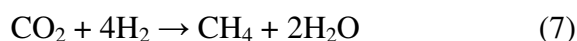
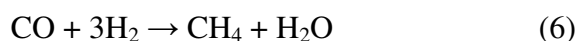


Figure 2.3: Yield of carbon containing products in ethane (left) and ethylene (right) steam reforming on Rh/YSZ as a function of temperature

Related reactions were investigated to determine the reason for the production of methane in the ethane reforming experiment. Tests for methanation eq. (6+7) and hydrogenolysis eq. (8) reactions were carried out at 600°C, since at this temperature the highest methane selectivity was obtained during steam reforming of ethane.



Comparative study of reforming of methane, ethane and ethylene

To investigate methanation on Rh/YSZ a mixture of CO₂ (10vol.%), H₂O (12vol.%) and H₂ (20vol.%) was fed. Hardly any methane was formed in this case, as shown in Figure 2.4 in the left bar. Only 1% yield was obtained. The main product was 3vol.% of CO, with still 17vol.% of hydrogen remaining (not shown). Thermodynamic calculations showed an equilibrium yield of methane of 1.7% under the present conditions.

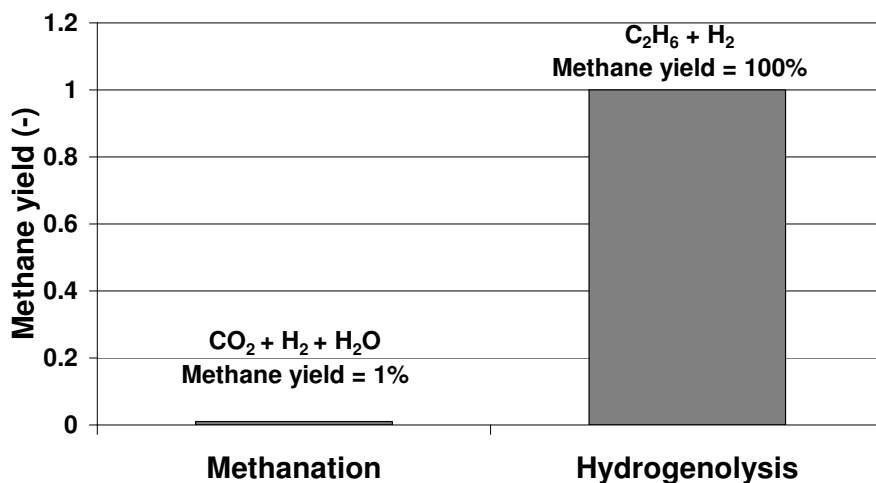


Figure 2.4: Comparison of methane yield in methanation and ethane hydrogenolysis tests at 600°C on Rh/YSZ at initial stage

During steam reforming reactions initially no hydrogen is present. Testing of hydrogenolysis reaction is however relevant as steam reforming of ethane will lead to hydrogen and CO_x, possibly enabling hydrogenolysis of ethane with hydrogen as a consecutive reaction. Moreover Rh-catalysts are well known to catalyze hydrogenolysis of ethane at temperatures around 300°C [21]; Rh/YSZ is tested here at 600°C.

Hydrogenolysis activity of Rh/YSZ was determined by feeding a H₂ (20vol.%) / ethane (5vol.%) mixture. At 600°C complete conversion of ethane to methane was observed (right bar in Figure 2.4) initially. After a short period of complete conversion, fast deactivation occurred and within two hours CH₄-yield dropped to 68% (not shown). This deactivation can be ascribed to coke formation on the catalyst,

as regeneration of the catalyst was possible by heating the catalyst to 850°C in a 20vol.% O₂/Ar-mixture (not shown).

Also the influence of hydrogenolysis under reforming reaction conditions was studied. Therefore a combined steam reforming/hydrogenolysis experiment was carried out. 5vol.% of ethane, 20vol.% of H₂ and 12 vol.% of H₂O in Ar were fed at 600°C. The results of this experiment are shown in Figure 2.5 (left bars). The experiment initially shows a methane yield of 54% while CO_x yield was 44%. For comparison, CO_x and methane yields in the normal reforming experiment (no addition of H₂, as shown in Figure 2.1) are included in Figure 2.5 (right bar). It shows that adding hydrogen clearly increases the methane production at the expense of the synthesis gas yield.

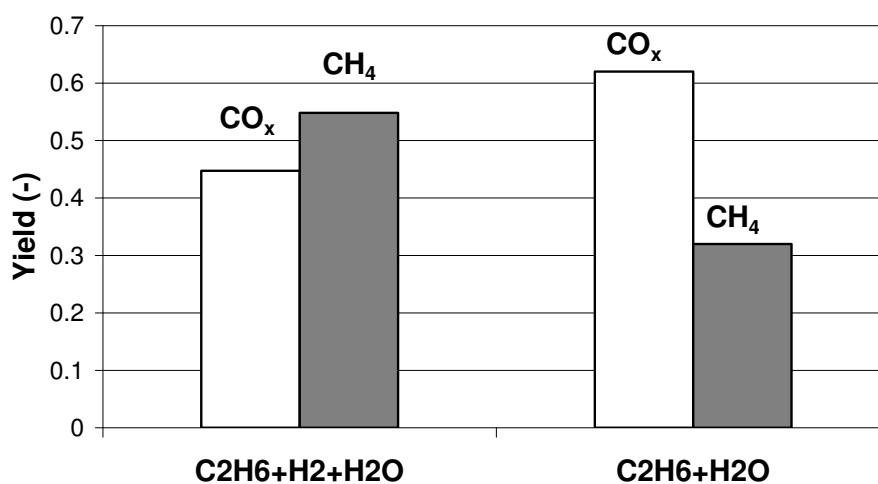


Figure 2.5: Yield of CO_x/methane in a combined ethane steam reforming/ethane hydrogenolysis experiment at 600°C (left side), yield of CO_x/methane in ethane steam reforming at 600°C (right side)

In addition, stability of the combined hydrogenolysis next to steam reforming of ethane was tested for 20 hours (not shown). Only a slight deactivation is observed for hydrogenolysis, as CH₄ yield decreased from 54% to 51%. During the entire reaction period the CO_x yield remains constant at 44%. This shows that ethane reforming and hydrogenolysis are stable processes under these conditions.

2.3.3 Pt/YSZ

Pt/YSZ was tested for steam reforming of methane, ethane and ethylene. The results are shown in Figure 2.6. On this catalyst methane shows the highest conversion under all conditions measured. Ethane and ethylene show similar conversions between 500°C and 600°C, while ethylene conversion is slightly lower at higher temperatures. It should be noted that this catalyst showed no deactivation for all three hydrocarbons over the entire temperature range. In all reactions tested on Pt/YSZ only CO, H₂ and CO₂ were produced; no methane or ethane was formed.

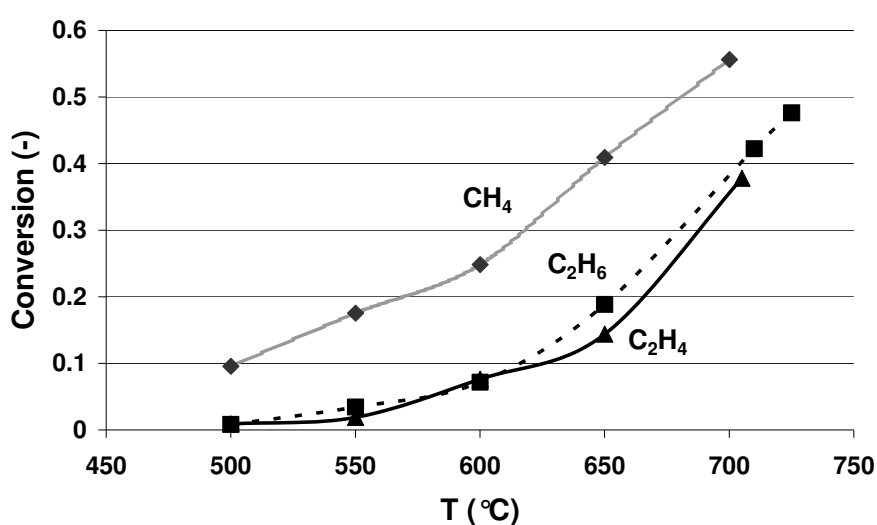


Figure 2.6: Conversion of methane (10vol.%), ethane (5vol.%) and ethylene (5vol.%) when fed separately in steam reforming on Pt/YSZ as a function of temperature

The water gas shift equilibrium was calculated and compared to the theoretical value for all experiments with Pt/YSZ (Figure 2.7). On the WGS reaction, it can be

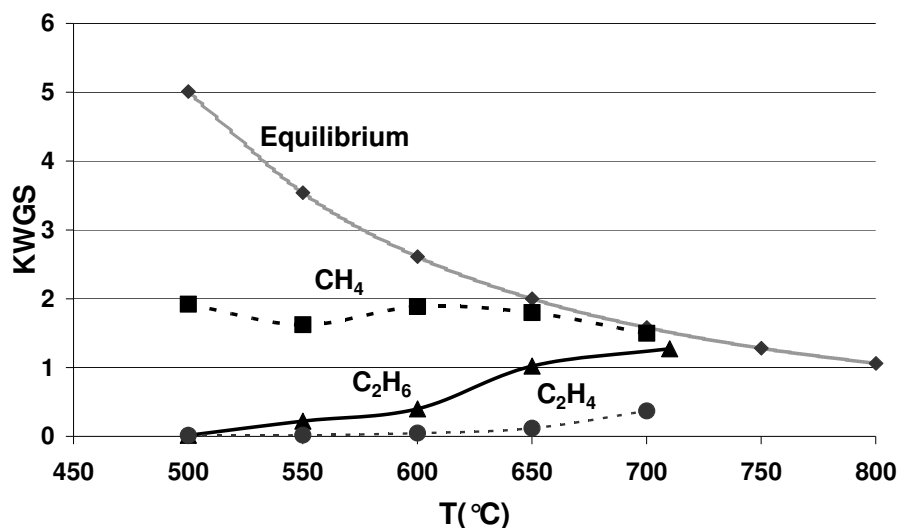


Figure 2.7: WGS equilibrium values between 500°C and 800°C compared to calculated WGS constants for steam reforming of methane, ethane and ethylene on Pt/YSZ. Conditions: 1vol.% CO in Ar, 12 vol.% of H₂O

concluded that equilibrium is only reached at temperatures above 650°C during methane reforming. In the case of ethane reforming, the amount of CO is higher than expected based on the WGS equilibrium, as indicated by a lower value for K compared to the equilibrium value. In the case of ethylene, almost only CO is formed, leading to K-values far from the equilibrium.

In addition, water gas shift experiments were performed to clarify the role of the hydrocarbons in the limitation to reach WGS equilibrium. A mixture of CO and H₂O in Ar was used to determine activity for WGS between 500°C and 700°C. The water gas shift constants calculated from experimental concentrations as compared to theoretical equilibrium constants are displayed in Figure 2.8a. Equilibrium was obviously reached between 500°C and 700°C. To test the influence of ethylene, 5 vol.% of ethylene was added to the CO/H₂O mixture at 700°C. Immediately the conversion of CO to CO₂ decreased significantly, suggesting that ethylene prevents equilibration of the WGS reaction (Figure 2.8b). Going back to the initial conditions (switching off ethylene) led to recovery of WGS activity and equilibrium was again achieved.

Comparative study of reforming of methane, ethane and ethylene

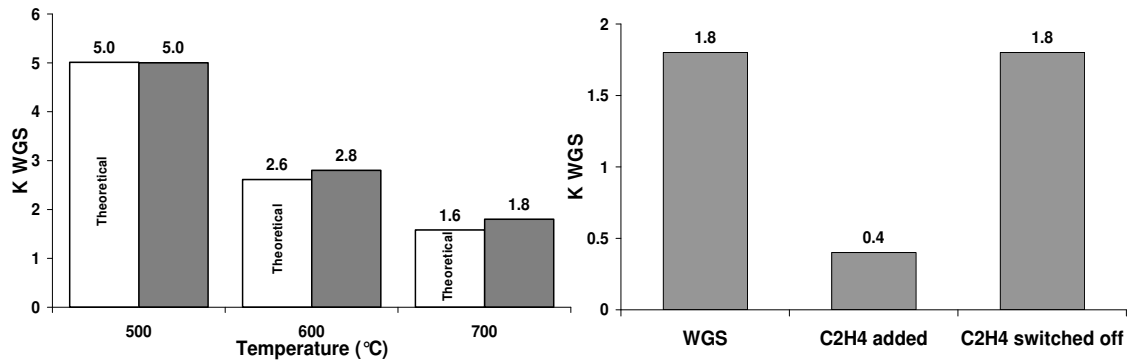


Figure 2.8 Left side (a): WGS equilibrium values (white bars) between 500°C and 700°C compared to calculated WGS constants for WGS experiments on Pt/YSZ (grey bars). Right side (b): effect of ethylene addition to WGS constant calculated from experimental data at 700°C

Next to behaviour of separate components as described above reactivity of hydrocarbons in mixtures was investigated. Steam reforming of a mixture of methane (5vol.%) and ethylene (2.5vol.%) was tested on PtYSZ to test competition effects of both hydrocarbons. The conversions of methane and ethylene are shown in Figure 2.9. It can be observed that ethylene strongly affects conversion of methane on PtYSZ: conversion of methane is limited to less than 10% in presence of ethylene under all conditions.

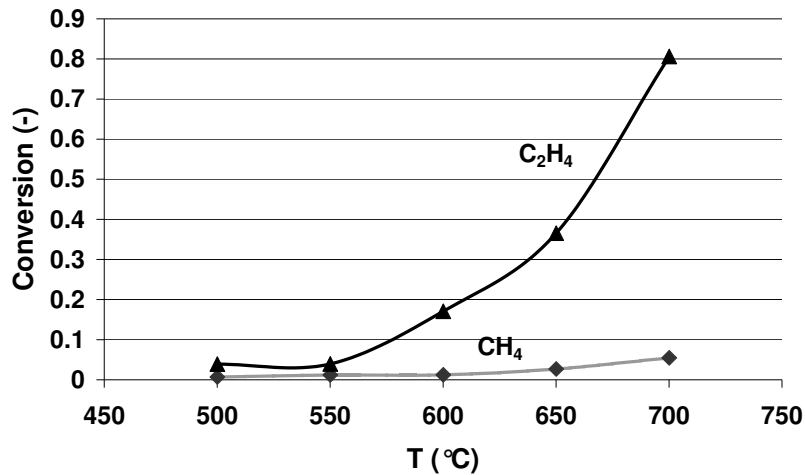


Figure 2.9: Conversions of methane (5vol.%) and ethylene (2.5vol.%) in mixture in steam reforming on PtYSZ

2.3.4 Pd/YSZ

Ethane reforming was carried out on Pd/YSZ. Immediate deactivation occurred when operating at 5vol% ethane at 600°C. In Figure 2.10, the ethane conversion is shown as a function of time on-stream. Conversion of ethane dropped from 38% to around 11% during the first three hours. The pressure drop over the reactor increased from 0.1 to 0.35 bar and the catalyst appeared strongly coked. In experiments with methane, Pd/YSZ showed stable conversion at temperatures from 500°C to 700°C (not shown).

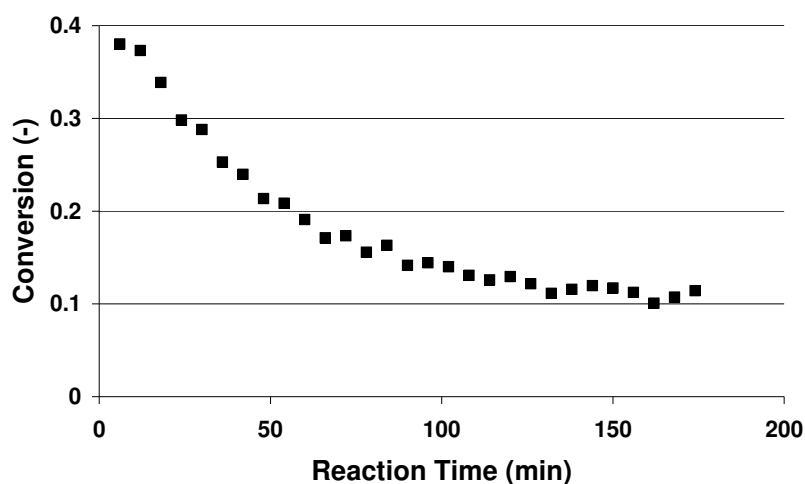


Figure 2.10: Conversion of ethane (5vol.%) in steam reforming on Pd/YSZ at 600°C

Reforming of ethane on Pd/YSZ led to complete blocking of the reactor. The same observation was made by Hegarty et al [22] after reforming of methane for 30 hours with higher water/carbon ratio. As ethane causes coking, experiments with ethylene would not make sense as ethylene usually leads to even faster formation of coke [9]. The high coking tendency eliminates Pd as reforming catalyst for combined methane coupling/steam reforming process. No further experiments were carried out on this catalyst.

2.4 Discussion

2.4.1 Activity of hydrocarbons on Pt and Rh

The comparative study of methane, ethane and ethylene steam reforming on Pt, Rh and Pd on YSZ shows large differences in both reactivity as well as product slate. The order of activity of Pt/YSZ was $\text{CH}_4 > \text{C}_2\text{H}_6 \approx \text{C}_2\text{H}_4$ (Figure 2.6). Interestingly, on Rh/YSZ the order of activity was completely different: $\text{C}_2\text{H}_6 > \text{C}_2\text{H}_4 > \text{CH}_4$ (Figure 2.1). Figure 2.10a illustrates that Rh/YSZ is much more active for ethylene reforming as compared to Pt/YSZ; for ethane a similar result is obtained (not shown). The conversion of methane on both Pt/YSZ and Rh/YSZ catalysts is shown in Figure 2.11b. The difference in conversion of methane on both catalysts is much smaller than in case of ethylene or ethane

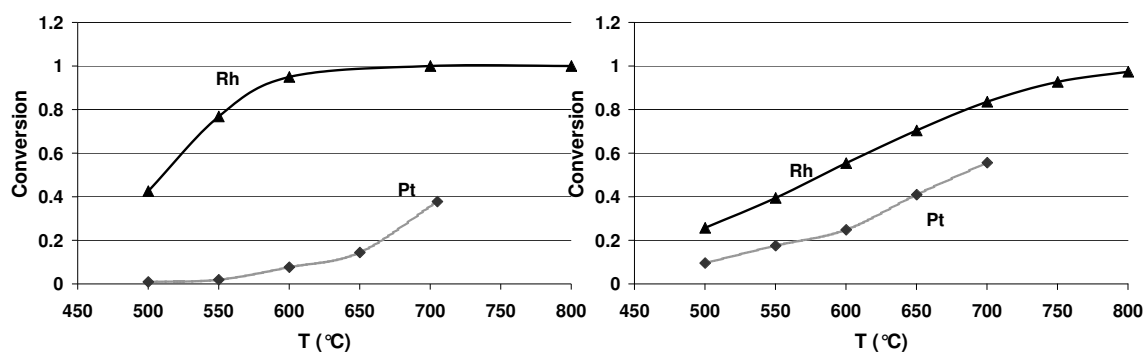


Figure 2.11: Comparison of conversion of ethylene (5vol.%) (a) and conversion of methane (10vol.%) (b) in steam reforming on Pt/YSZ and Rh/YSZ

The C2-hydrocarbons were converted much easier on Rh as complete conversion was observed already at 600°C (Figure 2.1). It is obvious that the differences between both metals cannot be explained by difference in metal dispersion (Table 2.1), since for both catalysts the metal particles are large, ruling out an ensemble effect. The high reactivity of Rh towards C2 hydrocarbons relates to findings in literature. Rh shows a higher binding strength towards carbon atoms than Pt, indicating a higher reactivity in C-C scission reactions [17].

Van Broekhoven and Ponc [19] related the reactivity of several metals towards higher hydrocarbons to the tendency to form multiple bonds between one carbon atom and the metal. It is stated that easy formation of multiple metal carbon bonds can be

correlated to higher activity in C-C splitting reactions. While rhodium is one of the better metals in this respect, Pt is inactive. This explains the observations in the present research, that Rh is more active than Pt in ethane and ethylene reforming. Pt/YSZ was the most stable catalyst. Pd/YSZ suffered from severe deactivation because of coking, while Rh/YSZ showed deactivation by coking only during ethylene reforming at temperatures below 600°C.

For the purpose of developing steam reforming catalysts which are able to convert selectively methane in hydrocarbon mixtures with ethane and ethylene, further research will be focused on Pt-catalysts. It was shown in Figure 2.9 that presence of ethylene can limit conversion of methane significantly. Similar to the water gas shift reaction (section 4.2), a blocking effect was noticed in this case. The strong adsorption of ethylene leads to low surface coverage of methane and low reaction rates of methane. Methane conversion was limited to less than 10% indicating that almost no methane adsorption on the catalyst is possible. In chapter 3 of this thesis, potassium will be added to Pt steam reforming catalysts and the effects to conversions of the hydrocarbons when fed in mixtures will be studied.

2.4.2 WGS equilibrium

The water gas shift equilibrium is achieved on Rh/YSZ during reforming of methane and ethane (Figure 2.2). This agrees with the results reported by Wei et al. [23], claiming that WGS is equilibrated during steam reforming of methane on supported metal catalysts. In the present study, too much CO was formed compared to CO₂ in case of ethylene, suggesting partial hindering of WGS during reforming of ethylene. On Pt/YSZ the equilibrium is only reached for methane at temperatures higher than 650°C (Figure 2.7). In reforming of C₂-hydrocarbons and especially ethylene, the amount of CO is much too high as compared to the water gas shift equilibrium. Probably, CO adsorption on the metal surface is suppressed, as water activation is obviously still taking place because steam reforming and WGS both need activation of water. Possibly, adsorption of CO is hindered by strongly adsorbed ethylene and ethane fragments. This indicates that carbon deposits can be involved during steam reforming.

The WGS reaction achieved equilibrium on Pt between 500°C and 700°C (Figure 2.8a) in the absence of hydrocarbons, while this was not the case during steam reforming experiments. The fact that water gas shift reaction equilibrated immediately when ethylene was switched off (Figure 2.8b) demonstrates that blocking by ethylene is fully reversible at 700°C. It can be concluded that ethylene blocks sites on the metal surface and that the responsible (hydro-)carbon fragments are easily removed.

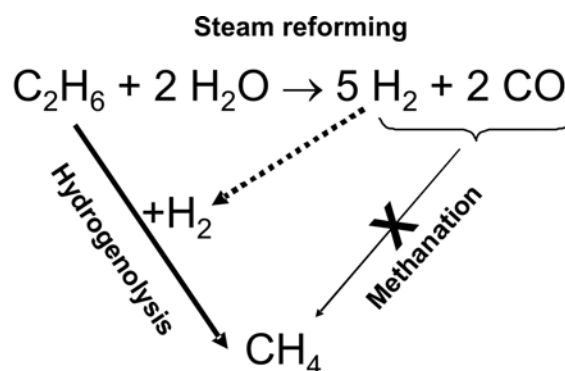
2.4.3 Mechanism of steam reforming of ethane on Rh

The results on Rh/YSZ provide new insights in the mechanisms involved during steam reforming of ethane. While on Pt/YSZ only reforming reactions occurred, surprisingly methane was one of the major products in case of ethane reforming on Rh/YSZ. In literature, it is assumed that the methane formation in reforming of higher hydrocarbons occurs through methanation reactions [24, 25]. In this study, however, tests of methanation reactions on Rh/YSZ show that essentially only the WGS reaction occurs; CO₂ and hydrogen are converted into H₂O and CO. Only a small amount of CH₄ (1% as shown in Figure 2.4) was detected at 600°C. This result excludes CO₂ methanation (equation (7)) as a source of methane during reforming. In addition, the final product composition, containing 3 vol.% CO and 17 vol.% H₂, also proves that methanation with CO (equation (6)) is not significantly contributing under these conditions. Consequently, it can be concluded that neither methanation of CO₂ nor CO is responsible for methane formation during ethane reforming, where methane yields up to 30% were found.

However, hydrogenolysis tests at 600°C showed that ethane and hydrogen (under conditions comparable to reforming) were converted to methane completely (Figure 2.4). This is a strong indication that methane formation is due to hydrogenolysis during ethane steam reforming. Nevertheless, fast deactivation of Rh/YSZ was observed during ethane hydrogenolysis, while methane formation was constant with time on stream during ethane steam reforming experiments on the same catalyst. The combined hydrogenolysis/reforming experiment (Figure 2.5) indicates that the deactivation of the catalyst is much slower in presence of water and that high methane concentrations can be detected for several hours. From this, it is proposed that the presence of water limits coke formation on the Rh surface and a stable conversion

level of ethane to methane is obtained. Generally, it is well known [9] that presence of steam is favorable to avoid coke formation.

Addition of hydrogen in the combined experiment increased the methane yield as compared to the standard ethane reforming experiment (Figure 2.5). Hydrogenolysis can occur throughout the reactor when hydrogen is added to the feed. During ethane reforming however, hydrogenolysis is only possible after hydrogen is produced from ethane and water. Therefore, addition of hydrogen to the feed significantly increases the methane yield. Furthermore, it can be concluded that ethane hydrogenolysis contributes as a consecutive reaction during ethane steam reforming on Rh/YSZ as schematically shown in scheme 2.1. Methanation does not significantly contribute to the production of methane (Figure 2.4), in contrast to propositions in literature [24, 25]. The conclusions on the reaction network based on experimental evidence are in full agreement with thermodynamics. Ethane and hydrogen can be completely converted to methane between 300°C and 800°C. In contrast, equilibrium yield of methanation is only 1.7% at 600°C, confirming that methanation is not significantly contributing.



Scheme 2.1: Reactions taking place during ethane steam reforming on Rh/YSZ

2.5 Conclusion

This comparative study of methane, ethane and ethylene steam reforming on Pt, Rh and Pd on YSZ shows substantial differences between the catalytic properties of the metals. Both reactivity and composition of products vary. The order of activity on Rh was $C_2H_6 > C_2H_4 > CH_4$. On Pt, methane reacted faster than the C2 hydrocarbons: $CH_4 > C_2H_6 \approx C_2H_4$. Concerning the target process of methane coupling combined with reforming, Pt is considered the most promising metal because C2 hydrocarbons are converted less than methane. Additionally, Pt/YSZ is the most stable catalyst. When fed in mixture with ethylene methane conversion was limited on PtYSZ.

On Pt/YSZ, the steam reforming reactions resulted in synthesis gas exclusively. However, more importantly, in this study all the occurring reactions during ethane steam reforming on Rh/YSZ have been elucidated. Additionally to synthesis gas, methane was formed during steam reforming of ethane on Rh/YSZ. It was shown that hydrogenolysis of ethane occurred on this catalyst as a consecutive reaction, converting hydrogen produced in ethane steam reforming *via* hydrogenolysis of unconverted ethane. This shows that effective steam reforming of higher hydrocarbons can only be achieved when the activity for hydrogenolysis is also considered to avoid production of methane.

2.6 References

- [1] M. Makri, C.G. Vayenas, *Applied Catalysis A-General* 244 (2003) 301.
- [2] V.R. Choudhary, B.S. Uphade, *Catalysis Surveys from Asia* 8 (2004) 15.
- [3] Istadi, N.A.S. Amin, *Fuel* 85 (2006) 577-592.
- [4] N. Lapena-Rey, P.H. Middleton, *Applied Catalysis A-General* 240 (2003) 207.
- [5] H. Zhang, J. Wu, B. Xu, C. Hu, *Catalysis Letters* 106 (2006) 161.
- [6] J.A. Hugill, F.W.A. Tillemans, J.W. Dijkstra, S. Spoelstra, *Applied Thermal Engineering* 25 (2005) 1259.
- [7] A. Machocki, A. Denis, *Chemical Engineering Journal* 90 (2002) 165.
- [8] D. Czechowicz, K. Skutil, A. Torz, M. Taniewski, *Journal of Chemical Technology and Biotechnology* 79 (2004) 182.
- [9] D.L. Trimm, *Catalysis Today* 37 (1997) 233.
- [10] X. Wang, R.J. Gorte, *Applied Catalysis A-General* 224 (2002) 209.
- [11] T. Takeguchi, Y. Kani, T. Yano, R. Kikuchi, K. Eguchi, K. Tsujimoto, Y. Uchida, A. Ueno, K. Omoshiki, M. Aizawa, *Journal of Power Sources* 112 (2002) 588.
- [12] D. Sutton, S.M. Parle, J.R.H. Ross, *Fuel Processing Technology* 75 (2002) 45.
- [13] T. Sperle, D. Chen, R. Lodeng, A. Holmen, *Applied Catalysis A-General* 282 (2005) 195.
- [14] O. Sidjabat, D.L. Trimm, *Topics in Catalysis* 11 (2000) 279.
- [15] J.R. Rostrup-Nielsen, J.H.B. Hansen, *Journal of Catalysis* 144 (1993) 38-49.
- [16] J.M. Wei, E. Iglesia, *Journal of Physical Chemistry B* 108 (2004) 4094.
- [17] A.V. Zeigarnik, R.E. Valdes-Perez, O.N. Myatkovskaya, *Journal of Physical Chemistry B* 104 (2000) 10578.
- [18] A.V. Zeigarnik, O.N. Myatkovskaya, *Kinetics and Catalysis* 42 (2001) 418.
- [19] E.H.v. Broekhoven, V. Ponec, *Progress in Surface Science* 19 (1985) 351.
- [20] K. Nagaoka, K. Seshan, K. Aika, J.A. Lercher, *Journal of Catalysis* 197 (2001) 34.
- [21] L.D. Schmidt, K.R. Krause, *Catalysis Today* 12 (1992) 269.
- [22] M.E.S. Hegarty, A.M. O'Connor, J.R.H. Ross, *Catalysis Today* 42 (1998) 225.
- [23] J.M. Wei, E. Iglesia, *Physical Chemistry Chemical Physics* 6 (2004) 3754.
- [24] G. Kolb, R. Zapf, V. Hessel, H. Lowe, *Applied Catalysis A-General* 277 (2004) 155.
- [25] C. Resini, M.C.H. Delgado, L. Arrighi, L.J. Alemany, R. Marazza, G. Busca, *Catalysis Communications* 6 (2005) 441.

Chapter 3

Influence of potassium on the competition between methane and ethane in steam reforming over Pt supported on yttrium-stabilized zirconia

Abstract

The effect of addition of potassium to Pt supported on yttrium-stabilized-zirconia (PtYSZ) catalyst for steam reforming of methane, ethane and methane/ethane mixtures was explored. Addition of potassium has a positive effect on preferential steam reforming of methane in mixtures of methane and ethane over PtYSZ catalysts. The activity of potassium modified catalysts increased with time-on-stream during steam reforming of mixtures of methane and ethane, while the ratio of reaction rates of methane and ethane remained constant. Most importantly, it was demonstrated that the presence of potassium prevents competition between methane and ethane during steam reforming. The reaction rate ratio in methane/ethane mixtures is changed from preferential ethane reforming on PtYSZ towards preferential methane conversion as a result of addition of potassium.

3.1 Introduction

Natural gas, mainly consisting of methane, is available in large quantities and is becoming one of the major resources for energy and chemicals. A new concept for utilization of methane is proposed in this study, as discussed in detail in earlier work [1]. Shortly, the intention is to combine oxidative coupling and inevitable combustion with reforming reactions of methane (equations (1) to (4)) in one multifunctional auto thermal reactor. This should lead to production of ethylene and synthesis gas in one auto thermal process, in which the energy released in reactions (1) and (2) is used to reform methane through reactions (3) and (4).



For the complete process, two catalysts are needed, one for oxidative coupling and one for the reforming reaction. The main focus in the current work is on the reforming steps (3+4) of the mixture produced in the oxidative coupling. In addition to ethylene, also ethane is produced during oxidative methane coupling. The oxidative coupling reaction thus leads to a mixture of unreacted methane and produced ethane and ethylene, plus CO, CO₂ and H₂O from the combustion reaction.

Due to the high temperature necessary for oxidative coupling (700°C), most of the CO₂ reacts to CO through the reversed water gas shift reaction, producing water next to CO. Therefore, the H₂O concentration will be much higher than the CO₂ concentration, making the steam reforming reaction (3) more relevant than the dry reforming reaction (4).

Steam reforming of the product stream from oxidative coupling leads to competition between methane, ethane and ethylene. All these hydrocarbons can be easily steam-reformed [2]. The main challenge in this project is, therefore, to prevent or limit the steam reforming of ethane and ethylene, while methane should be effectively

converted. The relevant temperature window is between 700°C and 800°C, because of the integrated operation of oxidative coupling.

Pt supported on zirconia proved to be a stable catalyst in steam and dry reforming of methane [3-6]. In earlier research [1], Pt supported on yttrium stabilized zirconia (YSZ) was found to be the most suitable metal catalyst for steam reforming of single reactants. Compared to Rh and Pd, PtYSZ showed the highest relative activity towards methane, for separate reforming of methane, ethane and ethylene. The relatively low reactivity of Pt towards ethane was in agreement with earlier results by Sinfelt et al. [7-9], reporting low activity of Pt in ethane hydrogenolysis, as compared to Rh. It was also found that methane hardly reacted in steam reforming when mixed with ethylene, which was attributed to strongly adsorbed ethylene fragments blocking the active Pt sites. Also carbon formation is an issue in steam reforming of ethylene [1, 2].

In literature, it is claimed that K prevents carbon formation on Ni catalysts by blocking step sites which are believed to be the nucleation sites for graphite formation [10]. In addition, potassium present on Ni catalysts enhances coke gasification [11]. For Ni/Al₂O₃, Juan-Juan et al [12] found decreasing activity in methane dry reforming with increasing potassium concentration in the catalyst. A reduction in catalytic activity by potassium was also confirmed by Trimm [13] and Rostrup-Nielsen [14]. The activity of Ni/MgO-Al₂O₃ for methane steam reforming was reported to decrease by 85% when 1.1wt% of K was added [15]. In short, addition of K to Ni catalyst decreases steam reforming activity and limits carbon formation and deactivation. Decreasing reforming activity by addition of potassium was also found on Rh/La-Al₂O₃ [16].

However, the effect of potassium on Pt catalysts on steam reforming of methane and ethane has not been reported so far. This study explores the effect of K addition to PtYSZ on catalyst activity and stability, for steam reforming of both ethane and methane as well as ethane/methane mixtures.

3.2 Experimental

Yttrium stabilized zirconia (YSZ), obtained from TOSOH (TZ-8Y) was used as support and was modified with 2 and 4wt.% potassium. 15g of YSZ was impregnated with 15 ml of an aqueous K_2CO_3 solution, containing resp. 0.5 or 1g of K_2CO_3 and calcined in synthetic air (30ml/min) for 4 hours at 600°C (temperature ramp 5°C min⁻¹).

Subsequently, 1wt% of Pt was impregnated on 10g of support with a H_2PtCl_6 (Alfa Aesar) solution containing 0.01g Pt per ml aqueous solution. PtYSZ was calcined at 750°C. The potassium modified samples were calcined at two different temperatures, 700°C and 750°C respectively. Catalysts were calcined in synthetic air (30ml/min) during 15h (ramp 5°C min⁻¹). Next to PtYSZ, four potassium modified catalysts were prepared, designated by initial potassium content (wt.%) and calcination temperature: Pt2K700, Pt2K750, Pt4K700 and Pt4K750.

Activity tests were carried out in a micro reactor flow setup. The reactor consisted of a quartz tube with inner and outer diameter of respectively 4 and 6mm. 200mg of catalyst was loaded between quartz wool plugs. Catalyst particles with a diameter between 0.3 and 0.6mm were used, resulting in a pressure drop around 0.1bar. The samples were heated to 500°C in argon and reduced in 2.5vol.% H_2 (Indugas 5.0) / Ar for 1h (flow rate: 200ml/min) before measuring the catalytic performance. No significant activity for steam reforming of methane and ethane was found for the support material YSZ at 700°C. Also the occurrence of gas phase reactions could be excluded based on experiments with quartz particles of 0.3 to 0.6 mm.

Methane (Hoekloos 4.5) and ethane (Indugas 4.0) were mixed with argon (Hoekloos 5.0) to a total flow rate of 200ml.min⁻¹, to ensure a constant space velocity. In the first series of experiments 2.2vol.% of ethane and 5vol.% of methane were used at a reaction temperature of 700°C. For comparison, identical concentrations were also applied separately in additional experiments with a single hydrocarbon. In the second series of experiments, methane and ethane concentrations and ratios were varied.

Water was added to the gas mixtures via a double saturation step: the gas stream was bubbled through water at 65°C in the first saturator, followed by condensation at 55°C

in a second saturator. This led to a stable water concentration of 12vol.%, resulting in a water/carbon ratio above 1 for all experiments. The product and reactant gas composition was analyzed with a Varian 3800 Gas Chromatograph equipped with two columns (Molsieve 5A and PoraPlotQ) and two TCD detectors. Water was analyzed in the PoraPlotQ column; the molsieve column was protected against water by a PoraPlotQ pre-column and a backflush system.

Elemental composition of the catalysts was determined with XRF on a Philips PW 1480 X-ray spectrometer.

3.3 Results

3.3.1 Catalyst characterisation

Table 3.1 shows the platinum and potassium contents of the samples as determined with XRF. The Pt content is similar for all catalysts and remained unchanged during reaction. The potassium content is shown for both fresh catalysts and after 20h and 85h time-on-stream (TOS). The initial content varies with calcination temperature: calcination at 700°C results in a higher potassium content than calcination at 750°C. All catalysts lost potassium during reaction. However, analysis of Pt4K700 after 85 hours of testing showed that the potassium content remained stable after 20 hours TOS.

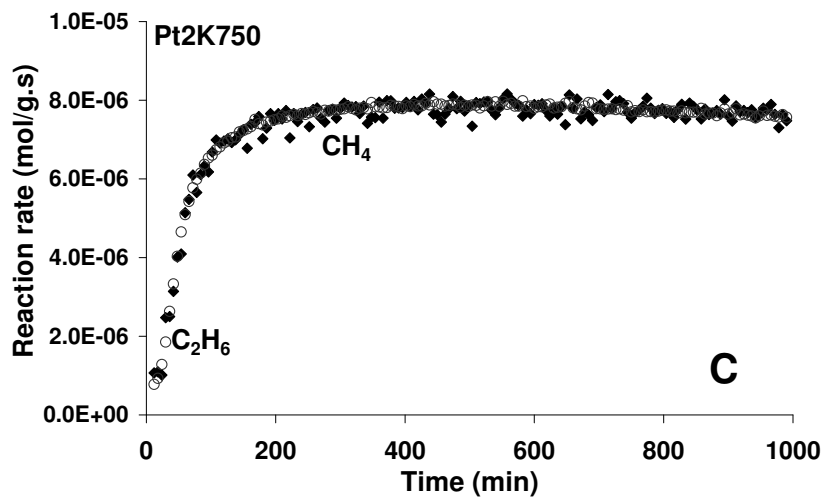
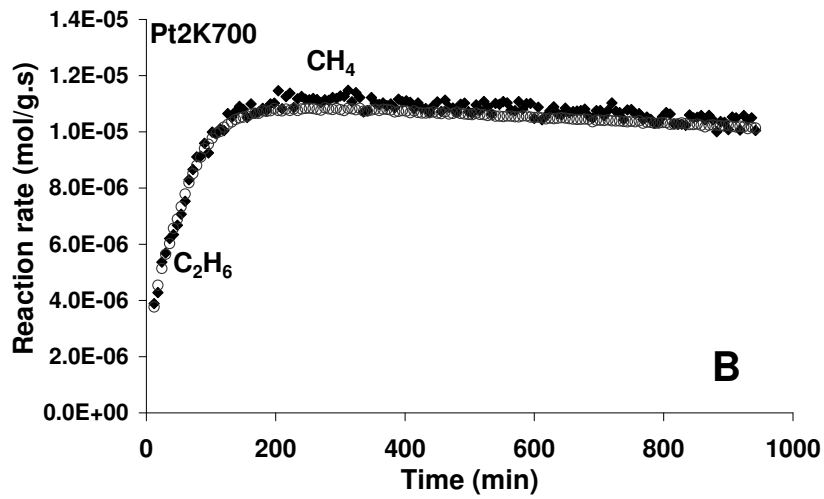
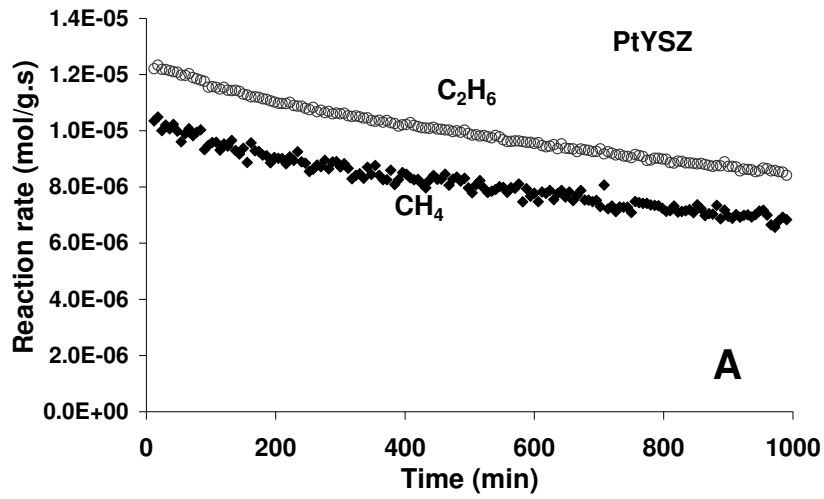
Table 3.1: Platinum and potassium contents of the applied catalysts as determined with XRF.

Catalyst	Wt.% Pt	Wt.% K (initial)	Wt.% K (20h)	Wt.% K (85h)
PtYSZ	1.04 ± 0.03	-	-	-
Pt2K700	1.05 ± 0.03	1.05 ± 0.03	0.45 ± 0.01	-
Pt2K750	0.96 ± 0.03	0.77 ± 0.02	0.35 ± 0.01	-
Pt4K700	1.03 ± 0.03	2.05 ± 0.06	0.90 ± 0.03	0.90 ± 0.03
Pt4K750	1.01 ± 0.03	1.60 ± 0.05	0.85 ± 0.03	-

3.3.2 Activity testing

The steam reforming activity was measured with a mixture of methane (5vol.%) and ethane (2.2vol.%). The reaction rates for both methane and ethane for a 20 hour period TOS are shown in Figure 3.1. Figure 3.1A shows the results for the unmodified Pt supported on yttrium stabilised zirconia (YSZ). The maximum reaction rate for ethane and methane was found during the initial stage of the experiment and the catalyst deactivated with about 30% in 20h for both reactants. The conversion at the initial stage was 70% for ethane and 28% for methane. The ratio between methane and ethane reaction rate remained constant at 0.81.

Influence of potassium on reforming of methane and ethane



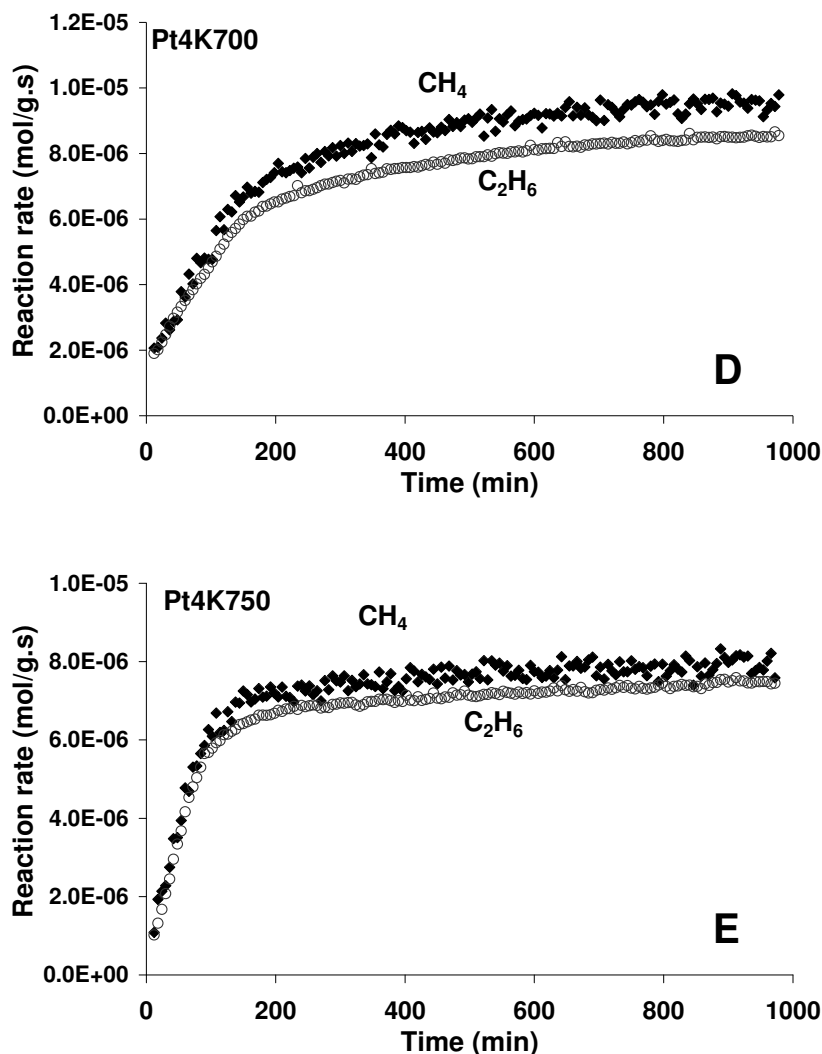


Figure 3.1: Reaction rates of a mixture of methane (\blacklozenge , 5vol.%) and ethane (\circ , 2.2vol.%) in steam reforming on PtYSZ (A) , Pt2K700 (B), Pt2K750 (C), Pt4K700 (D) and Pt4K750 (E)

Figure 3.1B to Figure 3.1E show the results of the steam reforming experiments with the methane/ethane mixture on the potassium-modified catalysts. These four catalysts showed a low initial activity for both reactants, but activity significantly increased during several hours. This phenomenon will be referred to as “activation” in the remainder of this paper.

The samples with the lower potassium amounts, namely Pt2K700 and Pt2K750 (Figure 3.1B and Figure 3.1C), activated within 200 minutes. After activation, methane and ethane reaction rates were fairly constant. A 10% decrease in the reaction rate in the final 800 minutes was noticed in the case of Pt2K700 (Figure 3.1B), while Pt2K750 (Figure 3.1C) showed a stable activity. The reaction rates

measured on Pt4K700 and Pt4K750 are shown in Figure 3.1D and Figure 3.1E. The activation for these two catalysts took longer, especially in case of Pt4K700, observing increasing activity during 1000 minutes. Continuation of the experiment for another 600 minutes showed no further changes in reaction rates (not shown). No deactivation was observed for both Pt4K700 and Pt4K750. The conversions of methane and ethane at maximum activity for Pt4K700 were 24% and 48%, respectively.

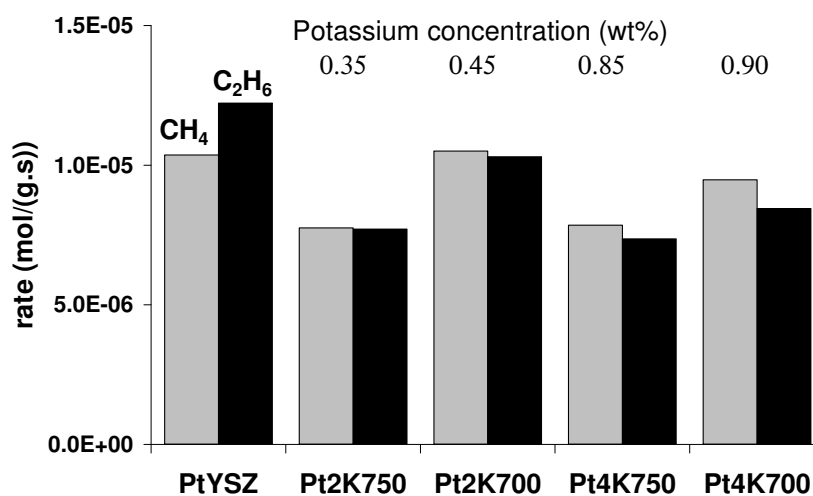


Figure 3.2: Overview of steam reforming reaction rates after stabilization in a mixture of methane (5vol.%) and ethane (2.2vol.%) for the catalysts shown in Figure 3.1

Figure 3.2 presents a comparison of the maximal reaction rates for both methane and ethane for all catalysts. The unmodified PtYSZ showed the highest activity expressed in mol per gram of catalyst per second. Both initial and final potassium content increases from left to right in Figure 3.2, and there is no obvious relation between the potassium content and the maximum rates. The maximum activity for the samples calcined at 700°C (Pt4K700 and Pt2K700) is 1.25 times higher than for the equivalent catalysts calcined at 750°C (Pt4K750 and Pt2K750). Interestingly, the relative reactivity of methane and ethane in the mixture is clearly influenced by the presence of potassium. As shown in Table 3.2, increasing the K concentration causes the ratio of reaction rates between methane and ethane (rate CH₄/ rate C₂H₆) to increase.

Table 3.2: Ratio of methane and ethane reaction rate on unmodified PtYSZ and potassium modified catalysts (5vol.% CH₄ / 2.2vol.% C₂H₆).

Catalyst	Ratio CH ₄ /C ₂ H ₆ converted
PtYSZ	0.81 ± 0.01
Pt2KYSZ750	1.00 ± 0.02
Pt2KYSZ700	1.02 ± 0.02
Pt4KYSZ750	1.07 ± 0.02
Pt4KYSZ700	1.12 ± 0.02

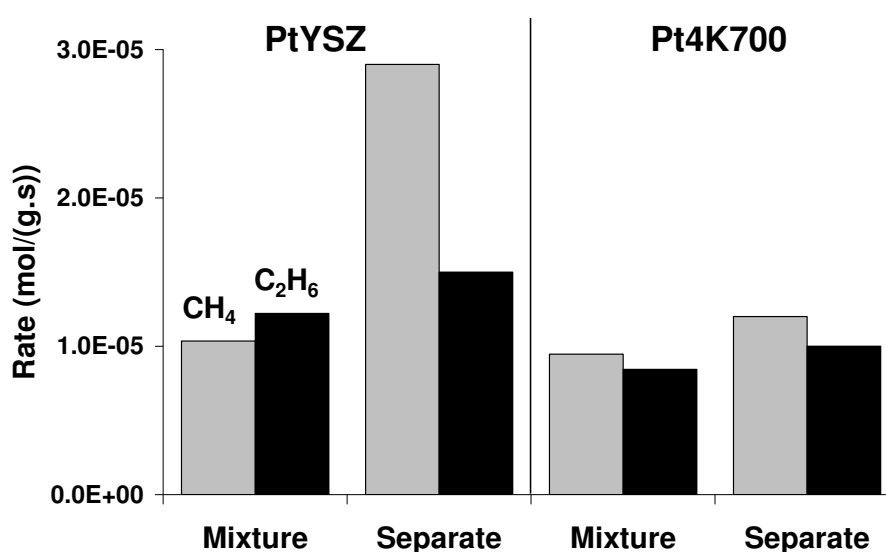


Figure 3.3: Reaction rates of methane (5vol.%) and ethane (2.2vol.%), when fed as a mixture versus fed separately on PtYSZ (left) and Pt4K700 (right).

In Figure 3.3, the reaction rates obtained with methane/ethane mixtures are compared with the reaction rates measured when feeding separately 5vol.% of methane or 2.2vol.% ethane for PtYSZ and Pt4K700. These experiments were performed with fully activated Pt4K700 and with fresh PtYSZ, respectively. The results clearly show that, operating with methane only, PtYSZ is almost 3 times as active for methane reforming as compared to feeding a mixture of methane and ethane. Interestingly on Pt4K700, the same effect is much smaller (factor 1.25). Moreover, while using the mixture both catalysts show similar methane and ethane conversion rates, Pt4K700 is about 2.5 times less active than PtYSZ for methane reforming when methane only is fed. For ethane the differences between operating with a mixture and separate feed are

smaller: the reaction rate of ethane fed separately is 1.23 times higher for PtYSZ and 1.18 times higher for Pt4K700 compared to the ethane conversion rate in the mixture.

Since the observed reaction rates of methane and ethane strongly depend on feed composition, a more detailed comparison of the effect of the composition of the mixtures on the performance of both catalysts is presented below.

Both catalysts were tested with varying ethane concentrations (0.74vol.% to 2.2vol.%) while keeping the methane concentration constant (7.7vol.%). The choice for these concentrations was based on keeping the carbon to H₂O ratio as close as possible to 1. In fact, it varies from 1.2 to 1.0. Pt4K700 was tested after activation and stabilization. To avoid influences of catalyst deactivation on PtYSZ, a water/Ar mixture was fed at reaction conditions for 15 minutes between measurements. This treatment was sufficient to fully reactivate the catalysts. Data were measured in random order and initial activities are reported for PtYSZ. The reaction rates and conversion for methane and ethane at 700°C are shown in Figure 3.5A (PtYSZ) and Figure 3.5B (Pt4K700).

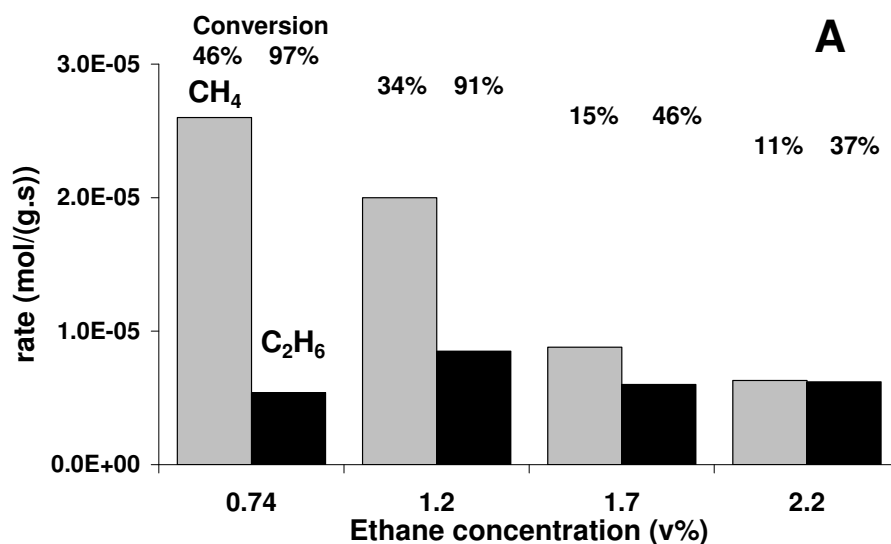


Figure 3.4A: Reaction rates and conversions for methane and ethane reforming on PtYSZ (A) in mixtures with constant methane concentration (7.7vol.%), varying the ethane concentration (0.74 – 2.2vol.%)

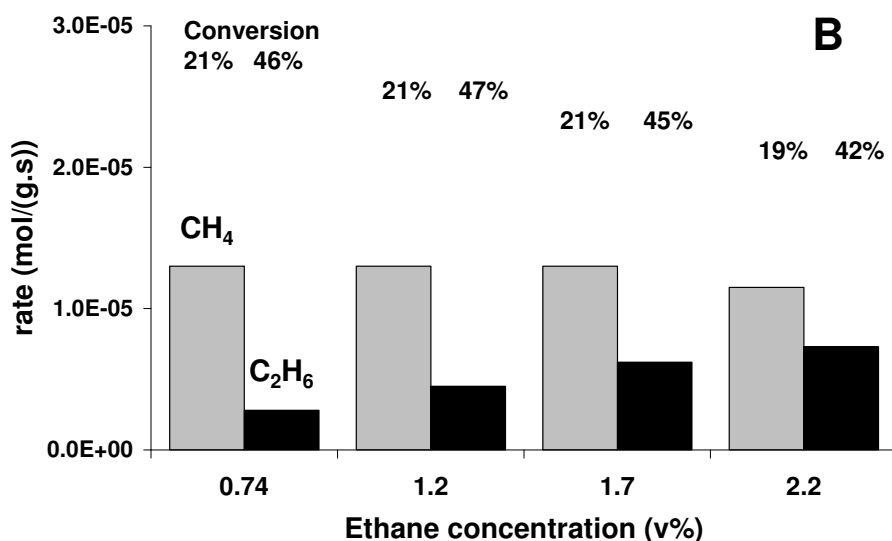


Figure 3.5B: Reaction rates and conversions for methane and ethane reforming on Pt4K700 (B) in mixtures with constant methane concentration (7.7vol.%), varying the ethane concentration (0.74 – 2.2vol.%)

For PtYSZ a high reaction rate for methane was observed at low ethane concentration (left side Figure 3.5A). The methane reaction rate reduced dramatically by a factor 4 when the ethane concentration was increased from 0.74 to 2.2vol.%. The methane conversion decreased from 46% to 11% in this range. No trend was observed in the ethane reaction rate and conversion. At low concentrations (0.74 and 1.2vol.%), ethane conversion was above 90%. Ethane conversion decreased to around 37%, when increasing the ethane concentration to 2.2vol.%. Further, the total number of hydrocarbon molecules converted per time over PtYSZ decreases with increasing carbon concentration in the feed.

On Pt4K700, the methane reaction rate was almost unaffected by increasing ethane concentration (Figure 3.5B), in contrast to PtYSZ. Only at the highest ethane concentration (2.2vol.%), methane reaction rate decreased by 10%. This almost constant reaction rate of methane also induces a constant conversion of 21% for the three lower concentrations of ethane, decreasing slightly to 19% when increasing ethane concentration to 2.2vol.%. The ethane reaction rate showed a linear increase with increasing concentration. Ethane conversion was constant around 45%. This indicates apparent first order behaviour of ethane reforming when fed together with

methane. Finally, in contrast to PtYSZ, the total number of molecules converted per time increased with increasing carbon concentration on Pt4K700.

The reaction rate of methane was higher than that of ethane on Pt4K700 for all conditions used in this series of experiments. Thus, Pt4K700 converts more methane than ethane when methane is present in excess. To investigate the behaviour of this catalyst with similar methane and ethane concentrations, methane concentrations were varied between 2.4 to 7.7vol.%, keeping the ethane concentration constant at 2.2vol.%. The results are shown in Figure 3.6. Other experiments (not shown here) demonstrated that changing the water to carbon ratio in this range did not influence reaction rates found on Pt4K700.

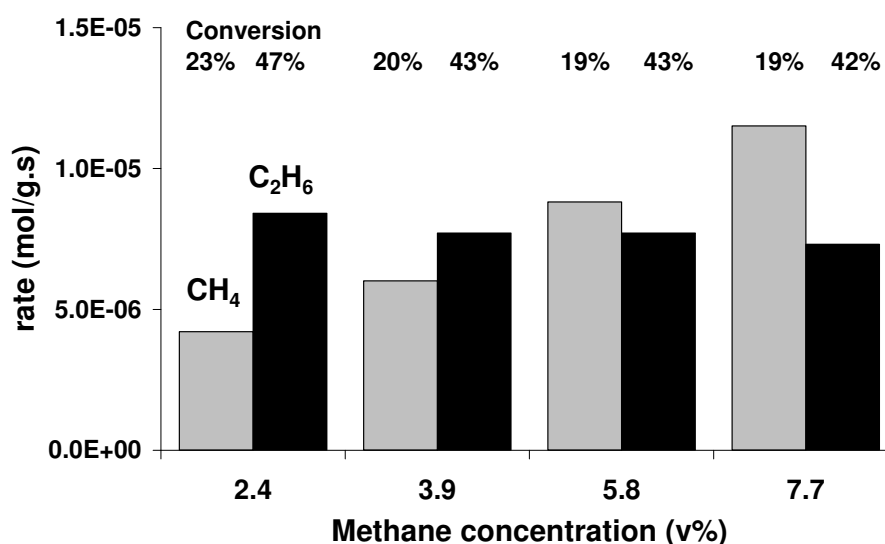


Figure 3.6: Reaction rates and conversion for methane and ethane on Pt4K700 in mixtures with constant ethane concentration (2.2vol.%) and variable methane concentration (2.4 – 7.7vol.%)

In the experiments shown in Figure 3.6, clearly the ethane reaction rate was hardly affected when increasing the methane concentration. Thus, the conversion of ethane was almost constant, only decreasing from 46% to 42% with increasing methane concentration from 2.4 to 7.7vol.%. Further, the reaction rate of methane increased linearly with methane concentration, indicating apparent first order in methane. Again, the total number of molecules converted increased with increasing hydrocarbon concentration.

Figure 3.7 shows the ratio of methane to ethane rates of conversion for PtYSZ and Pt4K700 as a function of the inlet $\text{CH}_4/\text{C}_2\text{H}_6$ ratio from experiments, varying both CH_4 and C_2H_6 concentrations. Only at very high methane/ethane inlet ratio (10.4), PtYSZ converts more methane than Pt4K700. In agreement, reforming of methane only (Figure 3.3) shows a higher reaction rate on the unmodified catalyst. For all other conditions, Pt4K700 showed an improved methane to ethane ratio.

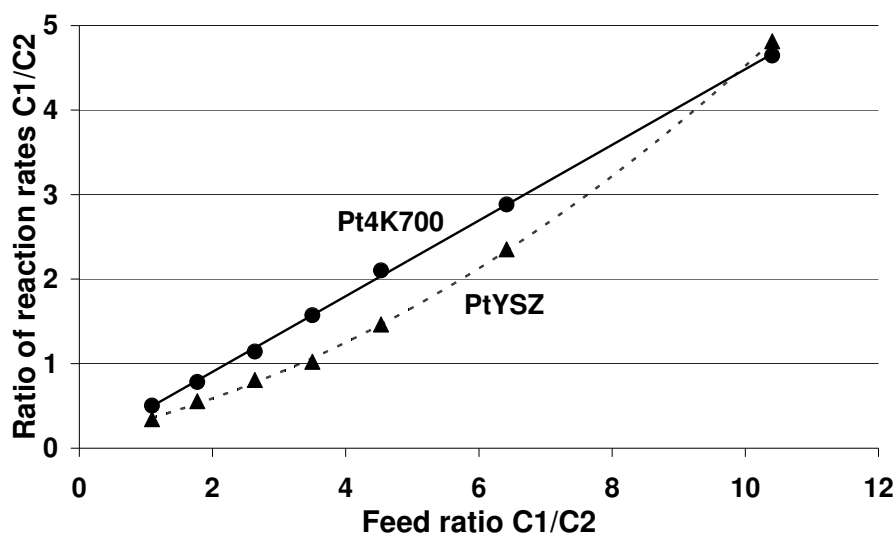


Figure 3.7: Ratio of reaction rates of methane/ethane as a function of methane/ethane feed ratio in steam reforming on PtYSZ and Pt4K700

3.4 Discussion

The addition of potassium to Pt supported on yttrium stabilised zirconia (YSZ) showed several effects on the catalytic performance in steam reforming of ethane and methane: 1. activation with TOS was observed, 2. maximum catalyst activity decreased, 3. the ratio between methane and ethane reaction rates changed and 4. the competition between hydrocarbons decreased. Each of these phenomena will be discussed below.

3.4.1 Activation behaviour of potassium modified catalysts

Clearly, the activity of the potassium modified catalysts increased with TOS, (Figure 3.1B to Figure 3.1E), while the unmodified catalyst deactivated during the whole experiment (Figure 3.1A). The time needed for activation is determined by the initial potassium content: with more potassium added, the time needed to reach steady state increased. Catalysts calcined at 700°C had a higher initial potassium content than the catalysts calcined at 750°C (Table 3.1) and consequently showed a longer activation period, ranging from 200 to 800 minutes. It was also found that potassium was removed during the activation process (Table 3.1). This can be explained by evaporation of K via the formation of volatile hydroxides at temperatures around 700°C [17]. It should be noted that after the activation period no further potassium evaporation between 20 and 85 hours of reaction (Table 3.1) was detected for Pt4K700. Although the concentration of K stabilized, very slow removal of K cannot be excluded, as the maximal time-on-stream was limited to 85 hours in this study.

It was noticed that the unmodified PtYSZ deactivated with TOS, whereas potassium addition led to a stable performance after an initial activation period (Figure 3.1A to Figure 3.1E). It is well known that potassium promotes the activation of water [18, 19], which helps to remove hydrocarbon fragments from the surface. This could explain stable performance over a longer period of time, in agreement with the observation that PtYSZ could be easily regenerated in a stream of 12vol.% water in Argon for 15 minutes at 700°C.

3.4.2 Activity of the catalysts

Figure 3.3 clearly shows a lower activity for the stabilized potassium modified catalysts during steam reforming of the single hydrocarbons ethane and methane as

compared to the unmodified PtYSZ catalyst. Potassium addition decreased the activity for methane decreased by 60%, while for ethane the effect was somewhat less, about 33%. In ethane/methane mixtures, the effect of added potassium is only visible at relative low ethane/methane ratios (Figure 3.5). The decreased activity is in agreement with results of Trimm and Rostrup-Nielsen [13, 14], who reported lower reactivity by more than one order of magnitude when adding potassium to Ni catalysts on several supports.

3.4.3 Influence of potassium on reaction ratio of CH_4/C_2H_6

The relative reactivity of methane and ethane is also influenced by potassium as shown in Figure 3.1A to Figure 3.1E and Table 3.2. It appears that the unmodified catalyst converted more ethane than methane (Figure 3.1A). The reaction rate of methane was close to the ethane reaction rate for low potassium amounts (Figure 3.1B and Figure 3.1C). For higher potassium amounts, the methane reaction rate is even higher than the ethane reaction rate (Figure 3.1D and Figure 3.1E). Interestingly, for all catalysts, a constant ratio of reaction rates of methane and ethane was found during the experiments. In addition, Figure 3.7 shows that the actual ratio of methane/ethane rates of conversion depends on the inlet methane/ethane ratio. Pt4K700 converts more methane than PtYSZ, when the methane/ethane inlet ratio is below 10. However, PtYSZ is more active for methane than Pt4K700 in case of high excess of methane. This agrees with Figure 3.3 showing higher methane reaction rates on PtYSZ when no ethane is present.

In Figure 3.8, the ratio of methane and ethane reaction rates from Table 3.2 is related to the potassium content for all catalysts in the activated state (Table 3.1). A linear relationship was found between the ratio of reaction rates of methane and ethane and the potassium content in the activated state. Moreover, the additional potassium present in the fresh catalyst, which evaporates during activation, does not influence the ratio between methane and ethane reaction rate, since this was constant during activation (Figure 3.1B to Figure 3.1E).

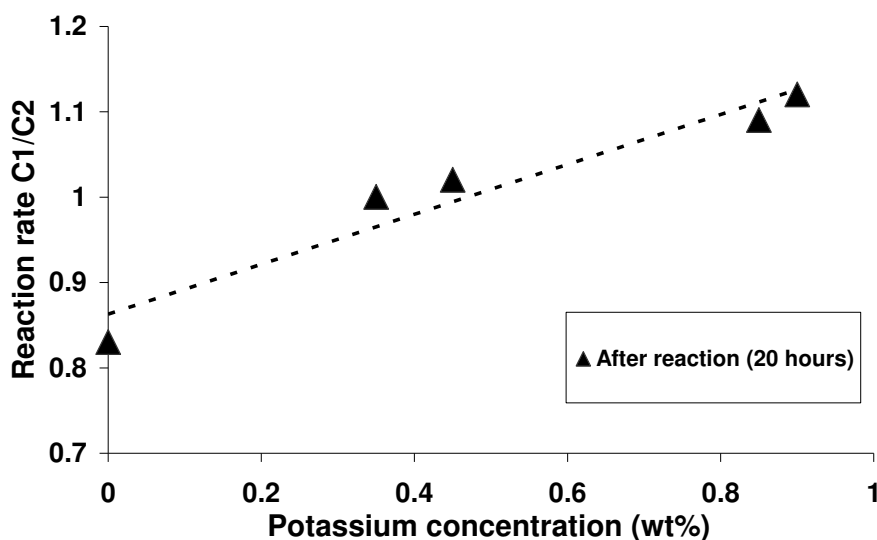


Figure 3.8: Ratio of methane reaction rate and ethane reaction rate, related to PtYSZ and potassium modified catalysts in activated state

3.4.4 Competition effects in hydrocarbon mixtures

Finally, addition of ethane had a drastic effect on the conversion of methane on PtYSZ (Figure 3.3, Figure 3.5A). Ethane and methane obviously compete for the same reactive Pt-sites and limit each others conversion: conversions of both components decreased. Consequently, high conversion of methane on Pt/YSZ is only possible in the absence of ethane and at low ethane concentrations (Figure 3.3, Figure 3.5A).

On Pt4K700, this behaviour was not observed. Methane and ethane seem to react independently and both showed first order behaviour when mixed (Figure 3.5B, Figure 3.6). Within the applied concentration range, increasing the concentration of one component hardly affected the other component's reaction rate. Further, Figure 3.3 shows that the reaction rates of methane or ethane separately on an activated potassium catalyst are similar to the rates in the mixture.

The initial aim of this study was to find a catalyst in which methane is effectively converted while the steam reforming of ethane is limited. The present results show that indeed the ratio of methane reaction rate to ethane reaction rate is improved when adding potassium to PtYSZ, via suppression of competition effects between the two reactants. As a result methane conversion is boosted compared to ethane.

Unfortunately, ethane conversion is hardly suppressed by the addition of potassium. A catalyst that clearly suppresses ethane conversion would be needed to make the overall concept of oxidative coupling combined with steam reforming applicable.

Nevertheless, the results show an unexpected effect of potassium on the catalytic behaviour of supported platinum catalysts. The most important conclusion in this respect is that potassium is able to prevent competitive behaviour between methane and ethane. The origin of this intriguing effect is currently investigated by characterization with FT-IR spectroscopy and will be the scope of a future publication.

3.5 Conclusion

The addition of potassium has a significant effect on the steam reforming of methane and ethane. Similar to results on Ni catalysts reported in literature, potassium improves catalyst stability at the expense of decreasing catalyst activity. The potassium modified catalysts activated with TOS which was attributed to partial potassium evaporation during steam reforming. Importantly, this study shows that the steam reforming rates of methane and ethane are affected quite differently by the presence of potassium. Potassium prevents inhibition of methane steam reforming by the presence of ethane. The reaction rate ratio in methane/ethane mixtures is changed from preferential ethane reforming on PtYSZ towards preferential methane conversion as a result of addition of potassium.

3.6 References

- [1] P.O. Graf, B.L. Mojet, J.G. van Ommen, L. Lefferts, *Applied Catalysis A: General* 332 (2007) 310-317.
- [2] D.L. Trimm, *Catalysis Today* 37 (1997) 233.
- [3] J.H. Bitter, W. Hally, K. Seshan, J.G. van Ommen, J.A. Lercher, *Catalysis Today* 29 (1996) 349-353.
- [4] J.H. Bitter, K. Seshan, J.A. Lercher, *Journal of Catalysis* 171 (1997) 279.
- [5] M.E.S. Hegarty, A.M. O'Connor, J.R.H. Ross, *Catalysis Today* 42 (1998) 225.
- [6] A.M. O'Connor, J.R.H. Ross, *Catalysis Today* 46 (1998) 203.
- [7] J.H. Sinfelt, *Journal of Catalysis* 27 (1972) 468-&.
- [8] J.H. Sinfelt, D.J.C. Yates, *Journal of Catalysis* 10 (1968) 362-&.
- [9] J.H. Sinfelt, D.J.C. Yates, *Journal of Catalysis* 8 (1967) 82-&.
- [10] J. Sehested, *Catalysis Today* 111 (2006) 103-110.
- [11] J.W. Snoeck, G.F. Froment, M. Fowles, *Industrial and Engineering Chemistry Research* 41 (2002) 3548-3556.
- [12] J. Juan-Juan, M.C. Roman-Martinez, M.J. Illan-Gomez, *Applied Catalysis A: General* 301 (2006) 9-15.
- [13] D.L. Trimm, *Catalysis Today* 49 (1999) 3.
- [14] J.R. Rostrup-Nielsen, *Journal of Catalysis* 31 (1973) 173.
- [15] M. Matsumura, C. Hirai, *Journal of Chemical Engineering of Japan* 31 (1998) 734.
- [16] M. Ferrandon, J. Mawdsley, T. Krause, *Applied Catalysis A: General* In Press, Corrected Proof.
- [17] R.J. Berger, E.B.M. Doesburg, J.G. van Ommen, *Journal of the Electrochemical Society* 143 (1996) 3186-3191.
- [18] F. Frusteri, S. Freni, V. Chiodo, L. Spadaro, O. Di Blasi, G. Bonura, S. Cavallaro, *Applied Catalysis A: General* 270 (2004) 1-7.
- [19] D. Sutton, B. Kelleher, J.R.H. Ross, *Fuel Processing Technology* 73 (2001) 155-173.

Chapter 4

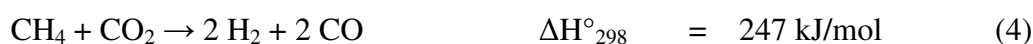
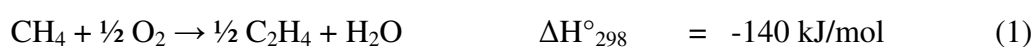
The effect of potassium addition to Pt supported on YSZ on steam reforming of mixtures of methane and ethane

Abstract

The influence of potassium addition on Pt supported on yttrium-stabilized zirconia (YSZ) was studied with FT-IR CO adsorption and CO FT-IR TPD, in order to understand the effect of potassium on the performance of the catalyst in reforming of mixtures of methane and ethane. Potassium modification of PtYSZ strongly influenced the conversion and rate determining steps in methane and ethane in steam reforming. Water activation is the rate determining step on PtYSZ, resulting in high surface coverage of hydrocarbon fragments during steam reforming of mixtures of methane and ethane. This led to blocking of active sites by ethane fragments and consequently low conversion of methane. If potassium is added to the catalyst, hydrocarbon activation on Pt is rate determining, resulting in low surface coverage of methane and ethane. As a result, competition effects of methane and ethane diminished on potassium modified PtYSZ, enabling simultaneous conversion of methane and ethane. The weakening of the interaction of the hydrocarbons with the Pt surface as a result of potassium addition is supported by the fact that the interaction with CO is weakened, as observed with FT-IR TPD.

4.1 Introduction

Natural gas, mainly consisting of methane, is available in large quantities and is becoming one of the major resources for energy and chemicals. A new concept for utilization of methane has been proposed by us, as discussed in detail in earlier work [1, 2]. Shortly, the intention is to combine oxidative coupling and inevitable combustion with reforming reactions of methane (equations (1) to (4)) in one multifunctional auto thermal reactor. This should lead to production of ethylene and synthesis gas in one auto thermal process, in which the energy released in reactions (1) and (2) is used to reform methane through reactions (3) and (4).



For the complete process, two catalysts are needed, one for oxidative coupling and one for the reforming reaction. This paper reports about the steam reforming step (3) of the mixture produced in the oxidative coupling, containing methane, ethane and ethylene. All these hydrocarbons are reactive in steam-reforming [3]. The main challenge in this project is to prevent or limit the steam reforming of ethane and ethylene, while methane should be effectively converted.

Pt supported on zirconia proved to be a stable catalyst in steam and dry reforming of methane [4-7]. In earlier research [2], Pt supported on yttrium stabilized zirconia (YSZ) was found to be the most suitable metal catalyst for steam reforming of single reactants. However, in mixtures of hydrocarbons methane conversion was suppressed by presence of ethane or ethylene [1]. It also was demonstrated that the presence of potassium on PtYSZ (Pt4K700) prevents competition between methane and ethane during steam reforming and relatively more methane can be converted [1]. In accordance with literature [8-12], potassium modified catalysts initially showed low activity. Potassium modified catalysts activated with TOS (Time On Stream), which

was attributed to partial evaporation of potassium during steam reforming. In the present paper, the characterization of the catalysts is discussed.

An easily accessible technique to study the surface properties of supported platinum catalysts is the adsorption of CO [13-15] (and references therein). The addition of potassium to noble metal catalysts is known to influence the electronic structure of the surface atoms via modification of the metal particle potential [16-20]. In turn, the electronic properties of the metal particle have been related to their catalytic properties in hydrogenolysis, hydrogenation and oxidation reactions [13-15, 21]. Usually characterization studies are performed on small metal particles (few nanometers). However, in the present study, the relevant temperature window for steam reforming is between 700°C and 800°C, because of the integrated operation of reforming and oxidative coupling. This means that Pt particles are relatively large (10-100 nm); with the lower number of surface sites characterization becomes a challenging issue.

In this paper, reactivity of methane and ethane in steam reforming on PtYSZ and potassium modified PtYSZ is investigated and the catalysts are characterized with FT-IR spectroscopy. TPD of CO on unmodified PtYSZ and potassium modified PtYSZ is used to estimate trends in the adsorption strength of methane and ethane. Also reaction kinetics of steam reforming of mixtures of methane and ethane on PtYSZ and Pt4K700 are investigated and related to the characterization data, resulting in an explanation why potassium is preventing reactant competition between methane and ethane.

4.2 Experimental

Yttrium stabilized zirconia (YSZ), obtained from TOSOH (TZ-8Y) was used as support and was modified with 4wt.% potassium. About 15g of YSZ was impregnated with 15 ml of an aqueous K_2CO_3 solution, containing 1g of K_2CO_3 and calcined in synthetic air (30ml/min) for 4 hours at 600°C (temperature ramp 5°C min⁻¹).

Subsequently, 1wt% of Pt was impregnated on 10g of support with a H_2PtCl_6 (Alfa Aesar) solution containing 0.01g Pt per ml aqueous solution. PtYSZ was calcined at 750°C. The potassium modified samples were calcined at two different temperatures, 700°C and 750°C respectively. Catalysts were calcined in synthetic air (30ml/min) during 15h (ramp 5°C min⁻¹). Next to PtYSZ, two potassium modified catalysts were used, designated by initial potassium content (wt.%) and calcination temperature: Pt4K700 and Pt4K750.

Activity tests were carried out in a micro reactor flow setup. The reactor consisted of a quartz tube with inner and outer diameter of respectively 4 and 6mm. Catalyst particles with a diameter between 0.3 and 0.6mm were used, resulting in a pressure drop around 0.1bar, when 200mg of catalyst was loaded between quartz wool plugs. The samples were heated to 500°C in argon and reduced in 2.5vol.% H_2 (Indugas 5.0) / Ar for 1h (flow rate: 200ml/min) before measuring the catalytic performance. No significant activity for steam reforming of methane and ethane was found for the support material YSZ at 700°C. Also the occurrence of gas phase reactions could be excluded based on experiments with quartz particles of 0.3 to 0.6 mm.

Methane (Hoekloos 4.5) and ethane (Indugas 4.0) were mixed with argon (Hoekloos 5.0) to a total flow rate of 200ml.min⁻¹. Measurements were performed at 700°C. Water was added to the gas mixtures with a Bronkhorst controlled evaporator mixer (CEM) in combination with a Liquiflow controller. To ensure constant space velocity, Ar flow was adjusted when water concentrations were changed. A 15 minute treatment of 11 vol.% water in Argon was applied between the separate experiments on PtYSZ to regenerate the catalyst. The product and reactant gas composition was analyzed with a Varian 3800 Gas Chromatograph equipped with two columns (Molsieve 5A and PoraPlotQ) and two TCD detectors. Water was analyzed in the PoraPlotQ column; the Molsieve column was protected against water by a PoraPlotQ

pre-column and a backflush system. Argon was used as internal standard to correct for volume changes during reaction.

Elemental composition of the catalysts was determined with XRF on a Philips PW 1480 X-ray spectrometer. The structure of the catalysts was studied with X-ray diffraction with a Philips PW1830 diffractometer using Cu K α radiation, $\lambda=0.1544\text{nm}$. XRD was performed in reflection geometry in the 2θ range between 20° and 70° . Average Pt particle size was estimated using the Scherrer equation [22]. Before XRD analysis of spent catalysts, samples were cooled to room temperature in He and exposed to air.

The transmission FT-IR CO adsorption measurements were carried out on a Bruker Vector 22 with MCT detector. A self supporting pellet was pressed, using 15 mg of the catalyst. Before measurements the samples were reduced in 5 vol.% H₂ at 400°C and subsequently cooled to room temperature in He. CO (Linde Gas 4.7) was absorbed at room temperature and subsequently desorbed with a heating rate of $2^\circ\text{C}/\text{min}$.

4.3 Results

4.3.1 Catalyst characterization

It was reported in an earlier paper [1] that potassium modified catalysts activated with time on stream during reforming of methane and ethane mixtures. The reaction rates initially increased and stabilized after 200 to 800 minutes of reforming of the methane and ethane mixture (a longer activation period was required with higher initial potassium content of the catalysts). The initial period of increasing activity will be referred to as “activation” in this paper. Potassium modified catalysts tested or characterized after activation are indicated with “act”. Catalysts indicated with “fresh” were tested or characterized directly after calcination. The unmodified PtYSZ was tested and characterized in fresh state. PtYSZ showed initially the highest activity and slowly deactivated as a result of carbon formation [1]. After measuring the performance of PtYSZ for one specific set of experimental conditions, the catalyst was regenerated following the procedure described in [1], before the next experiment was performed.

Table 4.1 shows the Pt particle size for all catalysts, measured by XRD-Line Broadening. All catalysts show Pt particles between 30 and 40 nm. Calcination of potassium modified PtYSZ at 700°C results in smaller Pt particles than calcination at 750°C (Table 4.1). It is also shown in Table 4.1 that Pt particle size remained unchanged during activation for both Pt4K700 and Pt4K750.

Potassium contents of fresh and used catalysts, as measured with XRF before and after steam reforming reaction, are given in Table 4.1. The potassium samples were initially impregnated with 4wt.% of potassium, and it was observed that calcination temperature influences the remaining potassium content. Calcination at 700°C leads to 2.05wt.% of potassium, Calcination at 750°C results in only 1.6 wt.% remaining. About 50% of the potassium is lost on Pt4K700 and Pt4K750 during activation.

Table 4.1: Pt particle size determined by XRD and potassium content determined by XRF for PtYSZ, Pt4K700act, Pt4K700fresh, Pt4K700act and Pt4K750initial

Catalyst	Pt content wt. %	Average Pt particle size	Potassium content wt. %
PtYSZ*	1.04 ± 0.03	32 ± 1 nm	-
Pt4K700act	1.03 ± 0.03	30 ± 2 nm	0.90 ± 0.03
Pt4K700fresh	1.03 ± 0.03	31 ± 3 nm	2.05 ± 0.06
Pt4K750act	1.01 ± 0.03	38 ± 3 nm	0.85 ± 0.03
Pt4K750fresh	1.01 ± 0.03	38 ± 3 nm	1.60 ± 0.05

*calcined at 750°C

The FT-IR spectra of adsorbed CO to characterize the accessible Pt surface are shown in Figure 4.1. Results of potassium modified samples are shown here for Pt4K700. For all samples 15 mg of catalyst was used.

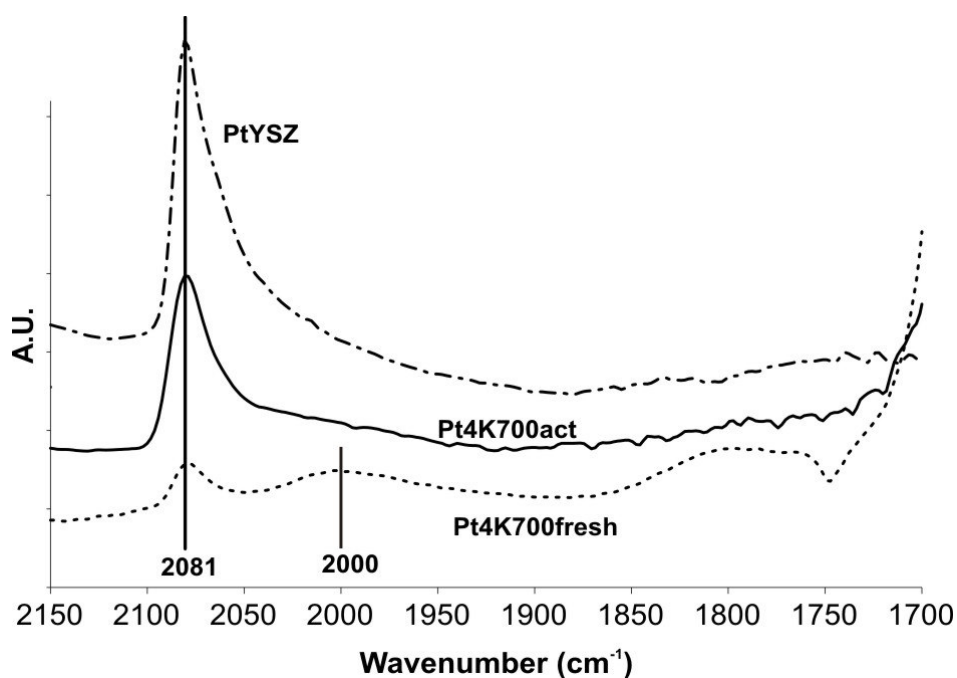


Figure 4.1 FT-IR CO adsorption spectra at room temperature for PtYSZ, Pt4K700fresh and Pt4K700act

PtYSZ, Pt4K700act and Pt4K700fresh all showed a band at 2081 cm⁻¹, attributed to CO linearly adsorbed on Pt [23]. This band had a low intensity on Pt4K700fresh. Further, a broad band around 2000 cm⁻¹ was found on Pt4K700fresh, which was assigned previously to a direct ion-dipole interaction between K⁺ and linear CO [24, 25]. Also, a broad band around 1800 cm⁻¹ was found on Pt4K700fresh, ascribed to CO coordinated in bridged position. Pt4K700act shows a larger peak at 2081cm⁻¹

compared to Pt4K700fresh, while the bands at 2000cm^{-1} and 1800cm^{-1} were absent. The total integrated intensities for the different peaks are given in Table 4.2. It should be noted that the area of the peak around 1800 cm^{-1} on Pt4K700 fresh is less accurate, as the large peak around 1700 cm^{-1} might partially contribute to its intensity. Clearly, on Pt4K700act, the peak at 2081cm^{-1} increased by a factor 5 compared to Pt4K700fresh. The total peak area of Pt4K700act is still significantly smaller than of PtYSZ.

Table 4.2: Peak area between 2100cm^{-1} and 1900cm^{-1} of FT-IR CO spectra of PtYSZ, Pt4K700act and Pt4K700fresh as shown in Figure 4.1 (Integration interval between brackets).

Catalyst	Band 2081cm^{-1}	Band 2000cm^{-1} (2030-1950)	Band 1800cm^{-1} (1880-1750)
PtYSZ	0.49 (2100-2000)	-	-
Pt4K700act	0.32 (2100-2000)	-	-
Pt4K700fresh	0.06 (2090-2050)	0.07	0.28

4.3.2 CO desorption

Figure 4.2a shows IR spectra of linearly adsorbed CO in a TPD experiment on PtYSZ. The first spectrum was taken at 35°C (used in Figure 4.1). The peak shifted to lower wave numbers with increasing temperature. This can be explained by reduced dipole-dipole coupling, as a result of lower surface coverage of CO [26]. At 99°C the peak maximum was observed at 2070cm^{-1} . More pronounced loss of intensity was observed when heating above 99°C and CO desorption is completed at 219°C .

Figure 4.2b shows IR spectra of linearly adsorbed CO on Pt4K700act as a function of temperature. The first spectrum was taken at 25°C and shows linear Pt-CO adsorption at 2081 cm^{-1} . The peak was shifted to 2073cm^{-1} when increasing temperature to 73°C , while the peak reduced around 10% in intensity. More pronounced desorption starts already at 73°C and is complete at 89°C .

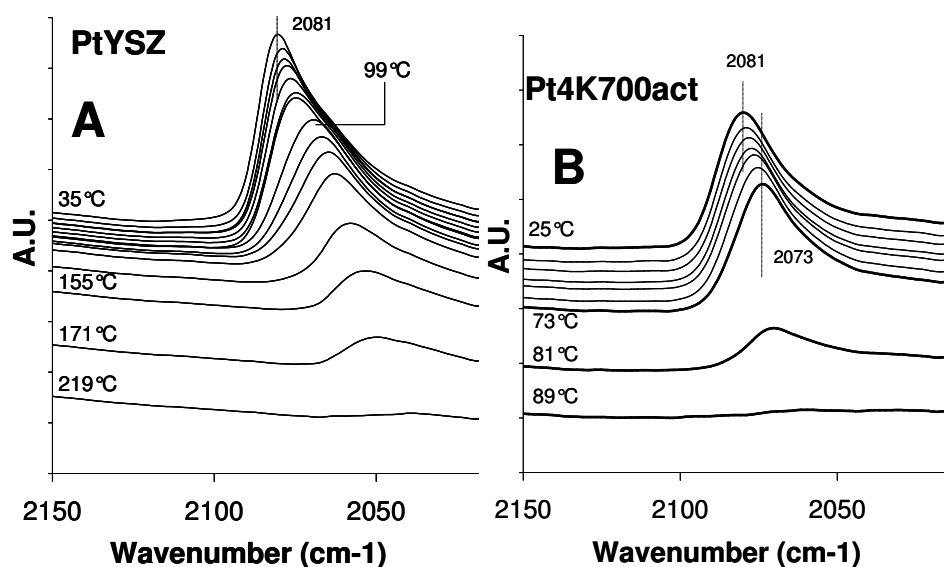


Figure 4.2: CO desorption on PtYSZ (A) and Pt4K700act (B) versus temperature, monitored by Transmission FT-IR spectroscopy. Heating rate was 2°C/min and spectra are shown every 8°C, unless indicated otherwise in Figure A.

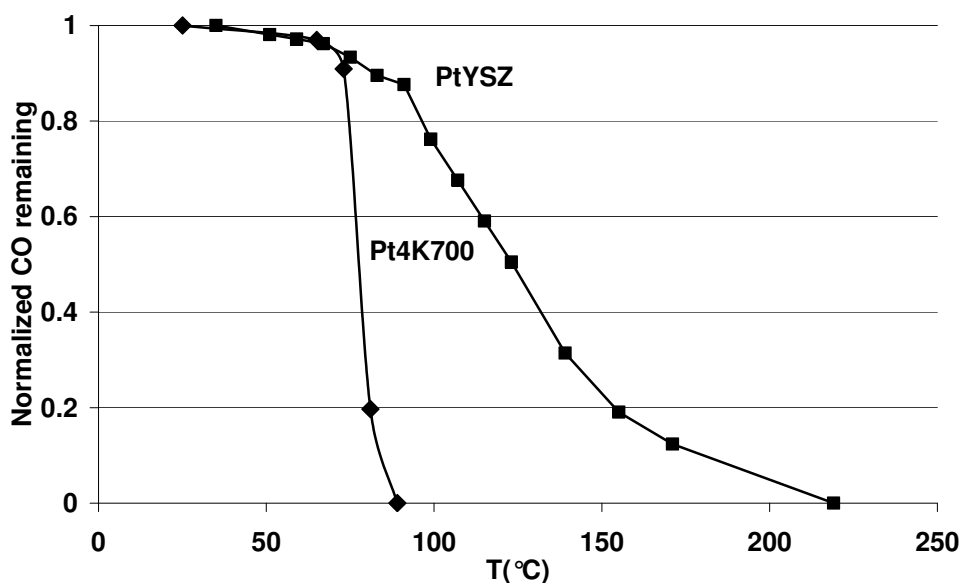


Figure 4.3: Remaining normalized CO on PtYSZ and Pt4K700 as a function of temperature.

Figure 4.3 shows the remaining CO fraction as a function of temperature obtained by integrating the peak area of the spectra shown in Figures 4.2a and 4.2b, defining the initial surface coverage as 1. On Pt4K700 CO desorption started approximately 25°C lower in temperature than on PtYSZ. Desorption of Pt4K700 is completed at 90°C,

while on PtYSZ more than 200°C is needed to achieve total desorption. Separate TPD experiments in a dedicated TPD apparatus equipped with a mass spectrometer confirmed the difference in temperatures necessary to desorb CO from PtYSZ and Pt4K700 (not shown).

4.3.3 Catalyst performance

Table 4.3 shows the reaction rates for methane and ethane as obtained in steam reforming experiments of a mixture of methane (5vol.%) and ethane (2.2vol.%) in argon. The corresponding figures and more detailed results have been published earlier [1] and are reported here for clarity reasons. As shown in Table 4.3, reaction rates for both methane and ethane are increasing on potassium modified catalysts with time on stream. It was also demonstrated that, depending on initial potassium content of the catalysts, stabilization of the rates was reached after 200 to 800 minutes of reforming of the methane and ethane mixture [1]. The experiments reported in this paper are performed on Pt4K700 after the initial activation, thus in stabilized state.

Table 4.3: Reaction rates in mixture of methane (5vol.%) and ethane (2.2vol.%) for PtYSZ, Pt4K700act, Pt4K700fresh, Pt4K750act and Pt4K750fresh. Conditions: 200 mg catalyst, 200 ml/min total flow, 700°C, water concentration 12vol.%

Catalyst	Reaction rate CH ₄ *10 ⁻⁶ (mol/g.s)	Reaction rate C ₂ H ₆ *10 ⁻⁶ (mol/g.s)	Ratio of reaction rates (CH ₄ /C ₂ H ₆)
PtYSZ	10	12	0.83
Pt4K700act	9.4	8.5	1.11
Pt4K700fresh	2.1	1.9	1.11
Pt4K750act	7.8	7.2	1.08
Pt4K750fresh	1.	1.0	1.10

The influence of varying the water concentration on the reaction rates of methane and ethane in the feed was compared on Pt4K700act and PtYSZ. The results for PtYSZ with a mixture of methane (4.5vol.%) and ethane (1.7vol.%) are shown in Figure 4.4.

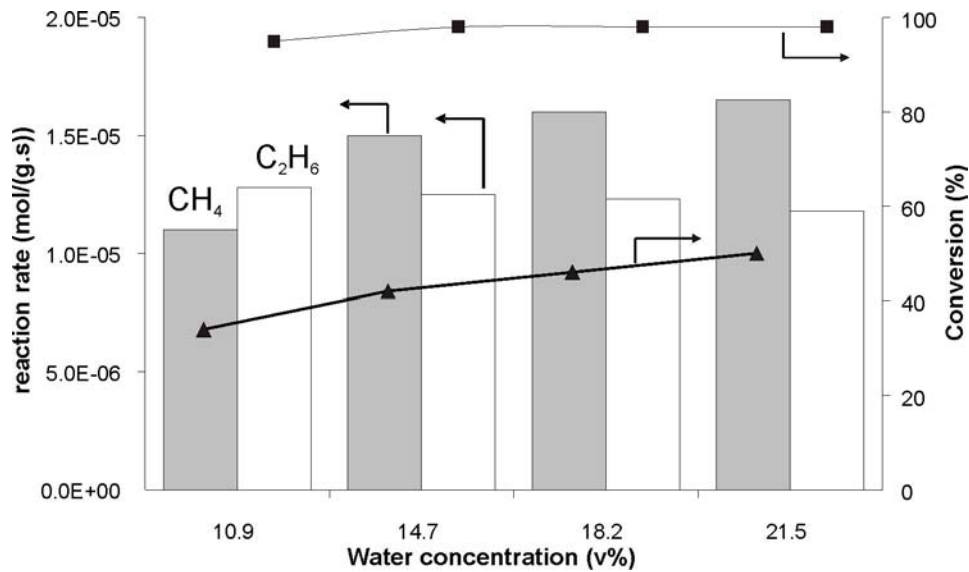


Figure 4.4: Reaction rates (bars) and conversions (markers) in steam reforming of a mixture of methane (\blacktriangle , 4.5vol.%) and ethane (\blacksquare , 1.7vol.%) on PtYSZ versus water concentration

It can be seen that the reaction rate of methane is increasing with increasing water concentration. Methane conversion increases from 34 to 50% when increasing the water concentration from 10.9 to 21.5vol.%. Ethane conversion was almost complete for water concentrations of 14.7vol.% and higher.

It should be noted that by changing the water concentration at identical hydrocarbon concentration, the water to carbon ratio changes, which could influence the reaction rates as well. For this reason, additional experiments were performed to separate effects of ethane concentration and the water to carbon ratio. In the experiments shown in Figure 4.5, water concentration was changed from 12 to 20 vol.%, while water/carbon ratio was kept constant at 1.8 by adjusting the ethane concentration.

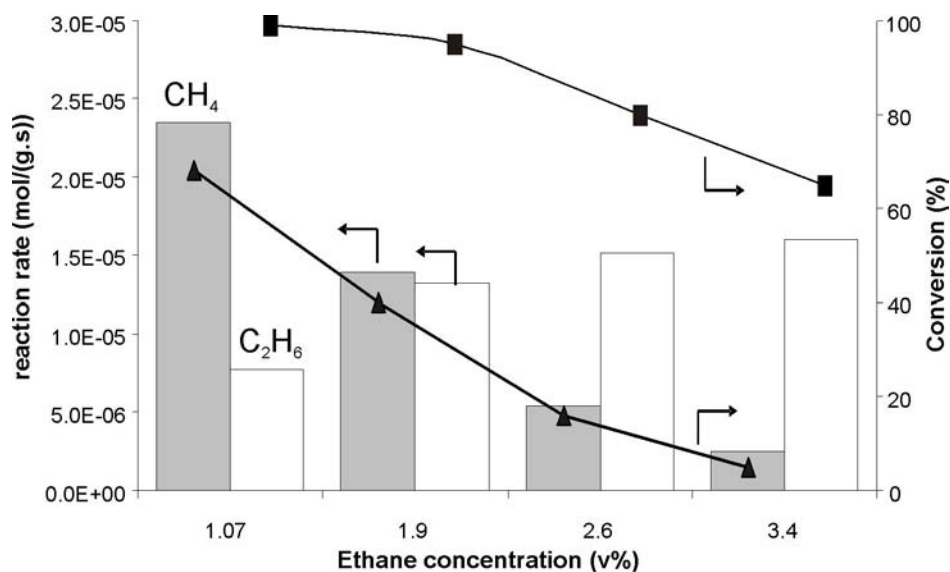


Figure 4.5: Reaction rates (bars) and conversions (markers) in steam reforming of a mixture of methane (\blacktriangle , 4.5 vol.%) and ethane (\blacksquare , 1.07 to 3.4 vol.%) on PtYSZ. Water/carbon ratio 1.8 and water concentration increased from left to right: 12, 15, 18 and 20 vol.%.

Methane concentration was kept constant at 4.5 vol.% and ethane was varied between 1.07 and 3.4 vol.%. This means that the methane/ethane feed ratio was changed from 4.3 to 1.3. At an ethane concentration of 1.07 vol.%, a methane reaction rate of $2.3 \cdot 10^{-5}$ mol/g.s was found, corresponding to a conversion of 68%. Methane conversion was decreasing down to 5% when ethane concentration was increased to 3.4 vol.%. It should be noted that the methane concentration was not changed. Ethane conversion level decreased from 98% at 1.07 vol.% to 65% at 3.4 vol.%.

A second series of experiments with constant water concentration (18 vol.%) and constant water to carbon ratio (1.8) was also carried out (not shown). The ratio of methane to ethane feed was changed from 1.1 to 5.7, keeping the total carbon concentration constant. It was found that the total carbon conversion (calculated in moles of C converted) increased with increasing methane to ethane ratio (not shown).

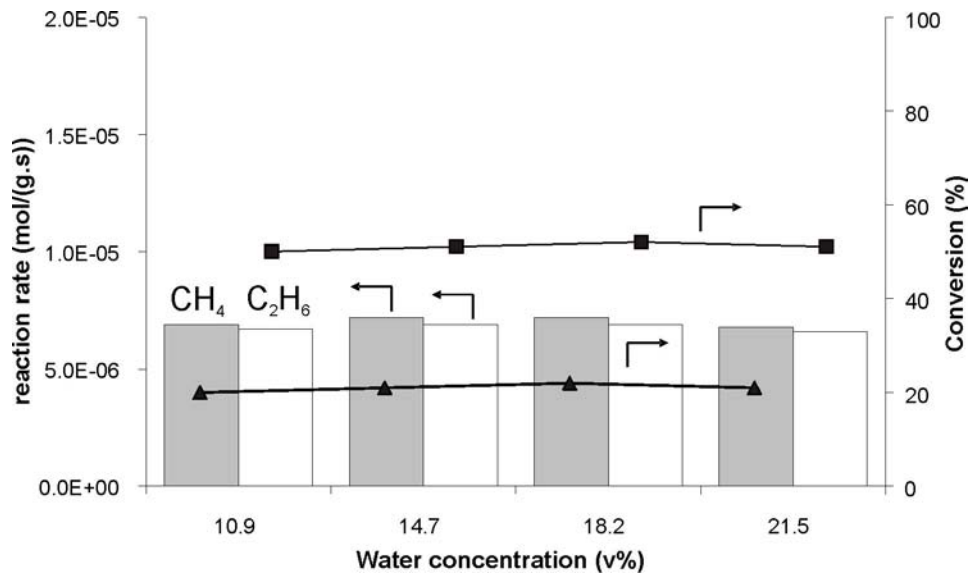


Figure 4.6: Reaction rates (bars) and conversions (markers) in steam reforming of a mixture of methane (■,4.5vol.%) and ethane(▲,1.7vol.%) on Pt4K700act versus water concentration

Figure 4.6 shows the influence of varying water concentration in steam reforming of a methane (4.5 vol.%) and ethane (1.7 vol.%) mixture on Pt4K700act. Water concentration was varied between 10.9 and 21.5vol.%. In this series of experiments reaction rates of methane and ethane were independent of the water concentration and thus conversions were constant, respectively 49% for ethane and 22% for methane.

4.4 Discussion

Potassium modified and unmodified PtYSZ show significant differences in both catalytic performance and characterization with XRD and FT-IR CO adsorption. The implications of the obtained results for steam reforming of methane and ethane will be discussed in the upcoming section.

4.4.1 Catalyst characterization

Table 4.1 showed a Pt particle size of 30-40 nm for all catalysts. The similar particle size of PtYSZ and the potassium modified sample indicates no direct influence of potassium on Pt particle sizes. A similar effect was observed by Juan-Juan on Ni/Al₂O₃ [8]: addition of potassium did not cause any change in Ni-particle size. Further, Table 4.1 shows larger Pt particle size at higher calcination temperature. In general, the calcination temperature affects the size of supported metal particles. High calcination temperatures result in larger metal particles due to increased surface mobility and agglomeration of particles. The difference in Pt particle size between Pt4K700act (30nm) and Pt4K750act (38nm) (Table 4.1) can explain the slightly higher reaction rates for Pt4K700act compared to Pt4K750act (Table 4.3). The activity per Pt surface area unit is identical within 5% for Pt4K750act and Pt4K700act, assuming hemispherical Pt particles of 38nm and 30nm, respectively. Furthermore, the rates of conversion of ethane and methane are in the same order of magnitude for PtYSZ and potassium modified catalysts under the applied conditions. However, it was observed that methane reaction rate is only 6% higher on PtYSZ than on Pt4K700act, while ethane reaction rate is 40% higher on PtYSZ (Table 4.3).

Methane and ethane reaction rates increased over 4 times with time on stream on both potassium modified Pt catalysts, as reported in previous work [1] and summarized in Table 1. It is shown in Table 4.1 that Pt particle size remains unchanged during time on stream for both Pt4K700 and Pt4K750. This clearly shows that activation phenomena do not relate to a change in Pt-particle size and that redistribution of platinum can be excluded. It was further found that the potassium content significantly decreased during activation (shown in Table 4.1), indicating that potassium content and catalyst activity are related.

FT-IR characterization (Figure 4.1) showed that three different CO adsorption bands were found in Pt4K700fresh: linear coordinated CO at 2081cm^{-1} , a band around 2000 cm^{-1} due to a direct ion-dipole interaction between K^+ and linear CO [24, 25], and CO coordinated in bridged position at 1800cm^{-1} [16]. Generally, the addition of potassium can lead to an electronic modification of (small) supported metal particles, resulting in a preferred bridge coordination of CO. Interestingly, in this study the average Pt particle size is approximately 30 nm (Table 4.1), and still an effect of potassium on the CO FT-IR spectra is observed. Because of the large Pt-particles the effect of potassium on adsorbed CO must be localized. Furthermore, potassium loss during the activation period (Table 4.1) led to increased intensity of CO adsorption at 2081 cm^{-1} and absence of the bands at 1800 and 2000 cm^{-1} for Pt4K700act. In addition, linear adsorbed CO on PtYSZ and Pt4K700act are at the same peak position (2081 cm^{-1}), but on PtYSZ this band was 1.5 times more intense than on Pt4K700act. Table 4.1 already showed that Pt particle sizes are around 30 nm for PtYSZ, Pt4K700fresh and Pt4K700act. All these observations lead to the conclusion that on Pt4K700fresh, the platinum surface is partly covered by potassium, which evaporates during the activation period. As a result the infrared bands at 1800 and 2000 cm^{-1} disappeared and the intensity at 2081 cm^{-1} significantly increased. Nevertheless, the lower amount of accessible surface sites on Pt4K700act compared to PtYSZ (Table 4.2) indicates that after activation still parts of Pt surface in Pt4K700act are covered with potassium.

In addition to the potassium loss, a large increase in reaction rates of methane and ethane (Table 4.3) was observed during TOS. The higher reaction rates combined with the increase in accessible metal surface as determined with FTIR, suggest that on Pt4K700act hydrocarbon activation on Pt is rate determining under the present reaction conditions. Moreover, the ratio of reaction rates between methane and ethane clearly increased after potassium addition and remained constant during the activation period on Pt4K700 and Pt4K750 (Table 4.3). For this reason, we propose that initially two types of potassium are present on the potassium modified catalysts. Type I only blocks active Pt sites and is gradually evaporating during activation, as indicated by the increased number of active sites after reaction and absence of the direct Pt K^+ CO adsorption band at 2000 cm^{-1} and bridged CO band at 1800 cm^{-1} in Pt4K700act.

Type II is proposed to influence the ratio of reaction rates of methane and ethane. This type of potassium proved to be more stable, as the potassium content did not change during reaction between 20 and 85 hours of time on stream, after activation had taken place [1]. The fact that potassium of type II is not lost, suggests a stronger interaction with either the YSZ support material or with Pt.

4.4.2 CO desorption in FT-IR TPD

CO temperature programmed desorption has been widely studied [27] and used in investigation of catalytic systems [28, 29]. TPD studies in IR spectroscopy have been used earlier by Visser et al. [15]. The intention of their experiments was to relate observations of CO adsorption strength to reactivity of hydrocarbons found in kinetic experiments, as reported earlier in literature on hydrogenolysis, hydrogenation and oxidation reactions [13-15, 21].

Here, it was found in FT-IR and CO desorption experiments that CO release from the Pt-surface occurred at lower temperature when potassium was added (Figures 4.2 and 4.3). It was also observed that CO desorption was completed at lower temperature on Pt4K700 compared to PtYSZ (Figure 4.3). The data convincingly show weaker CO bonding as a result of the addition of potassium.

Kuriyama et al. [17, 30] and Derrouiche et al. [16, 31] also investigated interaction of CO on potassium modified Pt/Al₂O₃ with FT-IR. Derrouiche reported IR bands on 2.9wt.% Pt/10wt.% K/Al₂O₃ located at 2074 cm⁻¹, 1990 cm⁻¹ and 1795 cm⁻¹, comparable to our results in Figure 4.1. The intensity of the peak of linear CO on Pt decreased significantly as a result of potassium addition, in agreement with our results in Figure 4.1. TPD experiments by Kuriyama showed complete CO desorption at about 150°C lower temperature on potassium modified K-10wt.%/2wt.%Pt/Al₂O₃ as compared to Pt/Al₂O₃, clearly showing weaker adsorption of CO. This is in agreement with our results in Figure 4.3, showing a similar difference of 130°C in temperature is needed to achieve complete desorption on Pt4K700 versus PtYSZ.

Derrouiche et al. determined the heat of adsorption with the Adsorption Equilibrium Infrared method (AEIR) on 2.9wt.% Pt/10wt.% K/Al₂O₃ [16] and reported a significant decrease in heat of adsorption of linear CO species and a strong increase in heat of adsorption for bridged CO species as a result of potassium addition to Pt. This

completely agrees with our results in Figure 4.3, showing a weaker interaction for linear CO species at 2081 cm^{-1} on Pt4K700act, which had only linear CO species present on the surface (Figure 4.1). Obviously, the C-O stretch frequency, which is identical for PtYSZ and Pt4K700act, does not reflect the Pt-CO bond strength.

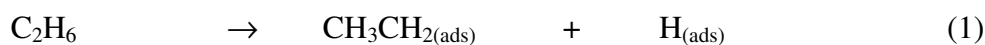
Bengaard et al. [32] observed weaker adsorption of hydrocarbons on Ni catalysts after adding potassium: a strong decrease in methane adsorption was found when potassium was added, resulting in slow hydrogen-deuterium exchange for methane compared to the unmodified catalyst Ni-catalyst. Cassuto et al. found more loosely bonded ethylene on potassium modified platinum surfaces [33]. Summarizing the results in literature, it is claimed that hydrocarbon adsorption on Pt can be weakened by addition of potassium to Pt or Ni catalysts. We propose, based on our results on CO desorption, that weakening of hydrocarbon adsorption occurs when modifying PtYSZ with potassium. The effects on kinetics on PtYSZ and Pt4K700 will be discussed below.

4.4.3 Steam reforming reaction mechanism on PtYSZ

For methane reforming, Wei et al [34, 35] proposed dissociative adsorption as the rate determining step in methane activation: $\text{CH}_{4, \text{gas}} \rightarrow \text{CH}_{3(\text{ads})} + \text{H}_{(\text{ads})}$. This means that the hydrocarbon surface coverage is low and reaction proceeds rapidly after dissociation of methane. Reaction to CO occurs as soon as the carbon atom is completely dehydrogenated. In literature, debate exists about the activation of water on Pt catalysts in steam reforming at high temperature: several sources claim a bi-functional mechanism for reforming reactions on Pt, proposing hydrocarbon activation on the Pt atoms and water activation on the support [36-38]. On the other hand, Wei and Iglesia [34, 39, 40] argued that water activation is a relatively fast step, implying that the question on which sites water is activated is not relevant for reaction kinetics.

To the best of our knowledge no detailed mechanism has been reported for steam reforming of ethane, but ethane hydrogenolysis has been investigated in detail on Pt and Ni catalysts. [41-43]. It was reported that activity trends in steam reforming and ethane hydrogenolysis are comparable on supported Ni-catalysts [9], suggesting similar mechanisms for ethane activation in both reactions. In hydrogenolysis,

activation of ethane on Pt or Ni takes place through dissociative adsorption on the surface (1), creating adsorbed ethylidyne and an hydrogen atom [41-43]:



Two pathways are possible after formation of the CH_3CH_2 fragment: (i) the CH_3CH_2 fragment can either split into a CH_3 and a CH_2 fragment after adsorption (2) or (ii) further abstraction of hydrogen atoms can occur (3a+3b+3c) [41, 42]. Both processes require additional empty surface sites. The C-C splitting is favored for the CH_3CH_2 fragment on Pt [41, 42]. After C-C splitting, further dehydrogenation of CH_x can occur, similar to the mechanism for methane, and subsequent conversion to CO is possible as explained above.

If further abstraction of hydrogen atoms on CH_3CH_2 fragments occurs (3a+3b+3c), much less reactive surface intermediates are formed, occupying the Pt sites. It is claimed that CCH_3 -fragments on the Pt surface are the most stable species that block the Pt surface sites [41, 42]. Very low reactivity of the CCH_3 -species on the surface was also reported by Anderson et al. [44] in ethylene dehydrogenation on platinum.

Our study focused on steam reforming of methane/ethane mixtures, requiring activation of both hydrocarbons on PtYSZ. Competition between methane and ethane in steam reforming was observed on PtYSZ (Figure 4.5). This leads to the proposition that methane and ethane are indeed activated on the same Pt-sites. The water concentration was also found to influence reaction rates in ethane/methane mixtures on PtYSZ as shown in Figure 4: higher reaction rates with increasing water concentration show that water activation on this catalyst is a limiting factor. This suggests that the Pt surface is highly covered with fragments originating from dissociative adsorption of methane and/or ethane.

The results in Figure 4.5 show that the relative increase of the reaction rates with higher water concentration is smaller than the decreasing effects caused by the increasing ethane concentration. This is confirmed by the total molar carbon conversion in the experiments of Figure 4.5, as shown in Table 4.4 (reaction of methane counts for one carbon atom converted, while ethane counts for two atoms). With higher ethane concentration in the feed, the percentage of carbon converted is decreasing, even when the water concentration is increased proportionally. Figure 4.5 thus shows that the methane reaction rate strongly decreased if more ethane is present, and that high methane conversions are only possible if ethane is converted completely, confirming competition between methane and ethane on the platinum surface.

Table 4.4: Total number of carbon atoms converted in the experiments shown in Figure 4.5, CH₄ (4.5vol.%), H₂O/C ratio 1.8:

Water (vol.%)	12	15	18	20
Ethane (vol.%)	1.07	1.9	2.6	3.4
Total C conversion ($\cdot 10^{-5}$ mol/g.s)	3.1	4.0	3.6	3.5
Carbon converted (%)	46.7	48.2	37.1	31.0

Furthermore, in Figure 4.5, ethane conversion decreased from 98% at 1.07vol.% to 65% at 3.4vol.%, implying that the apparent reaction order in ethane is smaller than 1. This indicates a self poisoning effect due to blocking of active sites by ethane fragments. The creation of stable C₂ intermediates as reported by Cortright [41, 42] on the Pt-surface could be a reason for limited adsorption and activation of methane at higher ethane concentrations (Figure 4.5). Higher ethane concentrations create more stable C₂-fragments on the Pt-surface, leaving a lower percentage of the active sites open for methane dissociation and reaction to CO and H₂. It is concluded that ethane induces a high surface coverage of C₂H_y fragments and water activation becomes the rate limiting step in mixtures of methane and ethane on PtYSZ.

4.4.4 Steam reforming reaction mechanism on Pt4K700

The addition of potassium could affect the reaction rates of methane and ethane in steam reforming in two ways: potassium either influences the activation of water or modifies the activation of the hydrocarbons, methane and ethane. In literature it is stated that potassium can indeed enhance water activation on the support [45, 46], but as indicated earlier, there is no agreement in literature on the kinetic relevance of water activation on the support on steam reforming [34-38, 40].

In our experiments with Pt4K700, it was observed that a changing water concentration had no influence on reaction rates for both methane and ethane (Figure 4.6), in contrast to PtYSZ (Figure 4.4). With the addition of potassium to PtYSZ, the competition between ethane and methane was diminished, as reported in an earlier paper [1]. First order kinetics in methane and ethane were reported, indicating low surface coverage of both hydrocarbons, even in mixtures of methane and ethane. The apparent first order in both methane and ethane suggests that hydrocarbon activation on Pt is the limiting step on Pt4K700 and activation of water is not kinetically relevant, as observed in Figure 4.6. The conclusion that hydrocarbon activation is rate limiting on Pt4K700 is also in agreement with the observation that increasing the number of accessible Pt sites with TOS (Figure 4.1) is accompanied by an increase in catalytic activity.

In an earlier paper [1], a lower activity was reported for the potassium modified catalysts during steam reforming of the single hydrocarbons ethane and methane, as compared to the unmodified PtYSZ catalyst. For methane the activity decreased by 60%, while for ethane reaction rate decreased by 33%. The IR experiments in this work indicate that potassium weakens the interaction with methane and ethane, leading to lower surface coverages of methane and ethane. The lower surface coverages can explain the observed lower reaction rates of methane and ethane on Pt4K700 as compared to PtYSZ.

Interestingly, contrary to the rate limiting step found for PtYSZ, the rate limiting step of hydrocarbon activation on Pt4K700 is well in agreement with the mechanism proposed by Wei and Iglesia [34, 35, 40]; competition effects as observed on PtYSZ, leading to high surface coverage, were eliminated on potassium modified catalysts. In

conclusion, our results show that adsorption for both ethane and methane was reduced on potassium modified PtYSZ. Blocking effects by ethane as observed on PtYSZ could be eliminated by reducing the alkane adsorption strength. However, this also resulted in reduced adsorption of methane, leading to lower reactivity for both hydrocarbons.

4.5 Conclusion

Potassium modification of PtYSZ strongly influenced the conversion and rate determining steps in methane and ethane in steam reforming. Water activation is the rate determining step on PtYSZ, resulting in high surface coverage of hydrocarbon fragments during steam reforming of mixtures of methane and ethane. This led to blocking of active sites by ethane fragments and consequently low conversion of methane. If potassium is added to the catalyst, hydrocarbon activation on Pt is rate determining, resulting in low surface coverage of methane and ethane. As a result, competition effects of methane and ethane diminished on potassium modified PtYSZ, enabling simultaneous conversion of methane and ethane. The weaker interaction of the hydrocarbons with the Pt surface due to potassium addition is also reflected in the lower adsorption strength of CO as found with CO FT-IR TPD.

4.6 References

- [1] P.O. Graf, B.L. Mojet, L. Lefferts, *Applied Catalysis A: General* In Press, Accepted Manuscript.
- [2] P.O. Graf, B.L. Mojet, J.G. van Ommen, L. Lefferts, *Applied Catalysis A: General* 332 (2007) 310-317.
- [3] D.L. Trimm, *Catalysis Today* 37 (1997) 233.
- [4] J.H. Bitter, W. Hally, K. Seshan, J.G. van Ommen, J.A. Lercher, *Catalysis Today* 29 (1996) 349-353.
- [5] J.H. Bitter, K. Seshan, J.A. Lercher, *Journal of Catalysis* 171 (1997) 279.
- [6] M.E.S. Hegarty, A.M. O'Connor, J.R.H. Ross, *Catalysis Today* 42 (1998) 225.
- [7] A.M. O'Connor, J.R.H. Ross, *Catalysis Today* 46 (1998) 203.
- [8] J. Juan-Juan, M.C. Roman-Martinez, M.J. Illan-Gomez, *Applied Catalysis A: General* 301 (2006) 9-15.
- [9] J.R. Rostrup-Nielsen, *Journal of Catalysis* 31 (1973) 173.
- [10] J. Sehested, *Catalysis Today* 111 (2006) 103-110.
- [11] J.W. Snoeck, G.F. Froment, M. Fowles, *Industrial and Engineering Chemistry Research* 41 (2002) 3548-3556.
- [12] D.L. Trimm, *Catalysis Today* 49 (1999) 3.
- [13] B.L. Mojet, J.T. Miller, D.E. Ramaker, D.C. Koningsberger, *Journal of Catalysis* 186 (1999) 373-386.
- [14] M.K. Oudenhuijzen, J.A. Van Bokhoven, D.E. Ramaker, D.C. Koningsberger, *Journal of Physical Chemistry B* 108 (2004) 20247-20254.
- [15] T. Visser, T.A. Nijhuis, A.M.J. Van Der Eerden, K. Jenken, Y. Ji, W. Bras, S. Nikitenko, Y. Ikeda, M. Lepage, B.M. Weckhuysen, *Journal of Physical Chemistry B* 109 (2005) 3822-3831.
- [16] S. Derrouiche, P. Gravejat, B. Bassou, D. Bianchi, *Applied Surface Science* 253 (2007) 5894-5898.
- [17] M. Kuriyama, H. Tanaka, S.-i. Ito, T. Kubota, T. Miyao, S. Naito, K. Tomishige, K. Kunimori, *Journal of Catalysis* 252 (2007) 39-48.
- [18] E.L. Garfunkel, J.E. Crowell, G.A. Somorjai, *Journal of Physical Chemistry* 86 (1982) 310-313.
- [19] P.A.J.M. Angevaere, H.A.C.M. Hendrickx, V. Ponc, *Journal of Catalysis* 110 (1988) 11-17.
- [20] H.P. Bonzel, *Surface Science Reports* 8 (1988) 43-125.
- [21] A.Y. Stakheev, Y. Zhang, A.V. Ivanov, G.N. Baeva, D.E. Ramaker, D.C. Koningsberger, *Journal of Physical Chemistry C* 111 (2007) 3938-3948.
- [22] H. Borchert, E.V. Shevchenko, A. Robert, I. Mekis, A. Kornowski, G. Grubel, H. Weller, *Langmuir* 21 (2005) 1931-1936.
- [23] S.D. Jackson, B.M. Glanville, J. Willis, G.D. McLellan, G. Webb, R.B. Moyes, S. Simpson, P.B. Wells, R. Whyman, *Journal of Catalysis* 139 (1993) 221-233.
- [24] M.J. Kappers, J.T. Miller, D.C. Koningsberger, *J. Phys. Chem.* 100 (1996) 3227-3236.
- [25] A.Y. Stakheev, E.S. Shpiro, N.I. Jaeger, G. Schulz-Ekloff, *Catalysis Letters* 32 (1995) 147-158.
- [26] P. Hollins, J. Pritchard, *Progress in Surface Science* 19 (1985) 275-349.
- [27] D.A. King, 1 ed., Utrecht, Netherlands, 1975, *Surf. Sci. (Netherlands)* Vol.47, pp. 384-402.

- [28] A.M. de Jong, J.W. Niemantsverdriet, *Vacuum* 41 (1990) 232-233.
- [29] D.L.S. Nieskens, A.P. Van Bavel, J.W. Niemantsverdriet, *Surface Science* 546 (2003) 159-169.
- [30] Y. Minemura, M. Kuriyama, S.-i. Ito, K. Tomishige, K. Kunimori, *Catalysis Communications* 7 (2006) 623-626.
- [31] P. Pillonel, S. Derrouiche, A. Bourane, F. Gaillard, P. Vernoux, D. Bianchi, *Applied Catalysis A: General* 278 (2005) 223-231.
- [32] H.S. Bengaard, J.K. Norskov, J. Sehested, B.S. Clausen, L.P. Nielsen, A.M. Molenbroek, J.R. Rostrup-Nielsen, *Journal of Catalysis* 209 (2002) 365-384.
- [33] A. Cassuto, S. Schmidt, M. Mane, *Surface Science* 284 (1993) 273-280.
- [34] J.M. Wei, E. Iglesia, *Journal of Catalysis* 225 (2004) 116.
- [35] J.M. Wei, E. Iglesia, *Journal of Physical Chemistry B* 108 (2004) 4094.
- [36] K. Nagaoka, K. Seshan, K. Aika, J.A. Lercher, *Journal of Catalysis* 197 (2001) 34.
- [37] K. Takanahe, K.-i. Aika, K. Inazu, T. Baba, K. Seshan, L. Lefferts, *Journal of Catalysis* 243 (2006) 263-269.
- [38] B. Matas Guell, I. Babich, K. Seshan, L. Lefferts, *Journal of Catalysis* 257 (2008) 229-231.
- [39] J. Wei, E. Iglesia, *Journal of Physical Chemistry B* 108 (2004) 4094-4103.
- [40] J.M. Wei, E. Iglesia, *Physical Chemistry Chemical Physics* 6 (2004) 3754.
- [41] R.D. Cortright, R.M. Watwe, J.A. Dumesic, *Journal of Molecular Catalysis, A: Chemical* 163 (2000) 91-103.
- [42] R.D. Cortright, R.M. Watwe, B.E. Spiewak, J.A. Dumesic, *Catalysis Today* 53 (1999) 395.
- [43] M.C. McMaster, R.J. Madix, *Surface Science* 275 (1992) 265-280.
- [44] A.B. Anderson, S.J. Choe, *Journal of Physical Chemistry* 93 (1989) 6145-6149.
- [45] F. Frusteri, S. Freni, V. Chiodo, L. Spadaro, O. Di Blasi, G. Bonura, S. Cavallaro, *Applied Catalysis A: General* 270 (2004) 1-7.
- [46] D. Sutton, B. Kelleher, J.R.H. Ross, *Fuel Processing Technology* 73 (2001) 155-173.

Chapter 5

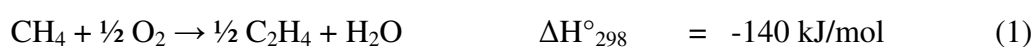
Reactive separation of ethylene from the effluent gas of methane oxidative coupling via alkylation of benzene to ethylbenzene on ZSM-5

Abstract

Separation of ethylene from the effluent gas of oxidative coupling has been a challenging issue for several years. In a combined process of oxidative coupling and reforming of methane, reactive separation of ethylene via alkylation of benzene to ethylbenzene (EB) is a promising option. Ethylene was successfully converted to the useful chemical intermediate ethylbenzene using ZSM-5. Yields of EB up to 90% were found at 95% conversion and 90% selectivity at 360°C. Methane and ethane present in the feed were not converted and can be used for steam reforming in the proposed reaction concept. None of the additional components present in the effluent gas of oxidative coupling (CO, CO₂, CH₄, C₂H₆ and H₂O) influences activity or selectivity of the alkylation catalyst. Stability of ZSM-5 is also not influenced by the added components, with the exception of water, which even increases stability.

5.1 Introduction

With the depletion of petroleum, it is expected that methane will eventually become a major resource for chemicals and liquid fuels. Much of the methane is found in regions that are far removed from industrial complexes and often located offshore, implying that transport is uneconomical or even impossible. This has led to worldwide efforts for directly converting methane into easy transportable value-added products. An interesting option is the slightly exothermic oxidative coupling of methane (1), with the highly exothermic complete oxidation to CO₂ and H₂O as side reaction (2), as reviewed by Choudhary et al [1].



A high selectivity to reaction (1) is always compromised with a low methane conversion. This means that the product stream after oxidative coupling will be a complex gas mixture consisting of the main product ethylene, combined with C₂H₆, CH₄, CO, CO₂, H₂O and small amounts H₂. Efficient separation of ethylene or creative ideas in process operation are needed to make the oxidative coupling commercially feasible.

The limitations of the oxidative coupling have led to development of several alternatives. Makri et al. used a gas recycle reactor [2], Choudhary proposed the use of a countercurrent moving bed [1]. Also research on plasma [3] and solid-state electrolyte reactors [4] has been carried out. Additionally combinations with other reactions have been proposed: catalytic oxidative coupling and gas phase partial oxidation [5], co-generation of ethylene and electricity through oxidative coupling [6], oxidative coupling of methane and oxidative dehydrogenation [7] and oxidative coupling of methane and pyrolysis of naphtha [8]. All of the processes face difficulties with economic and/or technical feasibility. Operation of oxidative coupling can be optimized by distributed feeding of oxygen [9, 10].

The objective of the current research is to create an autothermal process, combining the exothermic oxidative coupling of methane (1) and side combustion reactions (2) with the endothermic methane steam and dry reforming (3+4). The intention is to

convert methane to ethylene and synthesis gas (CO and H₂) in one multifunctional reactor. The essential advantage of this proposition as compared to the options listed above is the elimination of the methane recycle, because methane left unconverted in oxidative coupling is now converted via reforming.



Direct methane steam reforming of the product mixture of oxidative coupling (containing C₂H₄, C₂H₆, CH₄, CO, CO₂, H₂O and H₂) resulted in a loss of C₂H₄ and C₂H₆, as those components are also converted in steam reforming [11, 12]. Ethylene is the desired product and conversion to synthesis gas should therefore be avoided.

A process combining oxidative coupling and reforming of methane can still be valuable in terms of heat integration of the reactions, provided that ethylene is separated before steam reforming of the mixture produced in oxidative coupling. Cryogenic distillation has been considered for separation: the process takes place at around -160°C [13] and a flow sheet of OCM separation was demonstrated by Vereshchagin et al. [14]. A major drawback is the enormous temperature difference between oxidative coupling and this separation technique. An alternative separation technique is selective adsorption of ethylene on molecular sieves [2] or active charcoal [15]. However, disadvantages of this option are trapping of H₂O and CO₂ and the fact that desorption of ethylene requires a carrier gas, resulting in an inert carrier with only 1% C₂ content. Additionally, the adsorption process takes place at room temperature, which implies a large temperature difference with the oxidative coupling conditions.

A novel approach presented in this paper could be a reactive separation of ethylene, combining separation of ethylene and production of a useful product. The separation of ethylene by reaction with benzene to ethylbenzene (EB) could be promising as ethylbenzene is an important intermediate in styrene production. Benzene alkylation has been reported in vapor and liquid phase on various zeolite catalysts mostly under high pressure [16-24]. In our case it is important to operate benzene alkylation at

conditions similar to the conditions of oxidative coupling, i.e. 700°C and close to atmospheric pressure implying operation in gas phase.

In a review by Perego et al., several catalysts for benzene alkylation are compared [25]. ZSM-5 based catalysts are frequently used in vapor phase alkylation and offer low coking tendency and therefore long life cycles between regeneration are possible [26]. Excess benzene is applied to ensure high conversion of ethylene and selectivity to ethylbenzene, limiting di- or tri-alkylation [25, 27, 28]. Also toluene is reported as a byproduct [28].

The goal of this research paper is to demonstrate reactive separation of ethylene from the mixture produced in oxidative coupling, *via* alkylation of benzene. Yield of ethylbenzene, conversion of hydrocarbons (i.e. methane, ethane and ethylene) and selectivity to ethylbenzene will be reported for temperatures between 320°C and 440°C. Furthermore, the effects of byproducts of oxidative coupling (CO, CO₂ and H₂O) on benzene alkylation will be investigated, as CO₂ and H₂O are claimed to affect stability of alkylation of benzene [29].

5.2 Experimental

ZSM-5 with Si/Al ratio of 28 containing NH_4^+ cations was used (Exxon). Before activity test, ZSM-5 was heated to 400°C in argon and calcined for 5 hours in 20 vol.% O_2 (Linde Gas 5.0) / Ar (Linde Gas 5.0, flow rate: 200ml/min). Activity tests were carried out in a micro reactor flow setup with 200 mg of catalyst. The reactor consisted of a quartz tube with inner and outer diameter of respectively 4 and 6 mm. About 200mg catalyst was loaded in the reactor, held between quartz wool plugs. Catalyst particles with a diameter between 0.3 and 0.6 mm were used, resulting in a pressure drop around 0.1 bar.

Methane (Hoekloos 4.5), ethane (Indugas 4.0) and ethylene (Indugas 3.5) were used as hydrocarbon feedstock. Benzene (pro analysi, Alfa-Aesar 99.7%) was fed with a Bronkhorst controlled evaporator mixer (CEM) in combination with a Liquiflow controller. The reaction mixtures had the following composition: 4.3vol.% C_2H_4 , 3vol.% C_2H_6 , 5vol.% CH_4 , 30vol.% C_6H_6 in Ar. A total flow rate of 70 $\text{ml}\cdot\text{min}^{-1}$ was applied. H_2O , CO (Linde Gas 4.7) and CO_2 (Linde Gas 4.0) were added to this mixture. Water was added through a double saturation step of the gas mixture. In a first saturator the gas stream was contacted with water at 60°C, followed by condensation at 50°C in a second saturator. This led to a stable water concentration of 6vol.%.

The product and reactant gas composition was analyzed with a Varian 3800 Gas Chromatograph equipped with two columns (Molsieve 5A and PoraPlotQ) and two TCD detectors. 1,2 di-ethylbenzene and 1,4 di-ethylbenzene could be separated and analyzed in the PoraPlotQ column. A Balzers QMS 200 F mass spectrometer was used to check for higher alkylated benzenes or other by products. Conversion (X), selectivity (S_i) and yield (Y_i) were determined based on ethylene conversion, ethylbenzene (EB) and di-ethylbenzene (DEB) concentrations. Concentrations were corrected for volume changes of the reaction mixture, using Ar as internal standard. The calculations shown below are carried out with the amounts of reactants and products expressed in mole/sec.

$$X = 1 - \frac{C_2H_4out}{C_2H_4in}$$
$$S_{EB} = \frac{EB}{EB + 1,4DEB + 1,2DEB}, \quad S_{DEB} = \frac{1,4DEB + 1,2DEB}{EB + 1,4DEB + 1,2DEB}$$
$$Y_i = S_i * X$$

HSC Chemistry 4.0 software was used to calculate equilibrium compositions of the reaction mixtures including di-ethylbenzenes.

5.3 Results

5.3.1 Conversion of C_2H_4 , selectivity and yield to EB

Figure 5.1 shows the results of benzene alkylation experiments with a feed composition of 30vol.% C_6H_6 , 4.3vol.% C_2H_4 , 3vol.% C_2H_6 and 5vol.% CH_4 in Ar. The total flow rate was $70 \text{ ml}\cdot\text{min}^{-1}$. The data points were obtained in random order. The catalyst was regenerated by exposure to 20vol.% O_2 during 15 min at 400°C just before acquiring the data points at every temperature, in order to compensate for any deactivation (as will be discussed in Figure 5.3). The initial performance is reported in Figure 5.1.

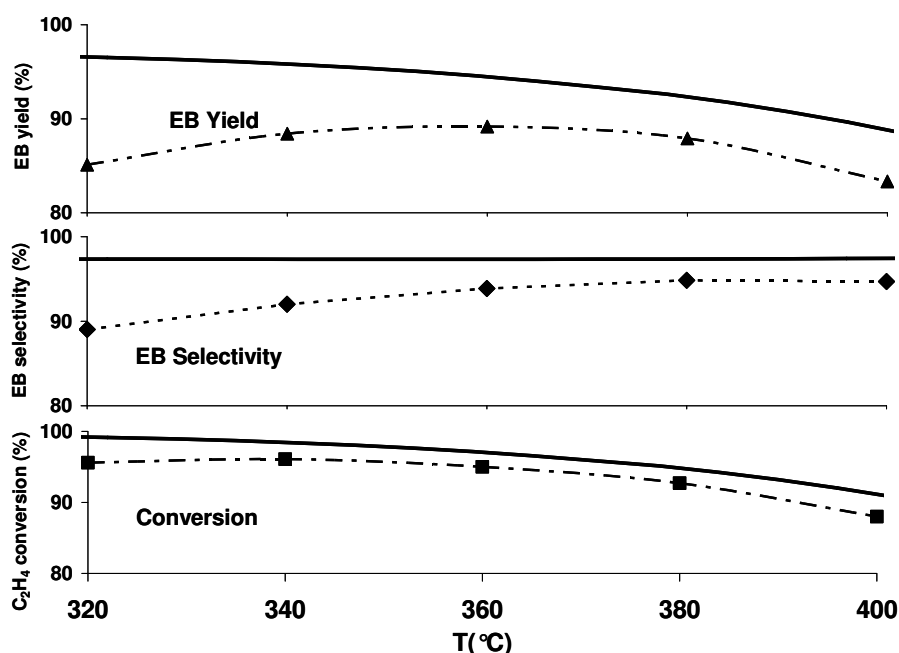


Figure 5.1: Comparison of experimental ethylene conversion (below), Ethylbenzene (EB) selectivity (middle) and EB yield (above) and thermodynamic equilibrium (solid line) in alkylation of benzene as a function of temperature. Concentrations: 30vol.% C_6H_6 , 4.3vol.% C_2H_4 , 3vol.% C_2H_6 and 5vol.% CH_4 in Ar (total flow rate $70 \text{ ml}\cdot\text{min}^{-1}$).

In all experiments in this work, no significant conversion of methane and ethane was observed (concentration changes in these components were smaller than 1%). Around 96% initial ethylene conversion was found at 320°C and 340°C , decreasing to 90% at 400°C . Thermodynamic equilibrium predicts 99% conversion at 320°C , decreasing at higher temperature. The experimental ethylene conversion was close to equilibrium for all temperatures.

Experimental selectivity to ethylbenzene increased with temperature from 89% at 320°C to 95% at 400°C. Equilibrium selectivity is approximately 97%, independent of temperature. The experimental results indicate a lower selectivity at lower temperature, resulting in a maximum experimental yield of EB at 360°C. Below 360°C the yield is limited because of lower selectivity while above 360°C conversion of ethylene is limited by thermodynamic constraints.

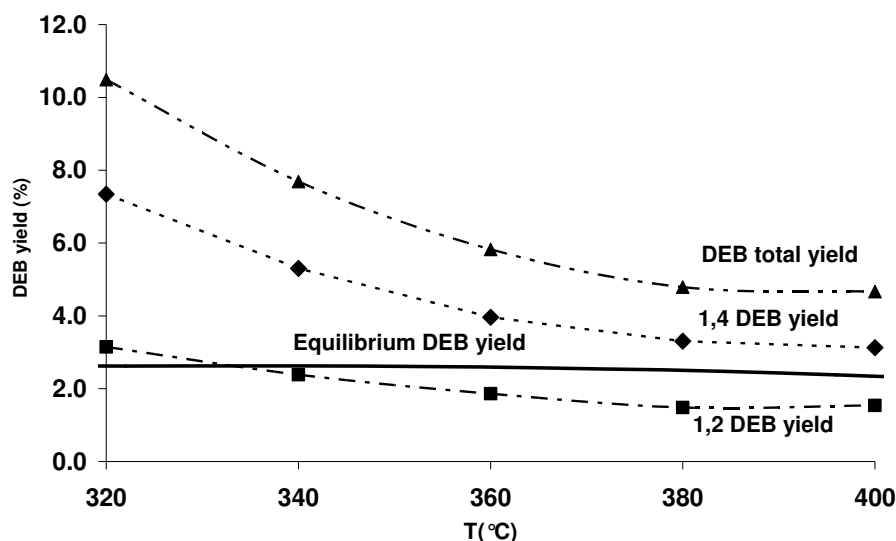


Figure 5.2: Equilibrium diethylbenzene yield in benzene alkylation as a function of temperature, total experimental DEB yield (\blacktriangle), experimental 1,4 DEB yield (\blacklozenge) and experimental 1,2 DEB yield (\blacksquare).

The experimental and equilibrium selectivity to diethylbenzene are shown in Figure 5.2. Other side products like tri-alkylated benzene could not be detected with mass spectrometry. Experimentally a DEB yield of slightly more than 10% was found at 320°C. With increasing temperature the yield of DEB reduced to 5%. The thermodynamic equilibrium predicts a constant DEB yield of just under 3%, which is clearly lower than the experimental results. The ratio between the yields of 1,4 DEB and 1,2 DEB varied experimentally between 0.65:0.35 and 0.7:0.3, in reasonable agreement with thermodynamic calculations, resulting in a 0.6:0.4 ratio (not shown).

5.3.2 Stability

Figure 5.3 shows the results of stability tests for alkylation of benzene with ethylene at 340°C, 360°C and 400°C. The conditions were identical to the experiment shown in Figure 5.1. All initial conversions were close to equilibrium, 98% (340°C), 97%

(360°C) and 91% (400°C) respectively. Conversion decreased with time on stream, observing the most pronounced deactivation at 400°C: conversion decreased to 75% after 20 hours at 400°C. It should be noted that selectivity to ethylbenzene remained unchanged at 95% during deactivation of the catalyst (not shown). At 340 and 360°C more stable conversions were observed. The highest stability was found at 360°C: conversion only decreases from 96 to 94% in 20 hours.

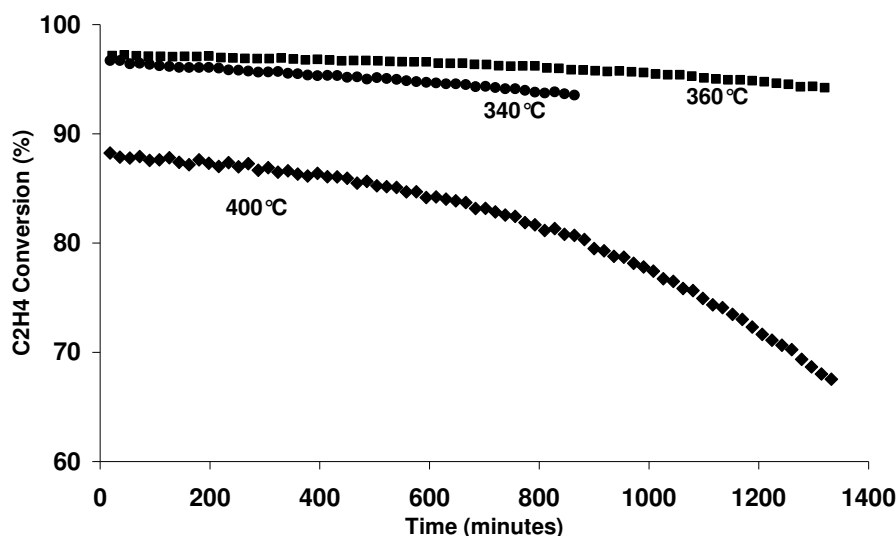


Figure 5.3: Stability of ethylene conversion in benzene alkylation at 340°C (●), 360°C (■), and 400°C (◆). Feed composition 30vol.% C₆H₆, 4.3vol.% C₂H₄, 3vol.% C₂H₆ and 5vol.% CH₄ in Ar (total flow rate 70 ml.min⁻¹).

The best stability (Figure 5.3) and the maximum yield (Figure 5.1) were both found at 360°C and therefore this temperature was selected for further stability tests under addition of CO, CO₂ and water (by-products of oxidative coupling) in the next paragraph.

5.3.3 Effect of by-products of oxidative coupling at 360°C

Figure 5.4 shows the relative conversion (measured conversion divided by initial conversion) of ethylene in 4 separate experiments at 360°C. The solid line in Figure 5.4 represents relative stability in the basic experiment at 360°C without any H₂O, CO or CO₂. Water, CO and CO₂ were added separately to check effects on catalyst stability and conversion.

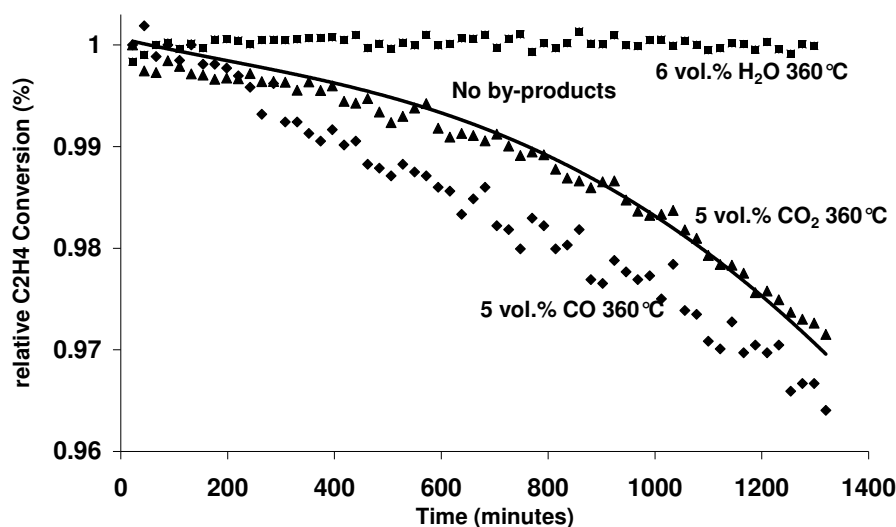


Figure 5.4: Stability of ethylene conversion in benzene alkylation at 360°C without adding by products (solid line) compared to stability in case of addition of 6vol.% H₂O (■), 5 vol.% CO₂ (▲) or 5 vol.% CO (◆), respectively. Feed composition: 30vol.% C₆H₆, 4.3vol.% C₂H₄, 3 vol.% C₂H₆ and 5vol.% CH₄ in Ar, total flow rate 70 ml.min⁻¹

None of these additional reactants was converted. The initial ethylene conversion was about 98% (water), 97% (CO₂ and basic experiment) and 95% (CO), respectively. No significant effect of 5vol.% CO₂ and only a small negative effect of 5vol.% CO on stability was observed: in both cases stability was comparable to the experiment at 360°C without addition of oxidative coupling products. Addition of water had a highly positive effect on stability, showing no deactivation during in 1400 minutes.

A gas mixture containing 4vol.% C₂H₄, 3vol.% C₂H₆, 5vol.% CH₄, 30vol.% C₆H₆, 5vol.% CO, 5vol.% CO₂, 6vol.% H₂O in Ar was fed to simulate benzene alkylation in the effluent stream of oxidative coupling. Conversion of ethylene, EB selectivity and EB yield as a function of temperature are compared in Figure 5.5. Thermodynamic equilibrium was calculated assuming that CO, CO₂ and water behave inert.

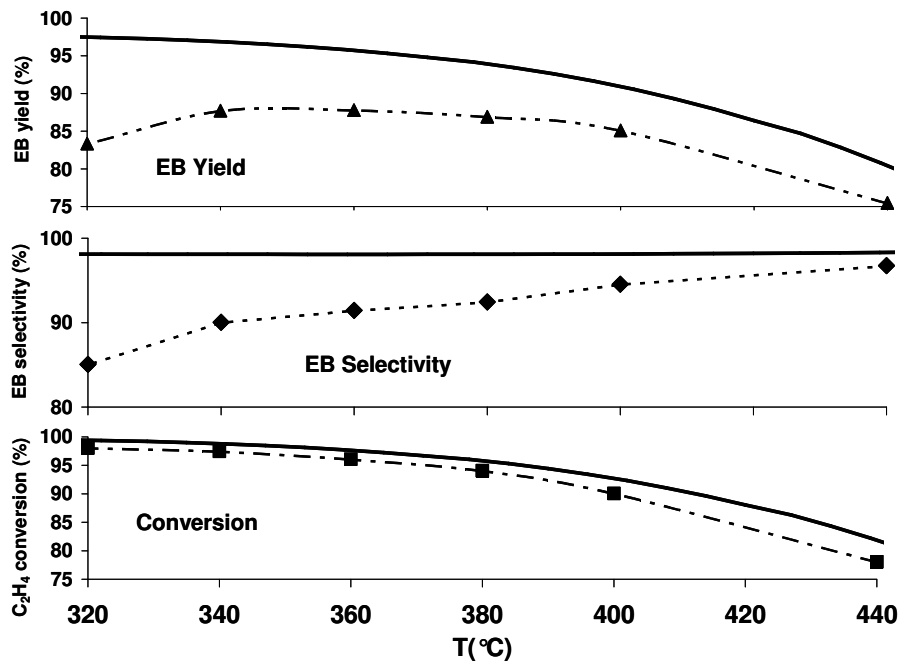


Figure 5.5: Ethylene conversion (■), Ethylbenzene (EB) selectivity (◆) and EB yield (▲) in alkylation of benzene in mixture containing 5vol.% CO, 5vol.% CO₂ and 6vol.% H₂O as a function of temperature, compared to thermodynamic equilibrium (solid lines)

Conversion is close to equilibrium under all conditions and a decreased selectivity is found at low temperature. High ethylbenzene yield is possible between 340°C and 380°C in the complete mixture containing water, CO and CO₂. The yield of DEB (not shown) did not differ significantly from the results in Figure 5.2. Above 400°C, EB yield decreases because of thermodynamic constraints.

Stable operation was found at all temperatures tested; as an example the results of a duration test at 360°C are shown in Figure 5.6. Constant ethylene conversion of 96% was combined with more than 90% selectivity to EB. This leads to a stable EB yield of 88% during 20 hours.

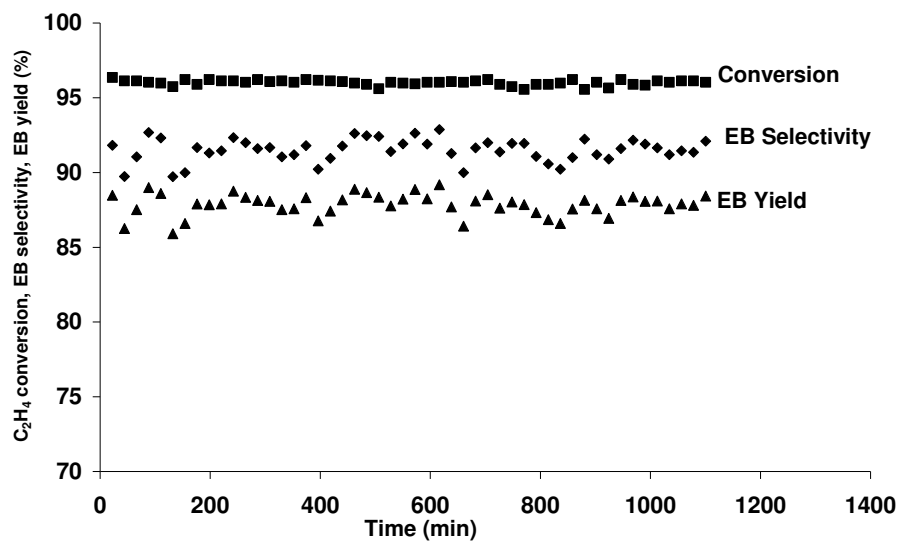


Figure 5.6: Stability of ethylene conversion (■), Ethylbenzene (EB) selectivity (◆) and EB yield (▲) in alkylation of benzene as a function of temperature. Feed composition 4vol.% C₂H₄, 3vol.% C₂H₆, 5vol.% CH₄, 30vol.% C₆H₆, 5vol.% CO, 5vol.% CO₂, 6vol.% H₂O in Ar, flow rate 70 ml/min

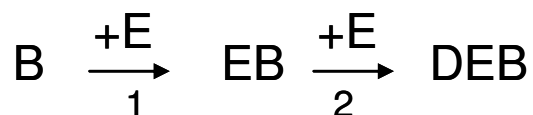
5.4 Discussion

5.4.1 Conversion and selectivity

Reaction of ethylene with benzene to ethylbenzene was investigated, with the intention to separate ethylene from the gas mixture produced in oxidative coupling. This gas mixture consists of CH₄, C₂H₆ and C₂H₄, together with the side products of oxidative coupling CO₂, H₂O and CO. In a first approach methane, ethane and ethylene were fed together with excess benzene over ZSM-5. Ethylene is the only reactive hydrocarbon, as no conversion of methane and ethane was detected. This was the case also in all other experiments shown, which means that the proposed concept is, in principle, suitable for reactive separation of ethylene from methane and ethane.

Figure 5.1 shows that ethylene conversion, ethylbenzene (EB) selectivity and ethylbenzene yield were close to thermodynamic equilibrium at 400°C. Decreasing temperature led to increased ethylene conversion, in agreement with the estimation of the equilibrium based on thermodynamics (Figure 5.1). The selectivity to ethylbenzene decreased with decreasing temperature, in contrast with what was expected based on thermodynamics, predicting constant selectivity.

Thermodynamic calculations predict a constant DEB selectivity of 2.7% between 300 and 440°C. However, the experimental yield of DEB was higher: 4.7% DEB yield was found at 400°C and increased further with decreasing temperature, reaching 10.5% at 320°C (Figure 5.2). Apparently, the conversions and product distribution are not determined by thermodynamics. Thus, the reactions are kinetically controlled according to Scheme 5.1 and selectivity is determined by the ratio of the rates of reactions 1 and 2.



Scheme 5.1: Schematic reaction pathway in alkylation of benzene

As stated by Qi et al. [28], the primary product ethylbenzene is more reactive in alkylation than benzene and thus a high benzene to ethylene ratio is required to reach reasonable selectivity to EB. Our results described in this paper are in agreement with

results of several other researchers [17, 20, 25, 30], who also reported higher DEB yields than predicted by thermodynamics. Selectivities of benzene ethylation obtained with different catalysts were compared in a review by Perego. In line with our results, selectivities to DEB of 8% were reported on zeolite Y and Beta, exceeding equilibrium yield to DEB by a factor 3. Christensen et al. [17] showed that use of a mesoporous ZSM-5 can enhance selectivity to EB and reduce DEB production, compared to conventional ZSM-5. In agreement with Scheme 5.1, this was explained by enhanced diffusion of EB out of the ZSM-5, resulting in lower concentration of EB in the zeolite pores and consequently less secondary alkylation than in normal ZSM-5.

5.4.2 Catalyst deactivation & effect of adding CO₂, H₂O and CO

The strongest deactivation of ZSM-5 was found at 400°C (Figure 5.3), while lower temperatures led to more stable operation. Regeneration with oxygen treatment was possible. Deactivation through coking on various zeolites has been widely studied and causes of deactivation are summarized in a review by Venuto [31]. Coking can range from simple olefin monomers chemisorbed at acid sites of the zeolite, to formation of highly aromatic hydrogen-deficient carbonaceous deposits. Both blocking of pores and deactivation of active sites were observed as cause of deactivation. It was found that deactivation of zeolites was most prominent at temperature above 375°C, leading to aromatic carbon deposits. Small amounts of coke, mainly consisting of easily removable oligomeric products can be formed at temperatures around 300°C [31].

Experimentally, maximum yield and highest catalyst stability were observed at 360°C (Figures 5.1 and 5.4). This temperature was selected for addition of CO₂, CO and H₂O. CO₂ had no effect and CO had a slightly negative effect on catalyst stability. The decrease in conversion as a function of time is similar to the base case without any additions (Figure 5.4). Water clearly improves catalyst stability, as the conversion was constant throughout the 1200 minute experiment (Figure 5.4). It should be noted that the conversion of ethylene is close to equilibrium under these conditions, which may imply that only part of the catalyst bed contributes. This may hide any possible deactivation effect. However, deactivation was clearly observed, in absence of water (Figure 5.4), in contrast to the performance in presence of water (Figures 5.4 and 5.6). The stabilizing effect of water is also reported in steam reforming reactions [32] as well as dehydrogenation reactions, e.g. alkanes and ethylbenzene to styrene [33]. The

increased stability of the catalysts was ascribed to coke gasification by steam, avoiding accumulation of carbon deposits.

Comparison of Figure 5.5 and Figure 5.1 shows that the selectivity pattern of reactions is not influenced by addition of the by-products of oxidative coupling. High conversions of ethylene to ethylbenzene are possible and yield of ethylbenzene is not affected by the addition of CO, CO₂ and H₂O.

Increasing the temperature to conditions closer to oxidative coupling operating conditions is unfortunately not feasible. When temperature is increased to above 400°C, conversion of ethylene reduces due to thermodynamic limitations (Figure 5.5). Optimum operating conditions were again found at 360°C with an EB-yield of 88%. It can be concluded from this study, that reactive separation of ethylene to ethylbenzene after oxidative coupling is a promising option. Operation of the alkylation reaction at atmospheric pressure between 320°C and 400°C was demonstrated and resulted in a high EB-yield. However, conditions as well as catalysts are not optimized here: increasing the pressure may further increase yield of EB [28].

5.4.3 Process scheme

A possible process scheme of oxidative coupling and reforming of methane combined with separation of ethylene via ethylbenzene production is shown in Figure 5.7. The exothermic oxidative coupling of methane takes place between 700°C and 800°C. C₂H₄ and C₂H₆ are produced in this reaction (1). A high selectivity to ethylene is desired as ethane cannot react with benzene and is thus converted to synthesis gas in the reforming step (4). Distributed feeding of oxygen can be used in oxidative coupling to optimize ethylene yield [9, 10]. Next to C₂-products, the product mixture after oxidative coupling also contains remaining CH₄ and byproducts CO, CO₂, H₂O as well as small amounts of H₂. Excess benzene is added to this stream, in order to react with ethylene to ethylbenzene at around 360°C (2).

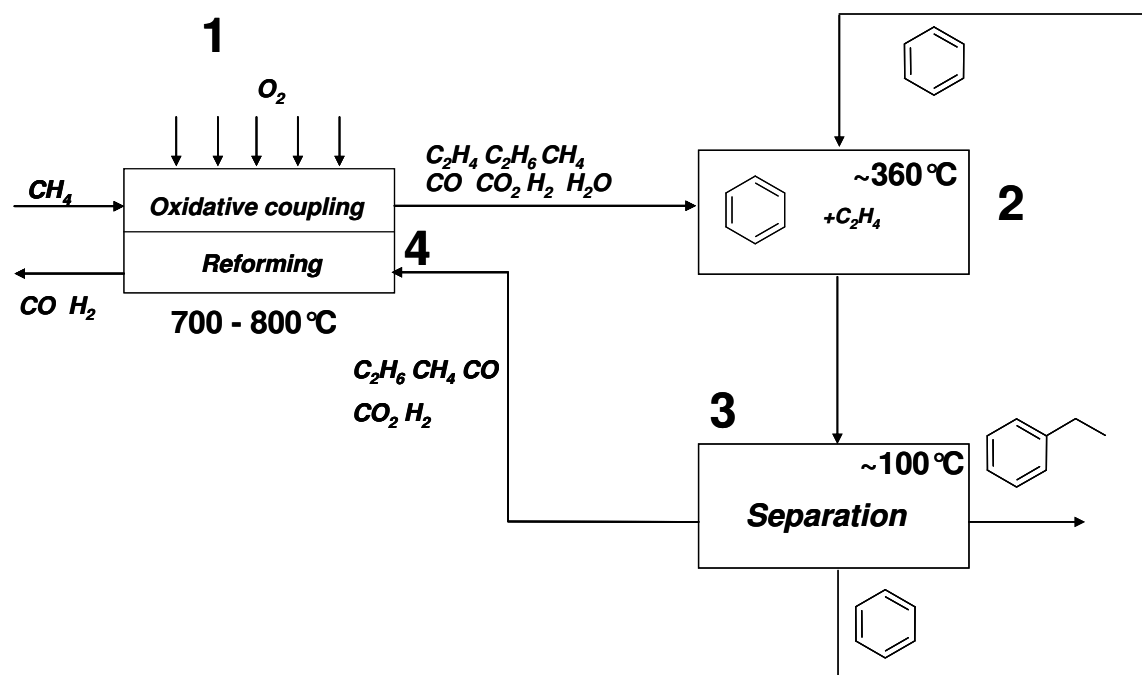


Figure 5.7: Possible process scheme of combined oxidative coupling and reforming of methane with ethylene reactive ethylene separation via alkylation of benzene

After alkylation, a separation step is required (3). The boiling points of ethylbenzene, benzene and di-ethylbenzene are 136°C, 80°C and 184°C, respectively, which provides sufficient difference for separation via a distillation process of the several components, as described by Faessler [34]. The approximate temperature in the separation would be about 100°C, depending on pressure. After separation, benzene has to be evaporated and heated to 360°C, before recycling to reactor (2). The remaining stream is fed to the reforming reactor (4). Water is also removed during the separation step, so additional steam has to be added in the steam reforming reactor.

The oxidative coupling and reforming reactor are combined to use excess heat generated in the coupling process, to drive the endothermic steam reforming reaction. The total process will convert methane and oxygen to synthesis gas and ethylbenzene. Efficient heat exchange is needed to make this concept feasible. Another aspect to consider is the impact of the energy cost of benzene recycling and evaporation.

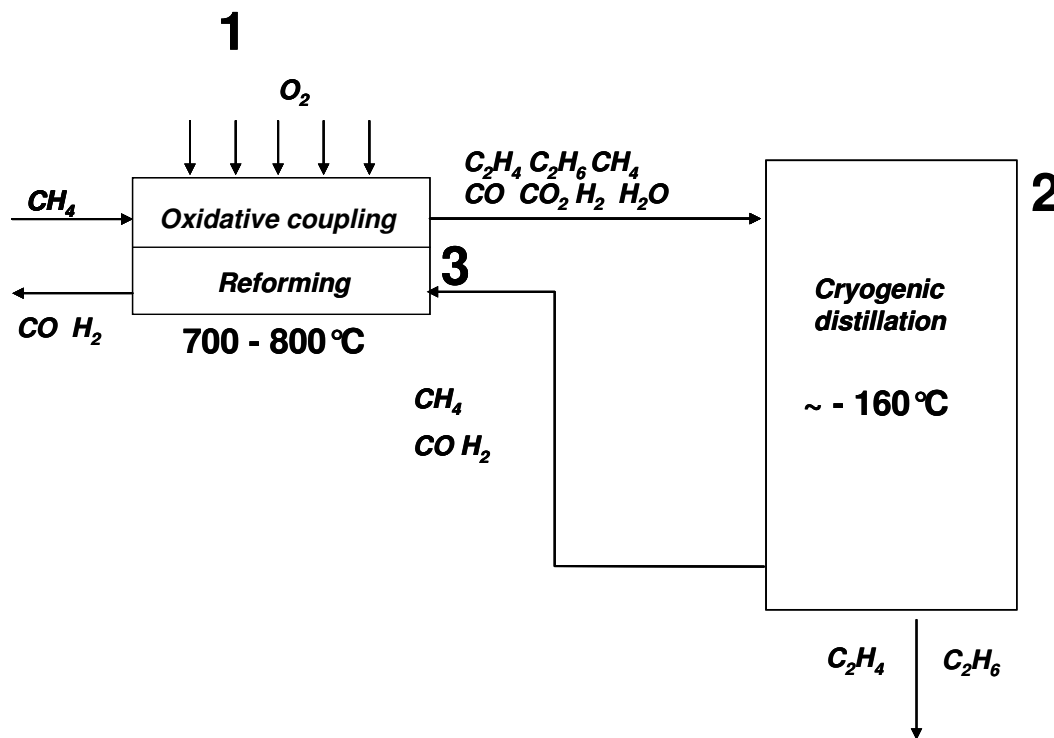


Figure 5.8: Possible process scheme of combined oxidative coupling and reforming of methane with included ethylene separation via cryogenic distillation

Figure 5.8 shows an alternative scheme with ethylene separation through cryogenic distillation (2) [13]. The oxidative coupling (1) and steam reforming part (3) of the process are identical to the scheme in Figure 5.7. The separation of ethylene needs rather extreme conditions, e.g. -160°C. With similar boiling points of ethane and ethylene, separation with cryogenic distillation is difficult and thus obtaining pure fractions of the desired product ethylene requires large and expensive columns. Parts of ethane and methane are lost during separation. This means additional loss of carbon source for production of synthesis gas in step 3. Also, water and CO_2 have to be removed before distillation, implying additional equipment costs. A major issue is the huge temperature difference of around 900°C between step 1 and 2, leading to high cost for heat exchange equipment.

The essential advantage of reactive separation to ethylbenzene (Figure 5.7) is easier and more selective separation of ethylene compared to cryogenic distillation. Further, the temperature differences between reaction and separation could be reduced by

250°C. In addition, the conversion of ethylene to the useful intermediate ethylbenzene is already included in the proposed scheme.

5.5 Conclusions

In a combined process of oxidative coupling and reforming of methane, reactive separation of ethylene via alkylation of benzene to ethylbenzene (EB) is a promising option to separate ethylene from the effluent gas of oxidative coupling. Ethylene was successfully converted to the useful chemical intermediate ethylbenzene using ZSM-5. Yields of EB up to 90% were found at 95% conversion and 90% selectivity at 360°C. None of the additional components present in the effluent gas of oxidative coupling (CO, CO₂, CH₄, C₂H₆ and H₂O) influences activity or selectivity of the alkylation catalyst. Stability of ZSM-5 is not influenced by the added components, with the exception of water, which even increases stability. It was concluded that reactive separation of ethylene to ethylbenzene is a promising option compared to cryogenic distillation, with the essential advantage of reduced temperature differences between oxidative coupling and ethylene separation.

5.6 References

- [1] V.R. Choudhary, B.S. Uphade, *Catalysis Surveys from Asia* 8 (2004) 15.
- [2] M. Makri, C.G. Vayenas, *Applied Catalysis A-General* 244 (2003) 301.
- [3] Istadi, N.A.S. Amin, *Fuel* 85 (2006) 577-592.
- [4] N. Lapena-Rey, P.H. Middleton, *Applied Catalysis A-General* 240 (2003) 207.
- [5] H. Zhang, J. Wu, B. Xu, C. Hu, *Catalysis Letters* 106 (2006) 161.
- [6] J.A. Hugill, F.W.A. Tillemans, J.W. Dijkstra, S. Spoelstra, *Applied Thermal Engineering* 25 (2005) 1259.
- [7] A. Machocki, A. Denis, *Chemical Engineering Journal* 90 (2002) 165.
- [8] D. Czechowicz, K. Skutil, A. Torz, M. Taniewski, *Journal of Chemical Technology and Biotechnology* 79 (2004) 182.
- [9] F.T. Akin, Y.S. Lin, *Catalysis Letters* 78 (2002) 239.
- [10] F.T. Akin, Y.S. Lin, *Aiche Journal* 48 (2002) 2298.
- [11] P.O. Graf, B.L. Mojet, L. Lefferts, *Applied Catalysis A: General* In Press, Accepted Manuscript.
- [12] P.O. Graf, B.L. Mojet, J.G. van Ommen, L. Lefferts, *Applied Catalysis A: General* 332 (2007) 310-317.
- [13] L. Mleczko, M. Baerns, *Fuel Processing Technology* 42 (1995) 217-248.
- [14] S.N. Vereshchagin, V.K. Gupalov, L.N. Ansimov, N.A. Terekhin, L.A. Kovrigin, N.P. Kirik, E.V. Kondratenko, A.G. Anshits, *Catalysis Today* 42 (1998) 361-365.
- [15] N.A.S. Amin, S.E. Pheng, *Chemical Engineering Journal* 116 (2006) 187-195.
- [16] C.H. Christensen, K. Johannsen, E. Törnqvist, I. Schmidt, H. Topsøe, C.H. Christensen, *Catalysis Today* 128 (2007) 117-122.
- [17] C.H. Christensen, K. Johannsen, I. Schmidt, C.H. Christensen, *J. Am. Chem. Soc.* 125 (2003) 13370-13371.
- [18] J.L. Goncalves de Almeida, M. Dufaux, Y.B. Taarit, C. Naccache, *Applied Catalysis A:General* 114 (1994) 141-159.
- [19] Y. Du, H. Wang, S. Chen, *Journal of Molecular Catalysis A: Chemical* 179 (2002) 253-261.
- [20] X. Sun, Q. Wang, L. Xu, S. Liu, *Catalysis Letters* 94 (2004) 75-79.
- [21] K.S.N. Reddy, B.S. Rao, V.P. Shiralkar, *Applied Catalysis A:General* 95 (1993) 53-63.
- [22] M. Han, S. Lin, E. Roduner, *Applied Catalysis A: General* 243 (2003) 175-184.
- [23] Y. Zhang, H. Xing, P. Yang, P. Wu, M. Jia, J. Sun, T. Wu, *Reaction Kinetics and Catalysis Letters* 90 (2007) 45-52.
- [24] H. You, W. Long, Y. Pan, *Petroleum Science and Technology* 24 (2006) 1079-1088.
- [25] C. Perego, P. Ingallina, *Catalysis Today* 73 (2002) 3-22.
- [26] N.Y. Chen, W.E. Garwood, *Catalysis Reviews - Science and Engineering* 28 (1986) 185-264.
- [27] X. Chen, S. Huang, D. Cao, W. Wang, *Fluid Phase Equilibria* 260 (2007) 146-152.
- [28] Z. Qi, R. Zhang, *Industrial and Engineering Chemistry Research* 43 (2004) 4105-4111.
- [29] Y. Song, S. Liu, Q. Wang, L. Xu, Y. Zhai, *Fuel Processing Technology* 87 (2006) 297-302.

- [30] G. Bellussi, G. Pazzuconi, C. Perego, G. Girotti, G. Terzoni, *Journal of Catalysis* 157 (1995) 227-234.
- [31] P.B. Venuto, *Microporous Materials* 2 (1994) 297-411.
- [32] D.L. Trimm, *Catalysis Today* 37 (1997) 233.
- [33] G.R. Meima, P.G. Menon, *Applied Catalysis A: General* 212 (2001) 239-245.
- [34] P.W. Faessler, K. Kolmetz, W.K. Ng, K. Senthil, T.Y. Lim, *DISTILLATION 2005 Spring AIChE Meeting* (2005).

Chapter 6

New insights in the water gas shift mechanism on PtZrO₂: the role of hydroxyl groups elucidated

Abstract

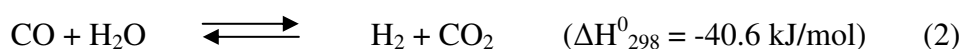
The reactivity of mono- and multi-coordinated hydroxyl groups on Pt/ZrO₂ with CO was investigated with *in-situ* Transmission FT-IR. It was found that mono-coordinated hydroxyl groups on the ZrO₂ support reacted with CO to formate. Multi-coordinated hydroxyl groups were needed for formate decomposition, producing H₂ and CO₂, taking place exclusively in the presence of Pt. The observed differences in reactivity of different types of OH groups are relevant for the WGS mechanism, assuming that formate is a reactive intermediate under the conditions used in this study (300-400°C). The fact that Pt is needed for decomposition of formate indicates that the reactivity of formate depends on the position on the ZrO₂ surface, *i.e.* in close vicinity or remote from metal particles. Our results show that reduction of the support was limited to structural defective zirconia sites at edges and kinks, hosting the mono-coordinated hydroxyl groups. These sites can be re-oxidized with water, re-establishing the hydroxyl groups.

6.1 Introduction

Environmental issues and the depletion of crude oil stimulate the search for alternative energy carriers. Hydrogen based fuel cells were widely investigated as replacement for conventional combustion engines and showed to be very promising [2-5]. The expected increase in hydrogen demand has led to extensive research to optimize hydrogen production. At the moment, natural gas is the biggest source for hydrogen. Synthesis gas ($\text{CO} + \text{H}_2$) can be produced from natural gas via steam reforming, CO_2 reforming, catalytic partial oxidation and auto thermal reforming. Steam methane reforming (SMR) is the most common process for hydrogen production (1):



Carbon monoxide is also formed in addition to hydrogen and the mixture is used directly in numerous industrial applications [6]. If direct use of the hydrogen is desired, CO has to be removed from the synthesis gas mixture. Water gas shift (WGS) (2) is an interesting reaction for reducing CO concentrations, additionally producing more H_2 . As fuel cell applications require CO-free hydrogen, further purification by selective oxidation of CO or methanation is necessary after water gas shift reaction [7-9].



PtZrO_2 was studied as a promising catalyst for water gas shift reaction [1, 10, 11]. The reaction mechanism on noble metals is generally considered bifunctional, with essential roles for both the active metal and the support [12-15]. It has been reported that Pt cannot activate water under water gas shift reaction conditions [16], and therefore activation of water has to take place on the support. Two mechanisms for WGS are indicated in literature: the formate associative mechanism [1, 17-19] and regenerative redox mechanism [12, 15, 20]. The regenerative redox mechanism requires a reducible support like CeO_2 or TiO_2 .

A hybrid mechanism, so called “the associative mechanism with redox regeneration” was proposed for PtZrO_2 [1]. In this mechanism, hydroxyls on the zirconia surface react with CO to form intermediate formate which can react/decompose into H_2 and

CO₂. Afterwards the hydroxyl groups on zirconia are regenerated by water. Formate formation between CO and hydroxyl groups was also proposed earlier by Ma et al. [21]. Formate decomposition was suggested to be facilitated by water [10]. Azzam et al. [1] showed that CO₂ and H₂ could also be formed when CO was pulsed over PtZrO₂ in the absence of water, using hydroxyl groups of the zirconia support and consequently removing oxygen from the zirconia support. Consequently the zirconia needs to be reactivated by decomposing water, thus filling the oxygen vacancy as well as generating OH groups. However, after regeneration of zirconia with N₂O instead of H₂O, resulting in the absence of OH-groups, CO is able to remove oxygen as well by forming CO₂. This confirms the ability of zirconia to provide oxygen under WGS conditions (300°C), even in absence of OH groups. However, clear evidence exists that the formate mechanism is not relevant for Pt/ZrO₂ when operating at mild temperature (200°C), based on DRIFT experiments in combination with isotopic transient experiments by Tibiletti et al [11]. Nevertheless, the formate mechanism continues to be a valid hypothesis for higher temperatures of operation (300-400°C).

Until now, the exact role of the hydroxyl groups in WGS has not been reported, while the presence of differently coordinated hydroxyl groups on the zirconia surface was already demonstrated with FT-IR in 1973 by Tsyganenko et al. [22]. In the following years, more studies were devoted to hydroxyl characterization on zirconia. Two different hydroxyl coordinations located at 3760cm⁻¹ and 3660cm⁻¹ in the FT-IR spectrum [23-26], respectively, were found on the surface of monoclinic zirconia. Mono-coordinated hydroxyls were assigned to IR signals at about 3760cm⁻¹ [26]. With increasing hydroxyl coordination number, the signal in FT-IR of the respective hydroxyl group shifts to lower wave number [22]. However, no consensus exists about the exact coordination of the hydroxyl peak located around 3660cm⁻¹. Quintard et al. [26] assigned this peak to bi-coordinated hydroxyl groups, while others assigned it to tri-coordinated hydroxyl groups [22, 27]. Korhonen et al. [28] concluded the presence of hydroxyl groups of mono, bi- and tri coordination on monoclinic zirconia from a combined study by DFT and FT-IR spectroscopy. In this study the more general term multi-coordinated hydroxyl groups will be used for the peak located around 3660cm⁻¹.

In this article, we report the reactivity of differently coordinated hydroxyl groups with CO. *In situ* transmission FT-IR was used to characterize hydroxyl groups on both monoclinic ZrO₂ and Pt/ZrO₂. ZrO₂ supported catalysts were selected because of the relative simplicity, as compared to TiO₂ and CeO₂, of both the OH band region in the IR spectrum as well as minimal reducibility of the oxide. Additionally, the respective reactivity of the OH groups with CO was studied at different temperatures (240-400°C). Gaseous product formation (CO₂ and H₂) during exposure to CO was monitored in a micro reactor flow setup. The results provide mechanistic information on the water gas shift reaction on Pt/ZrO₂, under the assumption that the associative formate mechanism is operative under conditions used here, i.e. high temperature.

6.2 Experimental

Monoclinic ZrO₂ obtained from Gimex Technical Ceramics (RC-100) was used as catalyst and as support for Pt. Zirconia, with particle sizes between 300 and 600µm, was treated at 600°C for 24h under a helium flow. The structure of the zirconia was not changed by this pre-treatment and remained monoclinic, as detected by XRD. 0.5wt.% PtZrO₂ was prepared by wet impregnation of 10g of ZrO₂ with aqueous solution, obtained by dissolving H₂PtCl₆ (Alfa Aesar) in 25ml of water. PtZrO₂ was calcined at 600°C in synthetic air (30ml/min) for 24h (ramp 5°C min⁻¹).

Platinum loadings on zirconia and the exact composition of the zirconia support were determined using a Philips X-ray fluorescence spectrometer (PW 1480). Platinum dispersion was determined with pulse H₂ chemisorption at room temperature on 0.3g of catalyst using a Micromeritics Chemisorb 2750, assuming a H/Pt ratio of 1. Before pulsing hydrogen, the catalyst was reduced in H₂ at 400°C for 15 minutes and cooled in He to room temperature subsequently.

The transmission FT-IR measurements were recorded with a Bruker Vector 22 with MCT detector. A self supporting wafer was pressed of 15mg of the sample and placed into a home made gold coated cell. Before measurements the samples were reduced in 5vol.% H₂ for 30 minutes (Linde Gas 5.0) at 400°C (heating rate 10°C/min, 40ml/min) and subsequently cooled to reaction temperature in He.

ZrO₂ was studied with FT-IR at 400°C under He (Linde Gas 5.0) to investigate the different hydroxyl groups in the IR spectrum. Helium was dried with a Varian Chromopack CP17971 Gas Clean Moisture Filter. The resolution was 4cm⁻¹ and 256 scans were taken. The reactivity of hydroxyl groups on ZrO₂ and PtZrO₂ towards CO was investigated by subjecting the catalysts to different CO (Hoekloos 4.7) concentrations in He (total flow 40ml/min). No water was present during these experiments.

A micro reactor flow setup was used in combination with a Balzers QMS 200 F mass spectrometer to study transient gaseous product formation during exposure to CO at different temperatures. The IR measurements were mimicked in the flow setup, as gas phase products in IR were not detectable because of too low concentrations. A detailed description of the micro reactor flow setup is given in an earlier publication [29]. About 250mg of 0.5wt.% PtZrO₂ (0.3 – 0.6 mm) was inserted in a quartz micro reactor with inner and outer diameter of respectively 4 and 6mm, reduced with 5vol.% H₂ in Ar for 15 minutes at 400°C ((heating rate 10°C/min, 100 ml/min) and flushed with Ar subsequently. CO (concentration: 8vol.%) in Ar (100ml/min) was fed to the reactor at different temperatures (240°C, 300°C and 400°C) and formation of gaseous products (i.e. CO₂ and H₂) was measured with MS detecting M/z=44 and M/z=2. The catalyst was treated with 6vol.% of water in Ar between experiments to regenerate hydroxyl groups.

6.3 Results

6.3.1 Characterization

The composition of the zirconia as determined with XRF is given in Table 6.1. The Pt content of PtZrO₂ was 0.58 ± 0.01 wt.%. Pt dispersion was 50% as determined with H₂ chemisorption, assuming a H/Pt ratio of 1.

Table 6.1: Catalyst composition

Zirconia Composition	Weight %
ZrO ₂	98.1
HfO ₂	1.7
TiO ₂	0.1
Y ₂ O ₃	0.1
Pt content PtZrO ₂	0.58

Hydroxyl groups on ZrO₂ and PtZrO₂ were studied under helium with Transmission FT-IR. Figure 6.1 shows the hydroxyl region (3900-3500cm⁻¹) of the spectra obtained at 240°C, 300°C and 400°C. Multiple peaks are found in the region between 3800cm⁻¹ and 3600cm⁻¹ with maxima at about 3745cm⁻¹ and 3658cm⁻¹. Peaks in the 3800-3700cm⁻¹ region can be assigned to mono-coordinated hydroxyl groups, while the 3700-3600cm⁻¹ can be assigned to multi-coordinated hydroxyl groups [22]. Multiple smaller peaks are observed in addition to the maxima in both regions indicating hydroxyl groups with different interactions with zirconia. Stabilization of hydroxyl groups by hydrogen interactions between neighbouring hydroxyl groups can induce a small shift to lower wavelengths, explaining the occurrence of multiple peaks [30].

Higher intensity of mono hydroxyls around 3760cm⁻¹ was found on PtZrO₂ as compared to ZrO₂ at 240°C. The intensities of mono hydroxyl groups on both materials are similar at 300°C and 400°C and are hardly affected by temperature increase above 300°C. In contrast, the intensity of multi-coordinated hydroxyl groups clearly decreases with increasing temperature on both ZrO₂ and PtZrO₂. The multi-coordinated hydroxyls show similar intensities under all conditions on both. In general, the intensities of the hydroxyl groups on ZrO₂ and PtZrO₂ are quite similar.

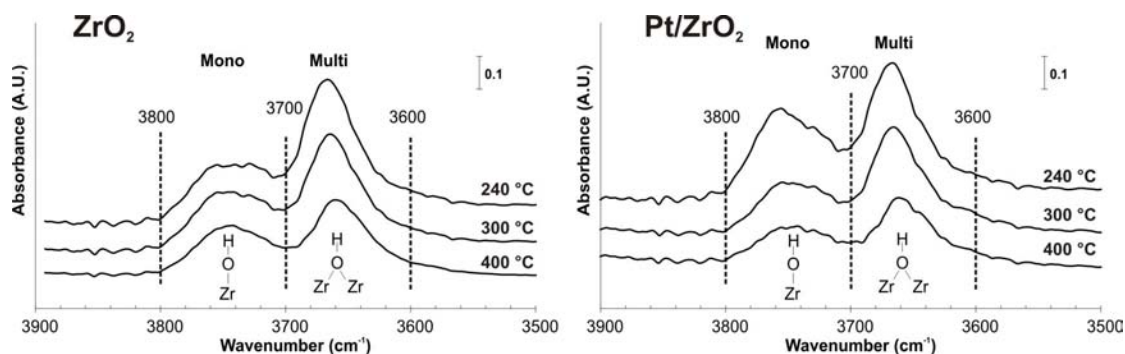


Figure 6.1: IR spectrum of ZrO_2 (left) and Pt/ZrO_2 (right) at 400°C under He

6.3.2 Reactivity of hydroxyl groups with CO on ZrO_2

Figure 6.2 shows close up spectra of the hydroxyl region ($3900\text{--}3500\text{cm}^{-1}$) and C-H and O-C=O formate regions ($3000\text{--}2850\text{cm}^{-1}$) / ($1700\text{--}1200\text{cm}^{-1}$) when ZrO_2 was subjected to CO at 400°C . The dotted lines represent the spectrum under helium, used as a reference. Addition of CO resulted in a decrease of the intensity of mono-coordinated hydroxyl peak ($3800\text{--}3700\text{cm}^{-1}$), while the multi-coordinated hydroxyl peak ($3700\text{--}3600\text{cm}^{-1}$ region) was hardly influenced.

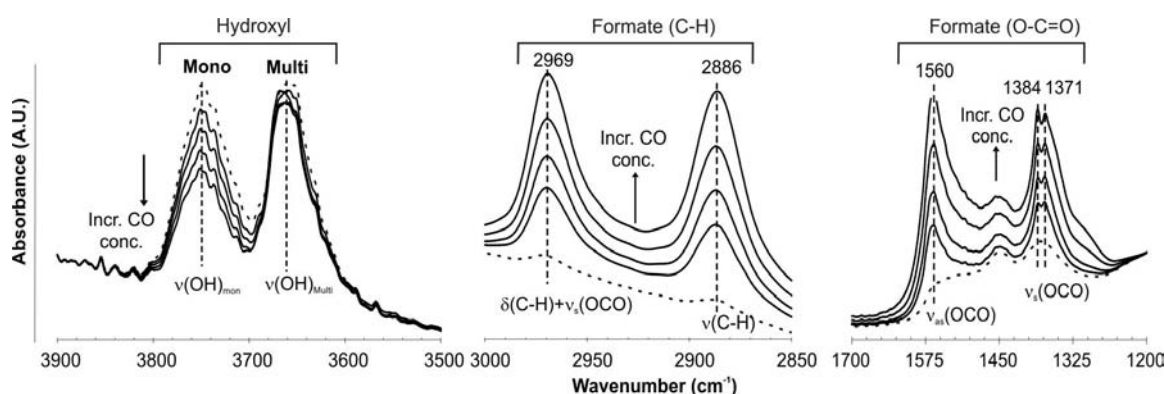


Figure 6.2: FT-IR spectra of addition of CO concentrations of 0, 8, 15, 37, 65vol.% on ZrO_2 at 400°C . Hydroxyl region ($3900\text{--}3500\text{cm}^{-1}$), formate region ($3000\text{--}2850\text{cm}^{-1}$) and ($1700\text{--}1200\text{cm}^{-1}$). Reference spectrum taken in He (dotted line).

As a result of CO addition new peaks appeared on ZrO_2 at 2969cm^{-1} , 2886cm^{-1} , 1560cm^{-1} , 1384cm^{-1} and 1371cm^{-1} . The peaks in the $3000\text{--}2850\text{cm}^{-1}$ and $1700\text{--}1200\text{cm}^{-1}$ region can be assigned to C-H bending and O-C=O stretching vibrations respectively and are representing surface formate [10].

Figure 6.3 shows the integrated intensities of FT-IR signals of the mono-coordinated and the formate representing C-H region ($3000\text{-}2850\text{cm}^{-1}$) as a function of CO concentration. It is shown that the intensity of the formate peak increased steadily with increasing CO concentration, accompanied by increased consumption of mono-coordinated hydroxyl groups. The experiments presented here were mimicked experimentally in the micro reactor flow setup to check the formate decomposition to CO_2 and H_2 . However, no gas phase products were detected with mass spectrometry when exposing ZrO_2 to CO between 240°C and 400°C .

It was found that formate formation was completely reversible: reducing CO concentration led to a decrease of surface formate and a simultaneous increase of mono-coordinated hydroxyl groups. Complete removal of CO led to the disappearance of surface formate and complete recovery of mono-coordinated hydroxyl groups (not shown).

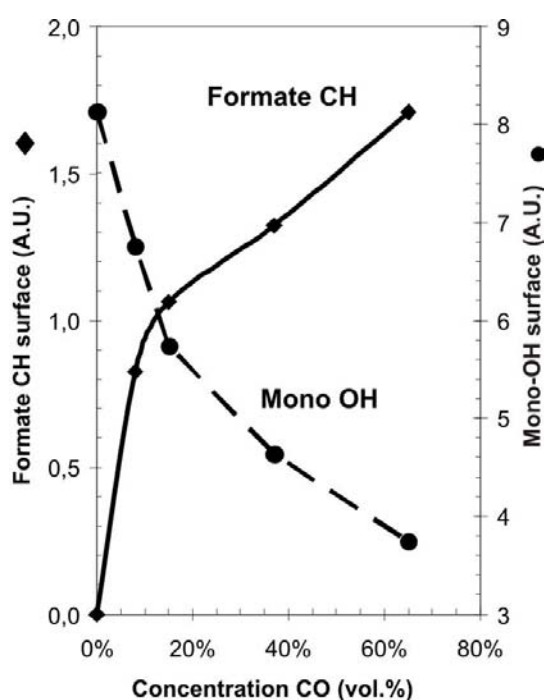


Figure 6.3: Integrated FT-IR regions of mono-coordinated hydroxyls (\bullet)(3745cm^{-1}) and formate (\blacklozenge)(2886cm^{-1}) as a function of CO concentration at 400°C .

The effect of temperature to formate formation on zirconia is shown in Figure 6.4, showing the FT-IR spectra of ZrO_2 of the hydroxyl region ($3850\text{-}3550\text{cm}^{-1}$) and formate region ($3025\text{-}2825\text{cm}^{-1}$ / $1750\text{-}1150\text{cm}^{-1}$) at 240°C , 300°C and 400°C after

exposure to 8vol.% CO (solid line). Temperature was increased under continuous presences of CO. The dashed lines in Figure 6.4 represent the spectra under He at the respective temperature (as shown in Figure 6.1). Two well defined hydroxyl peaks were observed at 240°C under helium (dashed) with maxima around 3745 cm^{-1} (mono-coordinated hydroxyls) and 3658 cm^{-1} (multi-coordinated hydroxyls). The mono-coordinated hydroxyl peak (3745 cm^{-1}) at 240°C decreased instantaneously when ZrO_2 was treated with 8vol.% CO (Figure 6.4A-I solid line). Simultaneously, large quantities of formate were formed (Figure 6.4B-I and 4C-I, solid line).

The amount of adsorbed formate decreased when the temperature was increased to 300°C (Figures 6.4B-II and 6.4C-II, solid line) and mono-coordinated hydroxyls (3700-3800 cm^{-1}) partly recovered (Figure 6.4A-II, solid line). Further increase of temperature to 400°C caused the amount of formate to decrease even more (Figures 6.4B-III and 6.4C-III, solid line). Simultaneously, the intensity of mono-coordinated hydroxyl groups increased further, becoming similar to the level obtained in helium at 400°C in the absence of CO (Figure 6.4A-III, solid line).

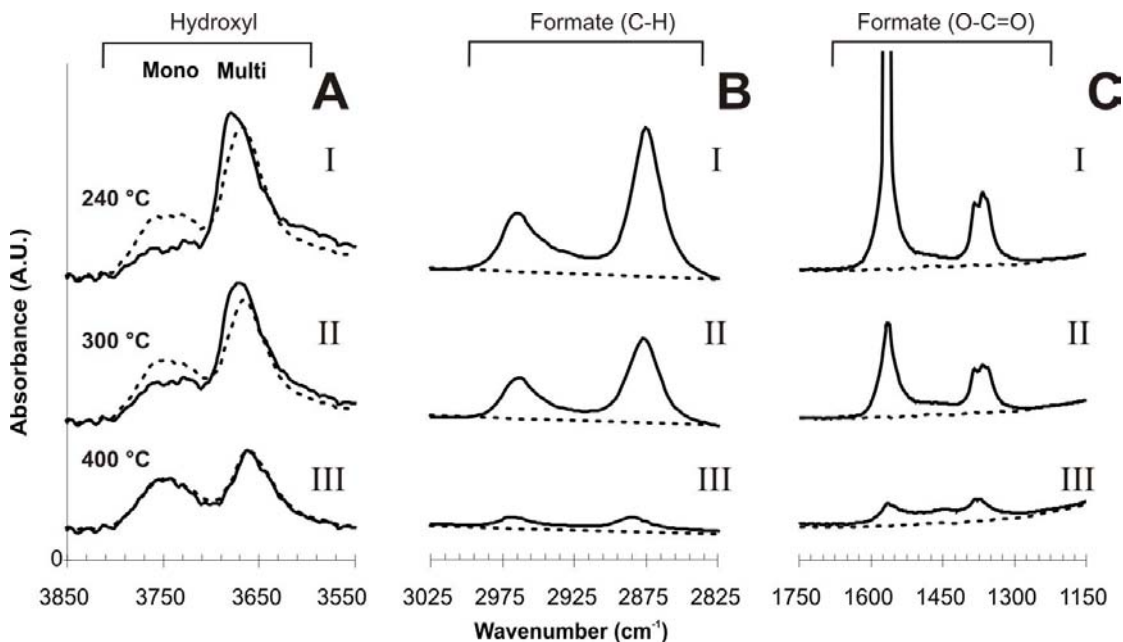


Figure 6.4: FT-IR spectra of ZrO_2 subjected to 8vol.% CO (solid lines) at 240°C (I), 300°C (II) and 400°C (III). Hydroxyl region (3850-3550 cm^{-1}) (A), Formate region (C-H 3025-2825 cm^{-1}) (B), O-C=O 1750-1150 cm^{-1} (C). Reference spectra under helium (dashed lines)

The intensities of multi-coordinated hydroxyl groups did not change as a result of CO addition during the experiments on ZrO_2 , as similar intensities of multi OH groups were found in presence and absence of CO between 240°C and 400°C. No gaseous products were detected on ZrO_2 between 240 and 400°C when this experiment was mimicked in experiments in the micro reactor flow setup.

6.3.3 Reactivity of hydroxyl groups with CO on PtZrO_2

Figure 6.5 shows Transmission FT-IR spectra, obtained by treating PtZrO_2 with 8% CO (solid lines) at 240°C, 300°C and 400°C, compared to reference spectra under helium (dashed lines, identical with results in Figure 6.1). Complete consumption of mono-coordinated hydroxyls was observed at 240°C (Figure 6.5A-I, solid line). Only marginal changes in the amount of multi-coordinated hydroxyls were observed at 240°C. Simultaneously, formate was formed (Figures 6.5B-I and 6.5C-I, solid line). The formate formation is still reversible: removal of CO leads to disappearance of formate species (not shown). A decrease of multi-coordinated hydroxyls was observed when the temperature was increased to 300°C. Also, the amount of formate on PtZrO_2 decreased as compared to the amount of formate observed at 240°C.

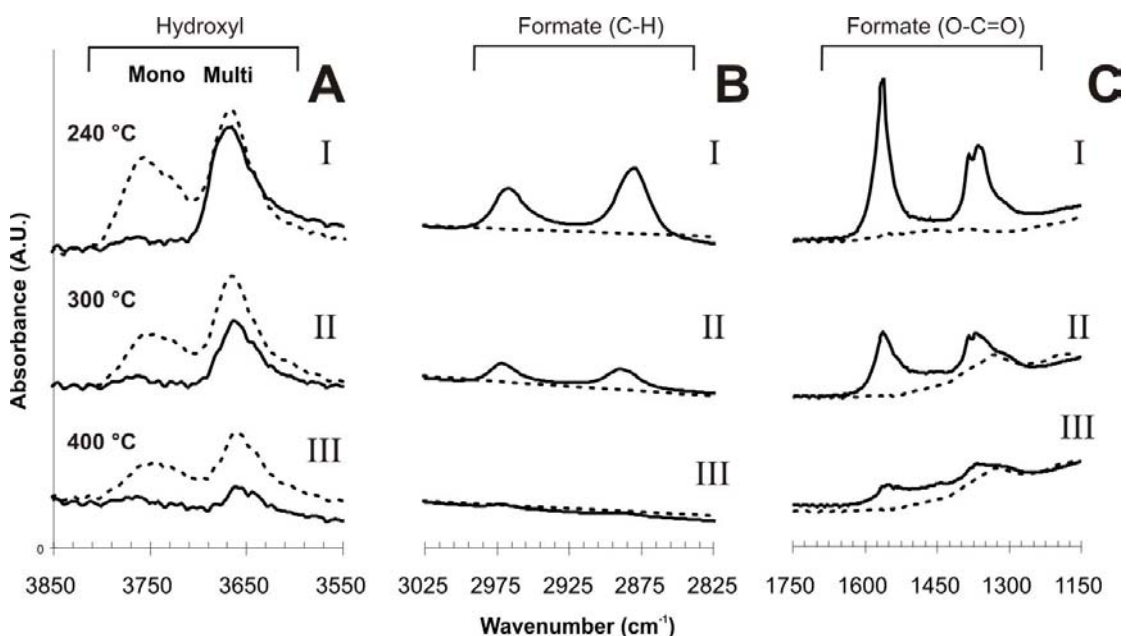


Figure 6.5: FT-IR spectra of 0.5wt.% PtZrO_2 subjected to 8% CO (solid lines) at 240°C (I), 300°C (II) and 400°C (III). Hydroxyl region (3850-3550 cm^{-1}) (A), Formate region (C-H 3025-2825 cm^{-1}) (B), O-C=O 1750-1150 cm^{-1}) (C). Reference spectra under helium (dashed lines).

When temperature is increased to 400°C, most multi-coordinated hydroxyls on PtZrO₂ were consumed and formate almost disappeared. In contrast to ZrO₂, mono-coordinated hydroxyls on PtZrO₂ did not reappear. Titration experiments of PtZrO₂ with CO in the micro reactor flow setup with MS analysis revealed formation of CO₂ and H₂ at 300°C and 400°C. Exposure of PtZrO₂ to CO at 240°C, however, did not result in any formation of CO₂ and H₂. The formation of CO₂ and H₂ at 300°C and 400°C stopped after a few seconds, indicating that surface hydroxyl groups were exhausted (as shown in Figures 6.5A-II and 6.5A-III). Treating PtZrO₂ with water restored the activity, regenerating hydroxyl groups (not shown).

6.3.4 CO adsorption on platinum

CO adsorption on platinum was studied on PtZrO₂ during the treatments with CO. Figure 6.6 shows Transmission FT-IR spectra between 2100cm⁻¹ and 2000cm⁻¹ of 0.5wt.% PtZrO₂ when subjected to 8vol.% CO in a temperature range of 240 to 400 °C. At 240°C, two peaks with a maximum at 2061cm⁻¹ and a shoulder at 2075cm⁻¹ are observed in the FT-IR spectrum and can be assigned to CO linearly adsorbed on platinum [31]. The intensity of both peaks was independent of temperature up to 280°C. A further increase to 300 °C decreased the amount of adsorbed CO. At 400°C, CO adsorption on Pt reduced significantly.

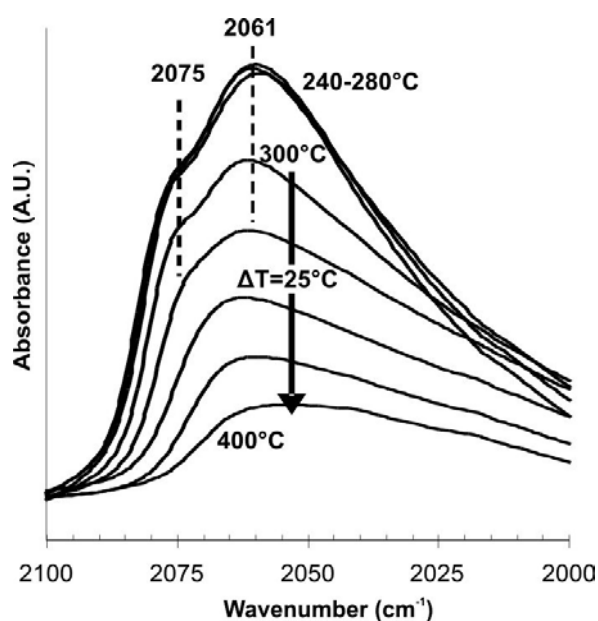


Figure 6.6: FT-IR spectra of CO adsorption on PtZrO₂ at different temperatures.

6.4 Discussion

6.4.1 Characterization of ZrO_2 and $PtZrO_2$

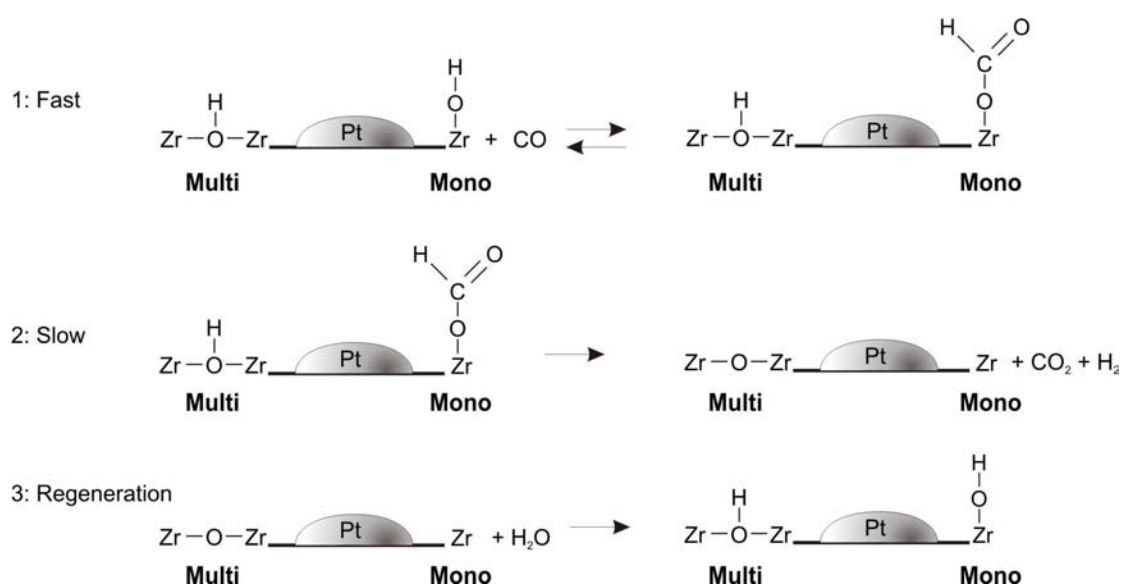
Transmission FT-IR characterization of monoclinic zirconia and $PtZrO_2$ revealed two peaks that can be assigned to mono and multi-coordinated hydroxyl groups respectively (Figure 6.1) in agreement with literature [23-26]. Only marginal differences in intensities of mono- and multi-coordinated hydroxyl groups were observed between ZrO_2 and $PtZrO_2$ above 300°C under He. Thus, the differences observed in reactivity of hydroxyl groups are not due to differences in the initial amount of OH groups, and must be due to the presence of Pt as discussed below.

6.4.2 Hydroxyl reactivity on ZrO_2 towards CO

It was demonstrated in Figure 6.2 that mono-coordinated hydroxyls on ZrO_2 reacted with CO, resulting in formation of surface formate on ZrO_2 . Formate formation as a result of CO addition can be concluded based on the appearance of peaks at 2969 cm^{-1} , 2886 cm^{-1} , 1560 cm^{-1} , 1384 cm^{-1} and 1371 cm^{-1} . The peaks at 1560 cm^{-1} , 1384 cm^{-1} and 1371 cm^{-1} can be assigned to symmetric and asymmetric stretching vibrations of O-C-O species. The presence of O-C-O is an indication for surface formate, but also surface carbonate could be responsible for O-C-O peaks [10]. However, the presence of C-H species is clear from the peaks at 2969 cm^{-1} and 2886 cm^{-1} . The combined presence of C-H and O-C-O vibrations indicate formate formation [10]. However, additional presence of surface carbonate cannot be ruled out. Several studies in literature claim the involvement of CO adsorbed on Pt in the formation of formate [1, 10]. However, formate was also formed on zirconia without any Pt in our experiments, demonstrating that Pt is not necessary on the present catalyst. This view is supported by Ma et al. [21], who also reported formate formation between hydroxyls on ZrO_2 and CO in the absence of platinum. In exact agreement with our results, formate formation in absence of Pt between CO and mono-coordinated hydroxyl groups on monoclinic zirconia was also reported in a recent paper by Korhonen et al. [32].

It was observed that increasing CO concentration resulted in increased consumption of mono-coordinated hydroxyls as well as formation of larger amounts of formate

(Figure 6.2). This formate did not decompose into gaseous products. Formate formation proved to be reversible as removal of CO resulted in total recovery of mono-coordinated hydroxyl groups and disappearance of formate species on ZrO₂ (Figure 6.3). Large amounts of formate were observed at 240°C but the amount decreased upon increasing the temperature to 400°C, also accompanied by recovery of mono-coordinated hydroxyls (Figure 6.4). This shows that formate is thermodynamically favoured at low temperature. At higher temperatures the equilibrium is shifted to gas phase CO and mono-coordinated hydroxyl groups, obviously because of high entropy of CO in gas phase. Multi-coordinated hydroxyls on ZrO₂ were not reactive towards CO. From these observations, we conclude that formate can be formed on ZrO₂ through an equilibrium reaction between CO and mono-coordinated hydroxyl groups as shown in Scheme 6.1 (step 1).



Scheme 6.1: Water gas shift reaction mechanism for PtZrO₂. 1: Formate formation through reaction between CO and mono-coordinated hydroxyls 2: Formate decomposition involving Pt and multi-coordinated hydroxyls 3: Hydroxyl regeneration with water

6.4.3 Hydroxyl reactivity on PtZrO₂ towards CO

Identical to ZrO₂, formation of formate through mono-coordinated hydroxyls was also observed on PtZrO₂ at 240°C (Figure 6.5A). The formate peaks were located at the same wavenumbers on PtZrO₂, indicating that the formate species on ZrO₂ and PtZrO₂ are identical. Apparently formate species on PtZrO₂ do not interact

significantly with the Pt particles. No H₂ and CO₂ formation occurred at 240°C on PtZrO₂. This demonstrates that step 1 in Scheme 6.1 is also valid in case of PtZrO₂.

Increasing the temperature to 300°C resulted in a decrease of surface formate and multi-coordinated hydroxyl groups on PtZrO₂ (Figure 6.5). At 400°C hardly any multi-coordinated hydroxyls and surface formate were present on PtZrO₂ (Figure 6.5). On PtZrO₂ mono-coordinated hydroxyl groups were not recovered at temperatures above 300°C in contrast to ZrO₂, which excludes formate decomposition to CO and mono-coordinated OH groups i.e. the reverse reaction 1 in Scheme 6.1 (comparing Figures 6.5A-I and 6.5A-III). Production of gas phase products (CO₂ and H₂) on PtZrO₂ was observed, starting at 300°C. This shows that formate on PtZrO₂ decomposes to CO₂ and H₂ at temperatures above 300°C.

It was found that next to H₂ and CO₂ formation, simultaneous decrease of both surface formate and especially multi-coordinated hydroxyl groups occurred above 300°C on PtZrO₂ (Figure 6.5). This suggests that multi-coordinated hydroxyl groups on PtZrO₂ are involved in formate decomposition to H₂ and CO₂. Furthermore, this study showed that formate decomposition to gas phase products only occurs in the presence of Pt. Step 2 in Scheme 6.1 schematically depicts formate decomposition into H₂ and CO₂ by consumption of multi-coordinated hydroxyl groups in the presence of Pt.

The relevance of these observations for the mechanism of WGS will now be discussed, assuming that formate is the relevant intermediate species at the relatively high temperatures used in this study. Formate formation proved to be an equilibrium reaction depending on the gas phase concentration of CO (Figure 6.2) and temperature (Figures 6.4 and 6.5). It was demonstrated that formate was already formed at 240°C. As higher temperatures were required for formate decomposition, it seems likely that the decomposition is rate determining. This is in agreement with Pigos et al. who identified C-H bond breaking in formate as the rate determining step in WGS mechanism [10]. Pigos et al. [10] proposed that platinum assists in abstracting H from the formate C-H bond to enable the complex to dissociate into H₂ and CO₂, based on hydrogen-deuterium exchange experiments in formate over ZrO₂ and PtZrO₂. H-D exchange in formate hardly occurred without Pt, whereas Pt increased the exchange rate significantly. Our results confirm that Pt is required for the formate

decomposition and additionally demonstrate the involvement of multi-coordinated hydroxyl groups in the decomposition of formate. However, hydrogen abstraction from formate and subsequent recombination of this hydrogen atom adsorbed on Pt with a hydrogen atom of a multi-coordinated hydroxyl group seems not very likely, as the O-H bond is very strong. Therefore, we suggest that a concerted mechanism occurs in formate decomposition. The multi-coordinated OH group and the Pt surface both interact with the formate complex simultaneously, breaking the C-H bond in the formate and the O-H bond in the multi-coordinated OH group, forming CO₂ and H₂ in one concerted step.

The experimental observation that decomposition of formate to CO₂ and H₂ takes place exclusively in the presence of platinum, would suggest that formate species located close to a metal particle decompose faster than a formate species positioned remotely from metal particles. This would seriously complicate the interpretation of the experimental result reported by Tibiletti et al. [11], showing a much slower response of the formate IR signals when feeding labeled CO in DRIFT measurements as compared to the kinetics of the reaction. Based on this, it was concluded that formate is not involved in the rate determining step and is a spectator instead in water gas shift reaction at 200°C. However, a slow response of formate species can also be explained by assuming that part of the formate species are located far away from Pt particles and surface diffusion is required for formate decomposition at the Pt particles. Relatively slow surface diffusion of formate could well result in slow response of the formate IR signals to the isotopic step change. It should be noted that mono-coordinated hydroxyl groups were almost completely converted (figure 5), when treating Pt/ZrO₂ with CO above 300°C. This demonstrates the mobility of both formate species as well as bridged OH groups in order to interact with Pt on the zirconia surface, eventually resulting in consumption of all available mono-coordinated surface OH-groups. Unfortunately, our experiments did not allow accurate determination of the dynamics of those events.

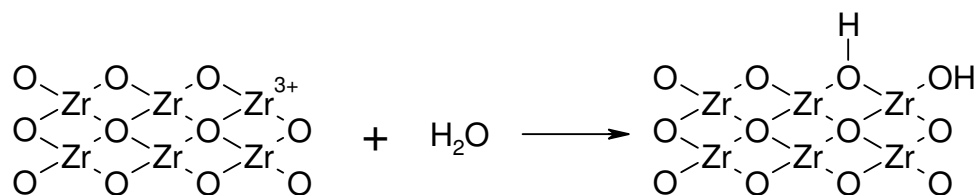
It should be noted that the conclusions drawn so far were obtained in experiments with surface hydroxyl groups, without any gas phase water present. Two possible roles for water in the reaction mechanism are proposed in literature [9]. The role of water is either decomposition of formate (and simultaneous reoxidation of zirconia

and regeneration of hydroxyl groups) or regeneration of the zirconia support exclusively. It was demonstrated in transient experiments that CO_2 and H_2 could be formed on hydroxylated PtZrO_2 during titration studies with CO , in the absence of water. As described extensively in earlier work by our group [1], product formation of PtZrO_2 stopped when the hydroxyl groups were exhausted. After pulsing water to the “exhausted” catalyst, complete regeneration of hydroxyl groups on PtZrO_2 was accomplished, demonstrated by complete recovery of the reactivity of the catalyst in reaction with CO to CO_2 . We therefore conclude that the exclusive role of water is regeneration of the hydroxyl groups and simultaneous re-oxidation of the support.

DFT calculations [28, 33] showed that the dissociation of water involves adsorption of water on a zirconium ion, resulting in the formation of one mono-coordinated and one multi-coordinated hydroxyl group. We showed that one mono-coordinated and one multi-coordinated hydroxyl group are consumed during water gas shift reaction of one CO molecule. Regeneration of both hydroxyl groups with one water molecule leads to a stoichiometrically balanced reaction for water gas shift.

Our current experiments with continuous presence of CO and earlier results in CO pulsing experiments by Azzam et al. [1] demonstrated that oxygen of the support was consumed during reaction with CO and thus partial reduction of the zirconia takes place. It was shown by Azzam et al. that after regeneration of an “exhausted” zirconia surface with N_2O , also reaction of CO to CO_2 was possible. It was found by Zhu [34] that activation of N_2O on zirconia takes place at structural defect sites (i.e. low coordinated Zr -cations located edges and corners). Zhu also showed that the structural defects did not react with O_2 . Based on the fact that the amount of CO_2 formed during exposure to CO is similar after re-oxidation with H_2O compared to N_2O [1], it follows that reduction of zirconia under WGS reaction conditions is limited to the structural defect sites. Scheme 6.2 illustrates the regeneration step with water on a defective Zr^{3+} -cation. Water dissociation creates a mono-coordinated OH -group on the structural defect site and a multi-coordinated OH -group on a neighbouring oxygen atom. It is proposed that in case of regeneration with water, the formed mono-coordinated OH -group on the defect site can react with CO to form formate. The surface formate can be converted with use of the multi OH group to H_2 and H_2O , assisted by Pt . To summarize, we need to precise our previous conclusion on the

reaction pathway for WGS on PtZrO₂ via “formate and redox regeneration” [1], in the sense that the redox step is limited to structural defect sites on zirconia.



Scheme 6.2: Proposed regeneration of surface hydroxyl and simultaneous reoxidation of ZrO₂, taking place on structural defects

The regeneration of the hydroxyl groups on ZrO₂ is also depicted more schematically in Scheme 6.1 (step 3). This leads to the following overall reaction steps in WGS: First, CO reacts with one mono hydroxyl group to form formate which is subsequently converted with a multi-coordinated hydroxyl group to H₂ and CO₂ in the presence of Pt. Finally, the hydroxyl groups on the ZrO₂ surface are regenerated by water dissociation.

In this mechanism CO activation on Pt is not required to produce formate on ZrO₂ (Figures 6.2, 6.3 and 6.4). Identical formate species were detected in presence of Pt (Figure 6.5). Figure 6.6 shows that high CO coverage on Pt can be expected below 300°C. Starting at 300°C, the intensity of adsorbed CO on Pt decreased, indicating a lower surface coverage. Exactly at the same temperature, formation of gas phase products was initiated. This demonstrates that adsorption of carbon monoxide on platinum could have a negative influence on water gas shift reaction, occupying Pt sites and preventing formate decomposition below 300°C. At temperatures above 300°C, the lower CO coverage on Pt increases accessibility of Pt sites, enhancing formate decomposition to H₂ and CO₂.

6.5 Conclusion

The main goal of this study was to determine the reactivity of hydroxyl groups on Pt/ZrO₂ in the water gas shift reaction. It was shown in this paper that two types of hydroxyl groups are present on monoclinic zirconia: mono- and multi-coordinated hydroxyls. Mono-coordinated hydroxyls are involved in formate formation, while multi-coordinated hydroxyls are needed for formate decomposition. Platinum is not involved in the formation of formate, in contrast, Pt is needed to enable formate decomposition, resulting in formation of CO₂ and H₂. These results imply that the reactivity of formate species depend on the distance to Pt particles.

In addition to the formate mechanism with redox regeneration proposed earlier for WGS on Pt/ZrO₂ by Azzam [1], it was found in this study that reduction of the support was limited to structural defective zirconia sites at edges and kinks. These sites can be regenerated with water, implying that the role of water in the WGS mechanism is regeneration of hydroxyl groups and simultaneous re-oxidation of ZrO₂.

6.6 References

- [1] K.G. Azzam, I.V. Babich, K. Seshan, L. Lefferts, *Journal of Catalysis* 251 (2007) 153-162.
- [2] W.C. Lattin, V.P. Utgikar, *International Journal of Hydrogen Energy* 32 (2007) 3230-3237.
- [3] K.B. Prater, *Journal of Power Sources* 51 (1994) 129-144.
- [4] W. Ruettinger, O. Ilinich, R.J. Farrauto, *Journal of Power Sources* 118 (2003) 61-65.
- [5] J.-H. Wee, *Renewable and Sustainable Energy Reviews* 11 (2007) 1720-1738.
- [6] F. Mueller-Langer, E. Tzimas, M. Kaltschmitt, S. Peteves, *International Journal of Hydrogen Energy* 32 (2007) 3797-3810.
- [7] T.V. Choudhary, D.W. Goodman, *Catalysis Today* 77 (2002) 65-78.
- [8] K. Takanebe, K.-i. Aika, K. Inazu, T. Baba, K. Seshan, L. Lefferts, *Journal of Catalysis* 243 (2006) 263-269.
- [9] K. Ledjeff-Hey, J. Roes, R. Wolters, *Journal of Power Sources* 86 (2000) 556-561.
- [10] J.M. Pigos, C.J. Brooks, G. Jacobs, B.H. Davis, *Applied Catalysis A: General* 328 (2007) 14-26.
- [11] D. Tibiletti, F.C. Meunier, A. Goguet, D. Reid, R. Burch, M. Boaro, M. Vicario, A. Trovarelli, *Journal of Catalysis* 244 (2006) 183-191.
- [12] T. Bunluesin, R.J. Gorte, G.W. Graham, *Applied Catalysis B: Environmental* 15 (1998) 107-114.
- [13] D.C. Grenoble, M.M. Estadt, D.F. Ollis, *Journal of Catalysis* 67 (1981) 90-102.
- [14] P. Panagiotopoulou, A. Christodoulakis, D.I. Kondarides, S. Boghosian, *Journal of Catalysis* 240 (2006) 114-125.
- [15] X. Wang, R.J. Gorte, *Applied Catalysis A: General* 247 (2003) 157-162.
- [16] K. Takanebe, K.-i. Aika, K. Seshan, L. Lefferts, *Journal of Catalysis* 227 (2004) 101-108.
- [17] S.Y. Choung, M. Ferrandon, T. Krause, *Catalysis Today* 99 (2005) 257-262.
- [18] H. Iida, A. Igarashi, *Applied Catalysis A: General* 303 (2006) 48-55.
- [19] T. Shido, Y. Iwasawa, *Journal of Catalysis* 141 (1993) 71-81.
- [20] F.C. Meunier, D. Tibiletti, A. Goguet, D. Reid, R. Burch, *Applied Catalysis A: General* 289 (2005) 104-112.
- [21] Z.-Y. Ma, C. Yang, W. Wei, W.-H. Li, Y.-H. Sun, *Journal of Molecular Catalysis A: Chemical* 231 (2005) 75-81.
- [22] A.A. Tsyganenko, V.N. Filimonov, *Journal of Molecular Structure* 19 (1973) 579-589.
- [23] P.A. Agron, E.L. Fuller, H.F. Holmes, *Journal of Colloid and Interface Science* 52 (1975) 553-561.
- [24] X. Chen, S. Huang, D. Cao, W. Wang, *Fluid Phase Equilibria* 260 (2007) 146-152.
- [25] C.K. Loong, J.W. Richardson, M. Ozawa, *Journal of Catalysis* 157 (1995) 636-644.
- [26] T. Merle-Méjean, P. Barberis, S.B. Othmane, F. Nardou, P.E. Quintard, *Journal of the European Ceramic Society* 18 (1998) 1579-1586.
- [27] B. Bachiller-Baeza, I. Rodriguez-Ramos, A. Guerrero-Ruiz, *Langmuir* 14 (1998) 3556-3564.

- [28] S.T. Korhonen, M. Calatayud, A.O.I. Krause, *J. Phys. Chem. C* 112 (2008) 6469-6476.
- [29] P.O. Graf, B.L. Mojet, J.G. van Ommen, L. Lefferts, *Applied Catalysis A: General* 332 (2007) 310-317.
- [30] E. Knozinger, K.H. Jacob, S. Singh, P. Hofmann, *Surface Science* 290 (1993) 388-402.
- [31] P. Pillonel, S. Derrouiche, A. Bourane, F. Gaillard, P. Vernoux, D. Bianchi, *Applied Catalysis A: General* 278 (2005) 223-231.
- [32] S.T. Korhonen, M. Calatayud, A.O.I. Krause, *J. Phys. Chem. C* (2008).
- [33] A. Ignatchenko, D.G. Nealon, R. Dushane, K. Humphries, *Journal of Molecular Catalysis A: Chemical* 256 (2006) 57-74.
- [34] Z. Jianjun, S. Albertsma, J.G. van Ommen, L. Lefferts, *Journal of Physical Chemistry B* 109 (2005) 9550-9555.

Chapter 7

Conclusions

7.1 Introduction

The research discussed in this thesis and the parallel work by Tymen Tiemersma evaluated the possibilities of combining the oxidative coupling and reforming of methane in one multifunctional reactor. Several aspects related to catalyst and reactor development were investigated and are described in the two PhD theses. The main conclusions are summarized in this chapter, leading to ideas for further research and future reactors in oxidative coupling and reforming. Figure 7.1 summarizes the reactions taking place in the combined process.

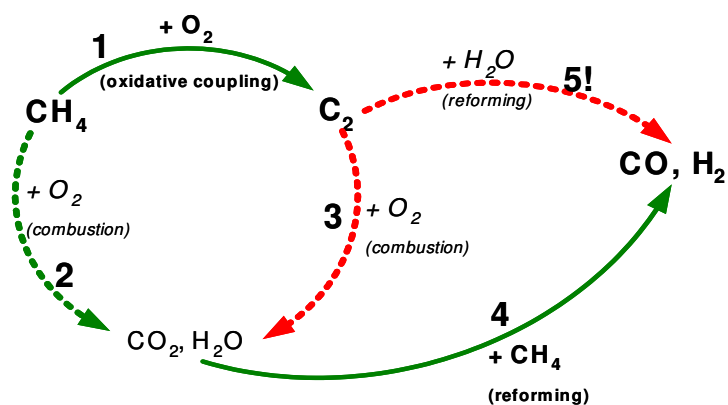


Figure 7.1: Reactions occurring in combined process of methane coupling and steam reforming

Methane coupling produces C₂ hydrocarbons (ethane and ethylene) and water (1). The side combustion reactions of methane (2) and C₂-hydrocarbons (3) produce water and CO₂, which can react with the remaining methane through steam or dry reforming

to CO and H₂ (4). The main challenge in the reaction concept is to suppress steam/dry reforming of ethane and ethylene (5!) in order to avoid complete reaction to synthesis gas. The main topics covered in the project were:

- (i) development of steam reforming catalyst able to reform only methane selectively in presence of ethane and ethylene
- (ii) optimization of oxidative coupling process and catalyst formulation
- (iii) development of a reactor concept based on the insights gained in both processes
- (iv) the mechanism of activation of water on zirconia was investigated, using water gas shift as a model reaction

7.2 Reforming competition (chapter 2, 3 and 4)

Chapter 2 discussed a comparative study of methane, ethane and ethylene steam reforming on Pt, Rh and Pd on YSZ (yttrium-stabilized zirconia). The intention was to develop a methane selective steam reforming catalyst, showing low reactivity towards ethane and ethylene. Both, reactivity and composition of products varied depending on the reforming catalyst. The order of activity of separate hydrocarbons on Rh was C₂H₆ > C₂H₄ > CH₄. On Pt, methane reacted faster than the C₂ hydrocarbons: CH₄ > C₂H₆ ≈ C₂H₄. Concerning the target process of methane coupling combined with reforming, Pt is considered the most promising metal because C₂ hydrocarbons are converted less than methane. Additionally, PtYSZ was the most stable catalyst. The higher reactivity of Rh towards C₂ hydrocarbons relates to findings in literature; Rh shows a higher binding strength of carbon atoms than Pt, indicating a higher reactivity in C-C scission reactions [1, 2]. On PtYSZ, the steam reforming reactions resulted in synthesis gas exclusively. It was shown that both synthesis gas and methane were formed during steam reforming of ethane on RhYSZ. Hydrogenolysis of ethane occurred on this catalyst as a consecutive reaction, consuming hydrogen produced in ethane steam reforming *via* hydrogenolysis of unconverted ethane. This showed that effective steam reforming of higher hydrocarbons can only be achieved when the activity for hydrogenolysis is limited, avoiding production of methane.

Reforming experiments with mixtures of methane/ethylene showed that preferential conversion of ethylene occurred on PtYSZ. It was also found that in methane/ethane

mixtures, methane and ethane competed for active sites on Pt. It was found that ethane provides a high surface coverage of C_xH_y fragments in steam reforming of methane and ethane mixtures. In mixtures of methane and ethane water activation is the rate limiting step in the mechanism on PtYSZ, in contrast to the mechanism for methane reforming as reported by Wei with hydrocarbon activation as the rate limiting step [3-5]. The addition of potassium to PtYSZ (chapter 3 and 4) resulted in weaker adsorption of methane and ethane on the Pt surface, indicated by weakened adsorption of CO in FT-IR TPD on Pt4K700. With potassium addition the hydrocarbon activation on Pt became rate determining for mixtures of methane and ethane, induced by low surface coverage of methane and ethane in this case, in agreement with the results of Wei [3-5]. As a result, competition effects of methane and ethane were diminished on potassium modified PtYSZ, enabling simultaneous conversion of methane and ethane. Unfortunately, ethane conversion is not suppressed by the addition of potassium. A catalyst that clearly suppresses ethane conversion would be needed to make the overall concept of oxidative coupling combined with steam reforming applicable in one reactor compartment. In conclusion it can be said that it is unlikely that a methane selective catalyst for the steam reforming process can be developed.

7.3 Role of hydroxyl groups in water shift on PtZrO₂ (chapter 6)

The activation of water on zirconia was investigated, using water gas shift as a model reaction (chapter 6). It was shown that water induces the presence of two types of hydroxyl groups on monoclinic zirconia: mono- and multi-coordinated hydroxyls. Both types are active in the water gas shift mechanism, but they have different functionalities. Mono coordinated hydroxyls are involved in reaction with CO to the intermediate formate, while multi coordinated hydroxyls play a role in formate decomposition. Platinum was not necessary for formate formation and was found to play a role in formate decomposition/product formation. The reaction products, CO₂ and H₂ were formed on Pt/ZrO₂ when subjected to CO, even in the absence of water. In addition to the formate mechanism with redox regeneration for WGS on Pt/ZrO₂ as proposed by Azzam [6], it was found in this study that reduction of the support was limited to structural defective zirconia sites at edges and kinks, hosting the mono-

coordinated hydroxyl groups. The mechanistic insights gained in this study provide new possibilities to improve water gas shift catalysts by optimizing the availability of mono- and multi-coordinated groups on the support. Also, application of a metal with low affinity towards CO-adsorption and the ability to efficiently decompose formate, could improve reaction rates in water gas shift.

7.4 Catalyst and reactor optimization oxidative coupling

Extensive tests on the Mn/Na₂WO₄/SiO₂ oxidative coupling catalyst in both co-feed and membrane reactors were performed in the parallel project by Tymen Tiemersma and are described in detail in his PhD thesis [7]. In co-feed tests a maximum C₂-yield of only 12% was obtained, lower than comparable to yields reported in literature on the same catalyst [8-12]. Use of a membrane reactor was a challenging issue: the currently available ceramic membranes deliver too high oxygen fluxes and showed stability problems at temperatures around 850°C. This shows that development of new membranes is required for optimal operation of oxidative coupling. However, already with the current membranes selectivity to C₂ products could be increased from 60% in co-feed operation to 65% in the membrane reactor, induced by lower oxygen partial pressure and better temperature control. As a result, C₂ yield was increased to 20%. The main advantage of operation in a membrane reactor is energy production over the entire length of the reactor, instead of instantaneous steep temperature increase at the reactor entrance, occurring in co feed operation because of higher oxygen concentration at the reactor entrance. This offers interesting possibilities to combine a coupling reactor for oxidative coupling with a steam reforming reactor.

7.5 Reactor concepts (chapter 5)

The type of reactor concept that can be used strongly depends on the following issues.

The main conclusions obtained are shortly mentioned for each issue:

1. Oxidation reactions of hydrocarbons on steam reforming catalyst should be prevented.
 - Avoiding combustion reactions on (metal) steam reforming catalysts seems too difficult and therefore no research was performed on this topic. This means that a reactor or catalyst concept that avoids contact between oxygen and the reforming catalyst is required.
2. Reforming activity of ethane and ethylene can convert the complete mixture to synthesis gas and has to be limited.
 - Development of a steam reforming catalyst that selectively converts methane was not successful. This means that a suitable reactor concept or catalyst configuration has to be chosen, in order to avoid contact between C₂ hydrocarbons and the reforming catalyst.
3. The overall process combines the highly exothermic coupling and combustion reactions with the endothermic reforming, requiring optimized heat transfer between both processes.
 - Combining both processes in one catalyst particle or using one multifunctional catalyst can provide autothermal operation, if a support material with good conductive properties is used.
 - Heat transfer in separate reactions zones or reactor compartments can be optimized by limiting the distance between exothermic and endothermic zones, e.g. using small reactor tubes or even micro reactor systems.
4. High oxygen concentration leads to unselective oxidation reactions in the OCM section, producing CO₂ and H₂O. To increase C₂ yield and minimize combustion reactions a low oxygen partial pressure is needed in the OCM section.
 - It was demonstrated that use of a membrane reactor with distributed oxygen feeding can significantly increase selectivity and yield of ethylene and distribute energy production in oxidative coupling more evenly over the reactor.

Based on the results summarized above, Figure 7.2 shows two promising reactor concepts selected from the options as discussed in the Introduction section (Figure 1.2) to combine the oxidative coupling and steam reforming of methane. Both concepts will be discussed more in detail here.

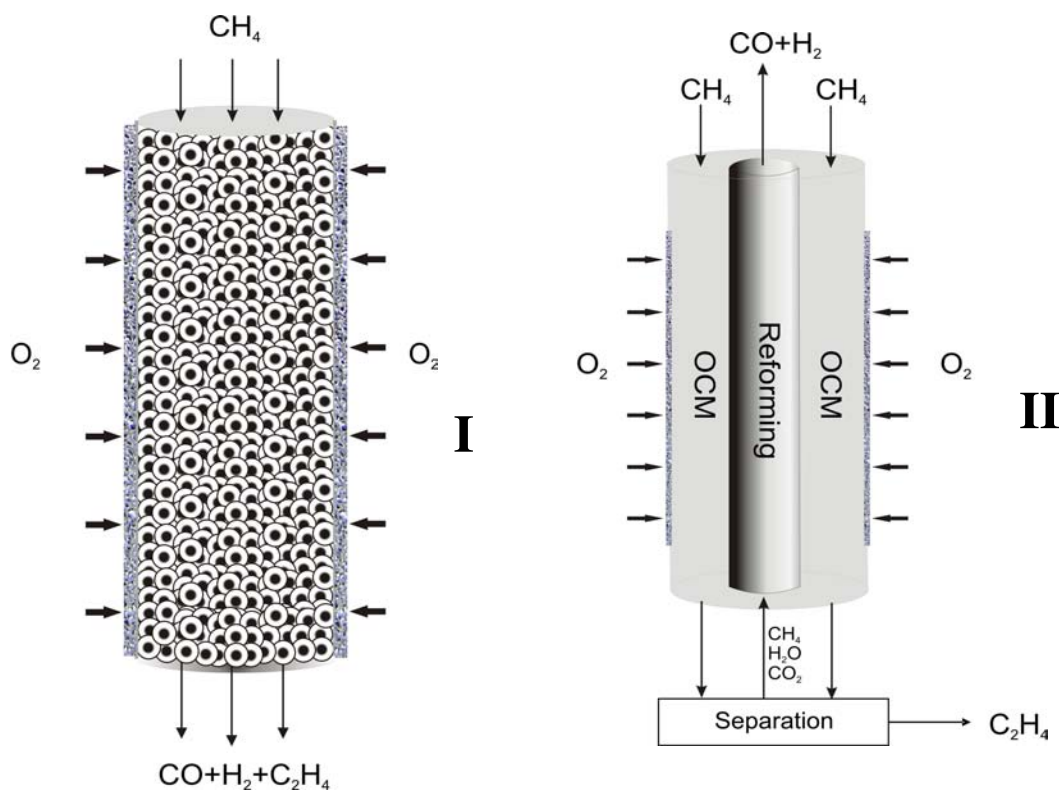


Figure 7.2: Selected reactor concepts for integration of oxidative coupling and reforming of methane, using combined catalyst particles (I) or combination of processes on reactor scale (II)

In the first concept, an eggshell catalyst is applied (Figure 7.2-I) to avoid contact between oxygen and the hydrocarbons on the reforming catalyst, eliminating combustions reactions on the reforming catalyst. The oxidative coupling catalyst is placed in the shell and the reforming function in the core of the catalyst. Oxygen present in the gas phase should be consumed in the outer layer of the particle to avoid diffusion to the core. In the core, in principle a methane selective reforming catalyst is required to avoid reforming of ethane and ethylene. This shell and core system enables excellent heat exchange between the processes, requiring support materials with good conductivity. However, the development of a methane selective catalyst was not successful, meaning that ethane and ethylene should not reach the particle

center. To reduce diffusion of these components to the particle center a catalyst particle with the structure indicated in Figure 7.3 is needed.

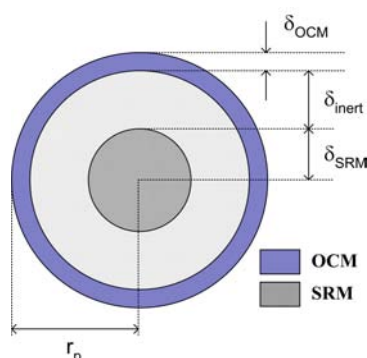


Figure 7.3: Schematic view of multifunctional catalyst particle, consisting of an outer layer of oxidative coupling catalyst (OCM), a diffusion layer and a core of methane steam reforming catalyst (SRM).

The reforming function (inner layer) and the oxidative coupling function (outer layer) are combined with an inert layer in one catalyst particle. Due to a higher diffusion coefficient of CH_4 , methane will reach the particle more easily than C2 hydrocarbons. As a result the amount of C2 hydrocarbons reformed will be relatively low. The combined catalyst particle should convert methane and oxygen to ethylene and synthesis gas. Numerical modelling of such a catalyst particle was performed using the kinetic model by Stansch [13] for oxidative coupling and reforming kinetics of Xu [14]. The possibility of auto thermal operation and net production of ethylene was demonstrated [7]. For low ethylene gas phase concentrations, it was shown that additional methane conversion to synthesis gas through steam reforming can consume energy produced in oxidative coupling, without significant consumption of ethane or ethylene. This concept only works at low C2 yield, because of much higher methane concentration, as compared to ethylene concentration. At high gas phase concentrations of ethylene, combustion reactions limit ethylene yields in oxidative coupling. The practical feasibility of synthesizing these catalyst particles and experimental demonstration of this concept offer challenging possibilities for future work.

As shown in figure 7.2 II, the oxidative coupling and reforming processes can also be separated on reactor scale by using separate reactor compartments. The advantage of concepts coupled on reactor scale is the higher flexibility in terms of intermediate reactions and separation steps: after the oxidative coupling process ethylene can be separated from the product mixture before the steam reforming section of the process (Figure 7.2 II), accepting that selective reforming of methane is not possible in presence of ethylene.

A possible concept was discussed more in detail in chapter 5 involving reactive separation of ethylene to ethylbenzene (equation 7.1):

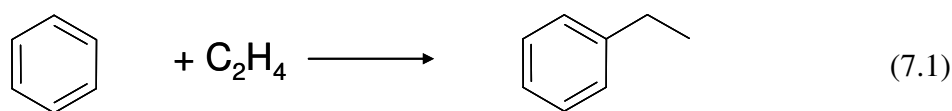


Figure 7.4 schematically shows a process scheme of the proposed concept. The oxidative coupling is carried out in a membrane reactor, producing C₂H₄ and C₂H₆ (1). The membrane reactor secures high selectivity to ethylene. Production of ethane should be avoided here: ethane is not reactive with benzene and is eventually lost to synthesis gas in the reforming step (4). The product mixture also contains remaining CH₄ and produced CO, CO₂, H₂O and small amounts of H₂. Excess benzene is added to this stream to react with ethylene to ethylbenzene around 360°C (2). Yields of EB up to 90% were found at 95% conversion and 90% selectivity at 360°C on ZSM-5. Methane and ethane present in the feed were not converted and can be used for steam reforming. None of the additional components present in the effluent gas of oxidative coupling (CO, CO₂, CH₄, C₂H₆ and H₂O) influences activity or selectivity of the alkylation catalyst. Stability of ZSM-5 is also not influenced by the added components, with the exception of water, which even improves stability.

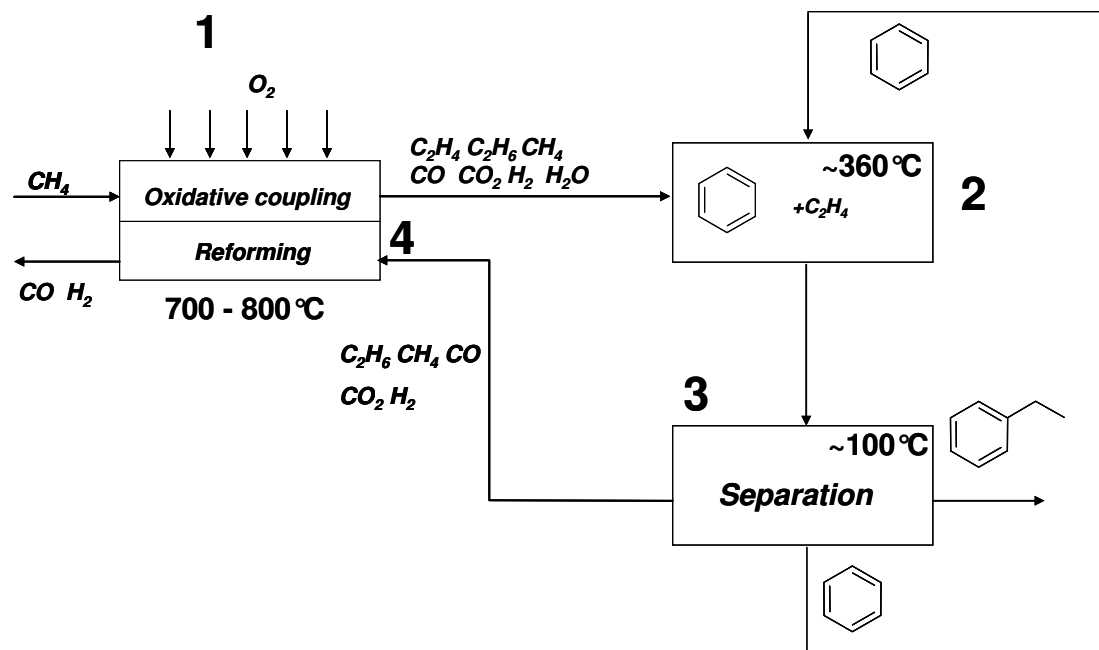


Figure 7.4: Possible process scheme of combined oxidative coupling and reforming of methane with ethylene reactive ethylene separation via alkylation of benzene

After the alkylation reaction, benzene and ethylbenzene are separated from the reaction mixture by distillation, recycling benzene to reactor (2). The remaining stream is fed to the reforming reactor (4), consuming the excess heat generated in the coupling process. The steam reforming catalyst needs to show high activity towards both methane and ethane, intending to convert all remaining hydrocarbons. An inexpensive commercial Ni catalyst could be an option, as deactivation through coking is less pronounced after removal of ethylene. The total process will convert methane and oxygen to synthesis gas and ethylbenzene. Efficient heat exchange between reactant and product streams is needed to make this concept feasible.

A remaining question in this concept is how to combine the oxidative coupling and reforming efficiently in one reactor. Performing oxidative coupling with distributed oxygen feeding proved to be beneficial [7] for ethylene selectivity and avoided the highly exothermic combustion reactions to a large extent. An additional advantage of using distributed feeding is that low oxygen partial pressure guarantees smaller temperature gradients and energy production over the entire length of the reactor, instead of instantaneous step increase of temperature at the reactor entrance. Reverse

flow operation of oxidative coupling could provide low temperature inlet and outlet streams[15, 16].

A possible configuration with oxidative coupling in horizontal tubes and reforming in the fluidized bed is shown in Figure 7.5. The processes are only coupled in terms of heat exchange between the endothermic reforming and exothermic oxidative coupling. With its excellent heat transfer properties, a fluidized bed reactor for the parallel steam reforming could provide an ideal heat sink for the reverse flow membrane reactor. The proposed total reactor concept consisting of reverse flow membrane tubes for oxidative coupling and a fluidized bed for steam reforming is schematically depicted in Figure 7.5. Numerical simulation [7] demonstrated the possibility of applying this concept and experimental demonstration of the concept is a challenging task for future research.

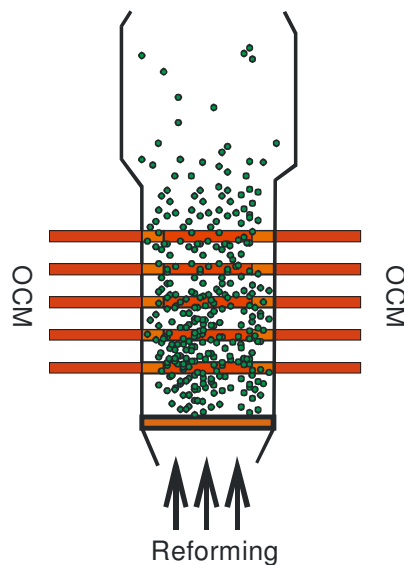


Figure 7.5: Schematic view of reactor concept with reverse flow membrane tubes for oxidative coupling of methane, integrated with fluidized bed for steam reforming

7.6 References

- [1] A.V. Zeigarnik, R.E. Valdes-Perez, O.N. Myatkovskaya, *Journal of Physical Chemistry B* 104 (2000) 10578.
- [2] E.H.v. Broekhoven, V. Ponec, *Progress in Surface Science* 19 (1985) 351.
- [3] J. Wei, E. Iglesia, *Journal of Physical Chemistry B* 108 (2004) 4094-4103.
- [4] J.M. Wei, E. Iglesia, *Journal of Catalysis* 225 (2004) 116.
- [5] J.M. Wei, E. Iglesia, *Physical Chemistry Chemical Physics* 6 (2004) 3754.
- [6] K.G. Azzam, I.V. Babich, K. Seshan, L. Lefferts, *Journal of Catalysis* 251 (2007) 153-162.
- [7] T. Tiemersma, PhD thesis, University of Twente, to be published (2009).
- [8] S.F. Ji, T.C. Xiao, S.B. Li, L.J. Chou, B. Zhang, C.Z. Xu, R.L. Hou, A.P.E. York, M.L.H. Green, *Journal of Catalysis* 220 (2003) 47.
- [9] A. Malekzadeh, M. Abedini, A.A. Khodadadi, M. Amini, H.K. Mishra, A.K. Dalai, *Catalysis Letters* 84 (2002) 45.
- [10] S. Pak, J.H. Lunsford, *Applied Catalysis A: General* 168 (1998) 131.
- [11] S. Pak, P. Qiu, J.H. Lunsford, *Journal of Catalysis* 179 (1998) 222.
- [12] A. Palermo, J.P.H. Vazquez, A.F. Lee, M.S. Tikhov, R.M. Lambert, *Journal of Catalysis* 177 (1998) 259.
- [13] Z. Stansch, L. Mleczko, M. Baerns, *Industrial & Engineering Chemistry Research* 36 (1997) 2568-2579.
- [14] J. Xu, G.F. Froment, *AIChE Journal* 35 (1989) 88-96.
- [15] M. van Sint Annaland, W.P.M. van Swaaij, H.A.R. Scholts, J.A.M. Kuipers, *Chemical Engineering Science* 57 (2002) 833-854.
- [16] M. van Sint Annaland, W.P.M. van Swaaij, H.A.R. Scholts, J.A.M. Kuipers, *Chemical Engineering Science* 57 (2002) 855-872.

Dankwoord

Acknowledgements

De afgelopen 4 jaar heb ik op de Universiteit Twente gewerkt aan mijn promotieonderzoek in de vakgroep katalytische processen en materialen. In deze tijd heb ik veel geleerd en me verder ontwikkeld op zowel vakkennis als op persoonlijk vlak. Ik ben iedereen die mij op welke manier dan ook heeft geholpen zeer dankbaar.

Leon, ik wil je bedanken voor de begeleiding gedurende dit onderzoek. Jouw kritische kijk op het onderzoek en precisie bij het schrijven van publicaties hebben dit werk wetenschappelijk naar een hoger niveau getild. Het was erg prettig om steeds snel reactie op documenten, posters en presentaties te krijgen.

Barbara, ontzettend bedankt voor alle hulp en ondersteuning in dit onderzoek. Ik vind het ontzettend knap hoe je steeds voor me klaar stond en heb erg van onze samenwerking genoten. Jouw enthousiaste inbreng en creativiteit zijn van onschatbare waarde voor het eindresultaat. Ik heb echt veel van je geleerd! Ook het samen verzorgen van onderwijs was erg prettig. Spontaan komt ook het weekje in Grenoble bij me op, waar het uiteindelijk toch wel erg gezellig was, ondanks dat EXAFS niet gauw mijn favoriete bezigheid zal worden...

Jan, ik waardeer jouw bijdrage aan dit onderzoek heel erg. Jouw positieve kijk op onderzoeksvragen en kennis op allerlei gebieden waren zeer waardevol en hebben tot leuke discussies en gesprekken geleid.

Tymen, bedankt voor de uitstekende en zeer prettige samenwerking en de mooie resultaten die je op jouw deel van het onderzoek hebt neergezet. Voor mijn gevoel vulden we elkaar uitstekend aan en hebben we echt iets moois van dit onderzoek gemaakt. Het gaf een heel sterk gevoel om bij presentaties en conferenties als duo op te treden en samen ons onderzoek te vertegenwoordigen. Verder denk ik ook met plezier terug aan de gezellige avonden op meetings en cursussen. Mijn dank gaat ook

naar je begeleiders Hans en Martin, voor hun bijdrage en de aangename en productieve samenwerking.

Dennis, ik wil je graag bedanken voor de uitstekende prestaties tijdens je afstuderen en de prettige samenwerking gedurende het laatste jaar. Ik weet zeker dat je de komende 4 jaar succesvol aan je promotie zal werken! Jordi, thanks for your contribution to my work. It is not described in this thesis but it gave very valuable information!

Lianne, uiteraard bedankt voor de secretariële ondersteuning, maar veel belangrijker ook bedankt voor het steeds klaar staan voor gesprekken over allerlei andere dingen, het helpen met van alles en nog wat en voor jouw gezellige inbreng in het dagelijks leven in onze groep en daarbuiten!

Bert, naast de uitstekende technische ondersteuning ook mijn dank voor de gezellige tijd tijdens koffiepauzes, borrels, beurzen en andere festiviteiten. Ook jij was van enorm belang voor de gezelligheid in de groep! Verder kom ik ook steeds op je hulp en adviezen rekenen bij allerlei vragen betreffende klusjes aan de auto, het huis, de fiets en andere kwesties in het leven.

Seshan, hartelijk bedankt voor alle hulp en discussies en je inbreng en begeleiding op water gas shift en op het gebied van wateractivering.

Jeroen, het was erg prettig om je bijna 3 jaar als collega te hebben. Bedankt voor de technische hulp en de hele fijne tijd! Hans, bedankt voor de 4 aangename jaren samen bij CPM, alle cursussen en conferenties waar we ons altijd uitstekend vermaakt hebben en ik met jou steeds een aangename kamergenoot had. Karin en Louise, bedankt voor alle ondersteuning op het lab en analyses van mijn samples.

A special thanks to my officemates during the 4 years for the nice time and talks we had together: Sune, Sergio, Miriam and Son. I would like to thank all present and former group members and colleagues for the nice time that we had during coffee breaks, lunches, dinners, courses, conferences, excursions, parties, soccer matches, Zhu, Jiang, Nabeel, Valer, Khalid, Dejan, Daryl, Igor (still remember our great victory of the NIOK cup), Berta (I always enjoyed your enthusiastic and outgoing personality), Iris (schitterende discussies, waren we het ooit ergens over eens?:)),

Cristiano (really like our friendship), Davide (our great defender, liked our dinners at Antica Villa), Vijay, Gacia, Hrudya, Marijana, Kazu, Kumar (what a great week we had in Korea!), all other (exchange) students, all other members of our CPM soccer team.

Martin Pijl van Varian, Gerard Wiecherink en Frans Arts van Bronkhorst en Huub Raterink van Brooks bedank ik voor de zeer prettige samenwerking en de gezellige borrels op de Instrumenten beurs.

Mark, Herman, Marinus, Ivo, Bas, Willem, Danny, Patricia, Elke, bedankt voor de etentjes, squashpartijen, stapavonden, weekendjes weg, enz.. de ontzettend gezellige tijd hier in Enschede, die wat mij betreft nog even doorgaat! Alle leden van ons zaalvoetbal team in Enschede!

Maurice, Koen, Raimond, Olaf, Rudi, Cyriel, Wouter, Hans, Hennie, Toonen, Jim en alle andere “Limburgers” die mij ontzettend mooie en gezellige weekenden hebben opgeleverd bij en rond de tafeltennisclub Kluis en op allerlei andere plekken zoals Eindhoven, Enschede, Warschau, Düsseldorf, enz. Een speciale dank ook aan Lia en Jos voor alle gezelligheid en ondersteuning.

Daniel en Inge, bedankt voor alle steun die ik van jullie heb gehad en alle andere leuke dingen die we samen hebben ondernomen.

Papa, Renate und Oma, ich moechte mich bei Euch fuer die Unterstuetzung waehrend der Promotion bedanken und ich bin immer gerne zu Besuch bei Euch!

Mam, ik waardeer heel erg dat jij er altijd voor me stond en me steeds ondersteund hebt! Het voelde heel prettig om in Beek steeds “thuis” te komen tijdens vakanties en weekenden.

Publications

P.O. Graf, B.L. Mojet, J.G. van Ommen, and L. Lefferts, Comparative study of steam reforming of methane, ethane and ethylene on Pt, Rh and Pd supported on yttrium-stabilized zirconia, *Applied Catalysis A: General* 332 (2007) 310-317

P.O. Graf, B.L. Mojet, and L. Lefferts, Influence of potassium on the competition between methane and ethane in steam reforming over Pt supported on yttrium-stabilized zirconia, *Applied Catalysis A: General* 346 (2008) 90-95.

P.O. Graf and L. Lefferts, Reactive separation of ethylene from the effluent gas of methane oxidative coupling via alkylation of benzene to ethylbenzene on ZSM-5, submitted to *Chemical Engineering Science*

P.O. Graf, B.L. Mojet and L. Lefferts, The effect of potassium addition to Pt supported on YSZ on steam reforming of mixtures of methane and ethane, *Applied Catalysis A: General* in preparation

P.O. Graf, D.J.M. de Vlieger, B.L. Mojet, L. Lefferts, New insights in the water gas shift mechanism on Pt/ZrO₂: the role of hydroxyl groups elucidated, submitted to *Journal of Catalysis*

Posters & Presentations

Patrick Graf, Tymen Tiemersma, Martin van Sint Annaland, Barbara Mojet, Hans Kuipers & Leon Lefferts, Simultaneous production of ethylene and synthesis gas: combining coupling and reforming of methane, Oral presentation at Netherlands Process Technology Symposium (NPS), 2007

Patrick Graf, Barbara Mojet & Leon Lefferts, Influence of potassium on Pt-catalysts in steam reforming of ethane and methane, Oral presentation at Netherlands' Catalysis and Chemistry Conference (NCCC), 2007

Patrick Graf, Barbara Mojet and Leon Lefferts, Influence of potassium on Pt-catalysts in steam reforming of methane & ethane, Poster Presentation at 14th International Catalysis Congress, July 13-18 2008, Seoul Korea

Patrick Graf: Poster presentations at Netherlands Catalysis and Chemistry Conference (NCCC 2006 and 2008)

Curriculum Vitae

Patrick Graf werd op 19 augustus 1979 geboren in Aachen (Duitsland). Na bezoeken van basisschool de Stutensee (Duitsland) verhuisde hij met zijn moeder en broertje naar Beek in Nederland en bezocht het gymnasium St Michiel in Geleen. Na het behalen van het diploma in 1998 begon hij met de opleiding Chemische technologie aan de TU Eindhoven. De bedrijfsstage bij Roche in Basel (Zwitserland) en het afstudeerproject bij de vakgroep Chemical Reactor Engineering waren de belangrijkste studieonderdelen. De studie werd in 2003 afgerond, waarna Patrick nog aan zijn afstudeerproject verder werkte als toegevoegd onderzoeker. Op 1 september 2004 begon Patrick aan zijn promotieonderzoek in de vakgroep Catalytic Processes and Materials aan de Universiteit Twente. De belangrijkste resultaten van dit onderzoek staan beschreven in dit proefschrift. Vanaf 15 oktober 2008 werkt Patrick als Basic Design Engineer bij Zeton BV in Enschede.



ISBN: 978-90-365-2778-1

